Drug-like Cell Permeability and Oral Bioavailability in Lipophilic Macrocycles Inspired by Natural Products

Andrew T Bockus,[†] Katrina W Lexa,[‡] Cameron R Pye,[†] Amit S Kalgutkar,[§] Jarret W Gardner,[†] Kathryn C R Hund,[†] William M Hewitt,[†] Joshua A Schwochert,[†] Emerson Glassey,[†] David A Price, [Δ] Alan M Mathiowetz,[Δ] Spiros Liras,[Δ] Matthew P Jacobson[‡]* & R Scott Lokey[†]*

[†]Department of Chemistry and Biochemistry, University of California Santa Cruz, Santa Cruz, California, USA.
[‡]Department of Pharmaceutical Chemistry, University of California San Francisco, San Francisco, California, USA.
[§]Pharmacokinetics and Drug Metabolism, Pfizer Inc, Groton, Connecticut, USA.
[Δ]Worldwide Medicinal Chemistry, Pfizer Inc, Groton, Connecticut, USA. *e-mail: slokey@ucsc.edu or matt.jacobson@ucsf.edu

Supporting Information

Table of Contents

I. General Information

Fmoc-protected amino acids and coupling agents were purchased from NovaBiochem, and all other reagents were purchased from Aldrich and used without further purification. Resins were obtained from Rapp Polymere. Dichloromethane, acetonitrile, tetrahydrofuran, and methanol were purchased from EMD; *N*,*N*-dimethylformamide was purchased from Acros. Moisture-sensitive reactions were run under N_2 in oven-dried glassware. Acetonitrile, toluene, methylene chloride, and tetrahydrofuran were dried by passage over a drying column by Innovative Technologies, Inc. NMR experiments were run on 500 or 600 MHz Varian instruments equipped with a cold probe at 25˚ C unless otherwise specified. Chemical shifts reported in ppm relative to reference solvent and coupling constants are reported in Hz. Key for multiplicity (s = singlet, d = doublet, t = triplet, q = quartet, m = multiplet). NMR data was processed with Mestranova on a MacBook Pro laptop. Optical rotations were measured using Jasco DIP-370 polarimeter. Flash chromatography of amino acid monomers was performed on Biotage Isolera Prime over silica gel 60. Analytical Tandem Liquid Chromatography/Mass Spectrometry was performed on a Thermo-Finnigan LCQ Classic equipped with a standard ESI ion trap and photodiode array detector. Samples were ejected on a reverse phase C18 column (HA 50 x 4.6 mm CS-0546-C158) with a 1.0 ml/min flow rate. Chiral chromatography was performed on a Waters MicromassZQ LC/MS using a Daicel Chiralcel column (OJ-RH 2.1x150 mm 5 um) with a flow rate of 1.2 ml/min. PAMPA well analytics were performed on a Finnigan MAT LTQ: quadrapole, using a Phenomonex synergi 2.5 um, 30 x 2.00 mm Fushion RP10 column with a 0.20 mL/min flow rate. Analytical TLC was performed using glass UV silica plates from Agela Techologies and a UV lamp or $KMnO_4$ stain. Mass-directed cyclic peptide purification was performed on the Waters MicromassZQ using an Xbridge BEH 130 Prep C18 5 um preparatory column at a flow rate of 20 ml/min. UV-directed peptide purifications were achieved using a Shimadzu LC-8A with a C18 prep column (250x20 mm C18 10 um) at a flow rate of 10 mL/min. MDCK-LE, HLM, Rat data, eLogD, and EPSA were acquired by Pfizer, Inc as described below.

II. SYNTHETIC PROCEDURES AND PHYSICAL PROPERTIES OF COMPOUNDS

Synthesis of Fmoc-Nme-leucine[1]

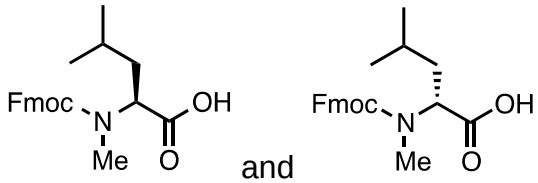

MW = 367.44

Fmoc-Leu-OH (5.10 g, 14.4 mmol), paraformaldehyde (5.0 g), and camphorsulfonic acid (0.15 equiv, 0.5 g, 2.24 mmol) were dissolved in toluene (200 mL) in a 500 mL round bottom flask and heated to 160°C in a stark apparatus for ~1.5 hours until only 30 mL of solution remained. The solution was cooled to room temperature, diluted with ethyl acetate (50 mL) and filtered. The filtrate was evaporated under reduced pressure, yielding a colorless oil. The crude oil was dissolved in 1:1 dichloromethane:trifluoroacetic acid (10 mL) and triethylsilane (3 mL, 18.6 mmol) was added. The solution was stirred overnight at room temperature. Upon completion, the solution was evaporated under reduced pressure and flash purified to yield an orange-white solid. A mixture of cis/trans-amide rotomers was observed in the NMR. Mass: 4.77 g, 12.98 mmol. yield: 90.1%, Rf (3:1 EtOAc:Hex) = 0.32.

(S): $[\alpha]_D^{25}$ = -20.8 (*c* 1.6, DCM), ee = > 98% Chiral RT = 5.75 min

(R): $[\alpha]_D^{25}$ = 24.2 (*c* 1.6, DCM), ee = > 98% Chiral RT = 8.26 min

^{1}H NMR (500 MHz, $CDCl_3$) δ 10.04 (s, 1H), 7.77 (d, *J* = 7.6 Hz, 1H) and 7.76 – 7.72 (m, 1H) integrate together for 2H, 7.61 (t, *J* = 6.5 Hz, 1H) and 7.58 – 7.54 (m, 1H) integrate together for 2H, 7.41 (t, *J* = 7.6 Hz) and 7.38 – 7.27 (m, 3H) integrate together for 4H, 4.95 (dd, *J* = 8.6, 7.2 Hz, 0.6H) and 4.62 (dd, *J* = 10.7, 5.9 Hz, 0.4H) integrate together for 1H, 4.48 (qd, *J* = 10.8, 6.7 Hz, 2H), 4.26 (dt, *J* = 30.2, 6.7 Hz, 1H), 2.88 (s, *2*H) and 2.86 (s, 1H) integrate together for 3H,

1.77 (dd, *J* = 8.4, 6.5 Hz, 1H), 1.67-1.43 (m, 2H) 0.97 (dd, *J* = 12.3, 6.5 Hz, 4H) and 0.89 (d, *J* = 6.6 Hz, 1H) and 0.76 (d, *J* = 6.5 Hz, 1H) integrate together for 6H.

^{13}C NMR (126 MHz, $CDCl_3$) δ 177.81, 157.30, 143.92, 141.4, 127.81, 127.19, 125.11, 120.09, 67.95, 56.83, 47.40, 37.33, 30.48, 24.98, 23.35, 21.37. Only the major isomer reported

LCMS (ESI) m/z: 368.47 (expected: 367.18 + H)

Vinylogue Synthesis

Synthesis of Fmoc-leucinol[2]

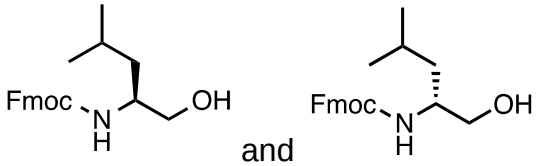

and

MW = 339.43

Fmoc-Leu-OH (5.0 g, 14.7 mmol) was dissolved in dry THF (100 mL) under inert atmosphere at room temperature. Carbonyldiimidazole (1.3 equiv, 2.9 g, 18.0 mmol) was added to the solution and allowed to stir for 20 minutes. The solution was cooled to 0 °C and sodium borohydride (1.6 equiv, 0.87 g, 0.23 mmol) was added slowly with 50 mL cold water. The reaction was stirred for 30 minutes determined complete by TLC. The reaction was quenched with 5% citric acid (10 mL) and the aqueous layer was extracted with ethyl acetate (3 x 50 mL) and evaporated onto silica. The compound was flash purified on a 100 g column with an ethyl acetate-hexanes 10-100% gradient, yielding a fluffy white solid (3.79 g, 10.3 mmol, 73% yield). Rf (3:1 EtOAc:Hex) = 0.44.
(S): $[\alpha]_D^{25}$ = -17.11 (*c* 1.9, DCM), ee = > 98% Chiral RT = 5.18 min

(R): $[\alpha]_D^{25}$ = +18.11 (*c* 1.5, DCM), ee = > 98% Chiral RT = 6.32 min

^{1}H NMR (500 MHz, $CDCl_3$) δ 7.76 (d, *J* = 7.5 Hz, 2H), 7.59 (d, *J* = 7.4 Hz, 2H), 7.40 (t, *J* = 7.4 Hz, 2H), 7.31 (t, *J* = 7.4 Hz, 2H), 4.83 (d, *J* = 7.6 Hz, 1H), 4.49 – 4.42 (m, 2H), 4.21 (t, *J* = 6.5 Hz, 1H), 3.78 (s, 1H), 3.67 (s, 1H), 3.51 (s, 1H), 2.27 (s, 1H), 1.64 (dt, *J* = 12.4, 6.2 Hz, 1H), 1.34 (m, 2H), 0.93 (m, 6H).

^{13}C NMR (126 MHz, $CDCl_3$) δ 156.89, 144.01, 141.47, 127.80, 127.17, 125.13, 120.09, 66.65, 66.11, 51.49, 47.47, 40.55, 24.90, 23.18, 22.27.

LCMS (ESI) m/z: 340.43 (expected: 339.18 + H)

Synthesis of Fmoc-leucinal

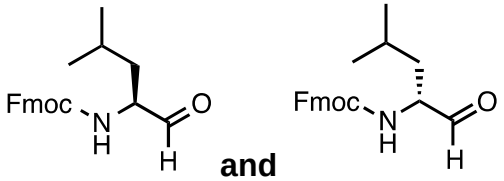

MW = 337.41

Fmoc-L-leucinol (1.69 g, 5.0 mmol) was dissolved in dry DCM (50 mL) under inert atmosphere and cooled to 0 °C for the addition of Dess-Martin Periodinane[3,4] with dry workup (1.2 equiv, 2.54 g, 6.0 mmol). The reaction was incomplete after 3 hours and allowed to stir overnight. An aqueous solution of 10% sodium thiosulfate and 5% sodium bicarbonate (20 mL) was added and stirred for 30 minutes. The aqueous layer was extracted with DCM (3 x 50 mL), and the pooled organic layers were back-extracted with water (50 mL), brine (50 mL), dried with MgSO4, and filtered through a plug of celite to yield a clear oil (1.43 g, 4.2 mmol, 84% yield). Rf (1:3 EtOAc:Hex) = 0.43.

(S): $[\alpha]_D^{25}$ = + 9.1 (*c* 1.5, DCM), ee = > 98% assumed regarding subsequent product
(R): $[\alpha]_D^{25}$ = -10.9 (*c* 1.6, DCM), ee = > 98% assumed regarding subsequent product

^{1}H NMR (500 MHz, $CDCl_3$) δ 9.58 (s, 1H), 7.77 (d, *J* = 7.6 Hz, 2H), 7.60 (d, *J* = 5.9 Hz, 2H), 7.40 (t, *J* = 7.3 Hz, 2H), 7.32 (t, *J* = 7.4, 2H), 5.22 (s, 1H), 4.45 (d, *J* = 6.8 Hz, 2H), 4.33 (dq, *J* = 8.5, 4.7 Hz, 1H), 4.23 (t, *J* = 6.8 Hz, 1H), 1.82 – 1.64 (m, 3H), 1.42 (ddd, *J* = 14.0, 9.3, 5.2 Hz, 1H), 1.03 – 0.91 (m, 6H).

^{13}C NMR (126 MHz, $CDCl_3$) δ 199.82, 156.29, 143.92, 141.45, 127.85, 127.19, 125.14, 120.12, 67.06, 58.92, 47.34, 38.19, 24.76, 23.21, 21.99.

LCMS (ESI) m/z: 338.48 (expected: 337.17 + H)

Synthesis of Fmoc-leucine vinyl tert-butyl ester[5,6]

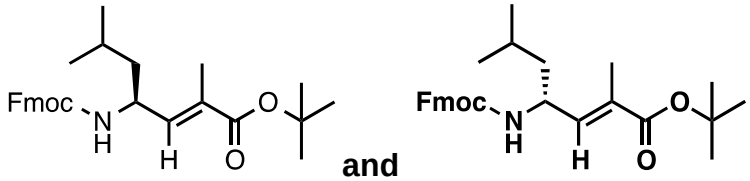

MW = 449.26

Fmoc-leucinal (0.26 g, 0.75 mmol) was dissolved in dry DCM (10 mL) in an oven-dried 100 mL round bottom flask under nitrogen. *tert*-butyl ester ylide (2.0 equiv, 0.59 g, 1.5 mmol) was added and the solution was stirred for 1.5 hours when the reaction was determined complete by TLC. The reaction mixture was evaporated onto silica gel and flash purified on a 5-40% EtOAc:Hexanes gradient on a 25 g

column. The purified product was a colorless oil (0.26 g, 0.58 mmol) recovered in 77.2% yield. Rf (1:3 EtOAc:Hex) = 0.57.

(S): $[\alpha]_D^{25}$ = -1.8 (*c* 1.7, DCM), ee = > 98% Chiral RT = 8.13 min

(R): $[\alpha]_D^{25}$ = +2.6 (*c* 5.3, DCM), ee = > 98% Chiral RT = 9.06 min

^{1}H NMR (500 MHz, $CDCl_3$) δ 7.76 (d, *J* = 7.5 Hz, 2H), 7.58 (d, *J* = 7.4 Hz, 2H), 7.40 (t, *J* = 7.5 Hz, 2H), 7.31 (t, *J* = 7.6, 2H), 6.39 (d, *J* = 8.8 Hz, 1H), 4.79 (d, *J* = 8.5 Hz, 1H), 4.56 (ddd, *J* = 8.8, 8.4, 7.7 Hz, 1H), 4.45 (dd, *J* = 10.7, 6.9 Hz, 1H), 4.37 (dd, J = 10.8, 6.7 Hz, 1H), 4.25 – 4.18 (m, 1H), 1.92 (s, 3H), 1.61 (q, *J* = 7.8, 6.8 Hz, 1H), 1.54 – 1.44 (m, 9H), 1.35 – 1.27 (m, 2H), 1.00 – 0.79 (m, 6H)

^{13}C NMR (126 MHz, $CDCl_3$) δ 167.29, 155.79, 144.00, 141.41, 140.30, 130.64, 127.75, 127.12, 125.10, 120.05, 80.60, 66.63, 47.40, 44.37, 28.19, 24.68, 22.88, 22.49, 12.97.

LCMS (ESI) m/z: 450.56 (expected: 449.26 + H)

Synthesis of Fmoc-leucine vinyl acid[7]

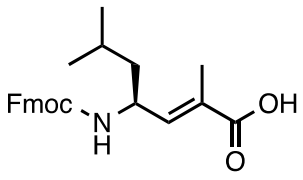

and

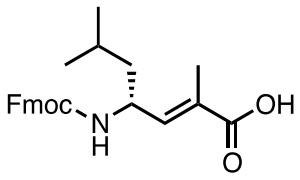

MW = 393.48

Fmoc-L-Leucine Vinyl *tert*-butyl ester (0.26 g, 0.58 mmol) was dissolved in dry DCM (4 ml) in a 25 mL round bottom flask. Trifluoroacetic acid (2 mL) was added and the reaction was stirred at room temperature for 30 minutes until determined complete by TLC. The reaction was diluted in 10 mL DCM and evaporated under

reduced pressure to remove residual TFA. The product was recrystallized from DCM/Hexanes to yield a white solid (0.11 g, 0.28 mmol, 48% yield). Rf = 0.48 (3:1 EtOAc:Hex).

(S): $[\alpha]_D^{25}$ = +2.6 (*c* 0.9, MeOH), ee = > 98%. Chiral RT = 3.75 min

(R): $[\alpha]_D^{25}$ = -4.4 (*c* 1.9, MeOH), ee = > 98%. Chiral RT = 5.93 min

^{1}H NMR (600 MHz, $CDCl_3$) δ 7.74 (d, *J* = 7.5 Hz, 2 H), 7.56 (d, *J* = 7.3, 2H), 7.38 (t, *J* = 7.4 Hz, 2H), 7.29 (t, *J* = 7.3, 2H), 6.56 (d, *J* = 9.2, 1H), 4.69 (d, *J* = 8.1 Hz, 1H), 4.54 (dt, *J* = 16.0, 8.1 Hz, 2H), 4.46 – 4.35 (m, 2H), 4.19 (t, *J* = 6.6 Hz, 1H), 1.94 (s, 2H), 1.59 (dd, *J* = 13.3, 6.5 Hz, 2H), 1.48 (dt, *J* = 14.2, 7.3 Hz, 1H), 1.31 (dt, *J* = 13.7, 6.9 Hz, 1H), 0.92 (dd, *J* = 10.6, 6.6 Hz 5H), 0.79 (m, 1H)

^{13}C NMR (126 MHz, $CDCl_3$) δ 172.90, 155.82, 143.98, 141.48, 127.83, 127.19, 125.12, 120.11, 66.73, 47.96, 47.44, 44.02, 24.74, 22.88, 22.51, 12.62

LCMS (ESI) m/z: 394.43 (expected: 393.19 + H)

Synthesis of *tert*-Butyl ester phosphorane ylide[8]

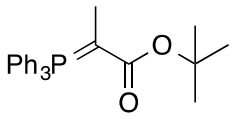

MW = 390.45 exact mass = 390.17

tert-Butyl-2-bromopropanoate (1.26 g, 6.02 mmol) and triphenyl phosphine (1.0 equiv, 1.57 g, 6.02 mmol) were dissolved in 7.5 mL of dry ACN, flushed with Nitrogen, and stirred at room temperature with 3 Å molecular sieves for 18 hours. The ACN was evaporated under reduced pressure and Toluene was added to crash out a white precipitate. The toluene was then decanted off and the white solid was dissolved in 30 ml DCM and transferred to a separatory funnel. A 30 mL solution of 10% NaOH was added to the funnel, shaken, and the organic

layer immediately turned yellow. The organic layer was collected. The aqueous layer was washed once with 30 mL DCM. The DCM layers were pooled and back extracted once with 10 mL H_2O, then dried over $MgSO_4$, filtered and evaporated, giving the ylide as a yellow solid in 28% yield. The crude was carried on to subsequent reactions. Comparable alternative syntheses using toluene solvent are outlined in **Table S1**.

^{1}H NMR (500 MHz, $CDCl_3$) δ 7.64 – 7.58 (m, 6H), 7.52 (td, *J* = 7.3, 1.7 Hz, 3H), 7.47 – 7.41 (m, 6H), 1.56 (d, *J* = 14.0 Hz, 3H), 0.99 (s, 9H)

^{13}C NMR (126 MHz, $CDCl_3$) δ 133.72, 131.60, 128.41, 28.73, 12.68.

Table S1: Synthesis of *tert*-Butyl ester ylide

Rxn	Solvent	Equiv. TPP	Time (h)	Temp (°C)	3 Å Sieves	Yield	Purity (1H NMR)
1	toluene	1	18	70	No	63%	50%
2	toluene	1	18	25	No	0%	-
3	toluene	1	18	25	Yes	0%	-
4	toluene	1	18	70	Yes	59%	90%
5	toluene	1.2	114	25	No	16%	98%
6	acetonitrile	1	18	25	Yes	28%	95%

All reactions run with 6.02 mmol of *tert*-Butyl 2-bromopropanoate at 0.8 M in 7.5 ml dry solvent.

Statine Synthesis

Fmoc-(*R,R*)-Leu-statine and Fmoc-(*S,S*)-Leu-statine

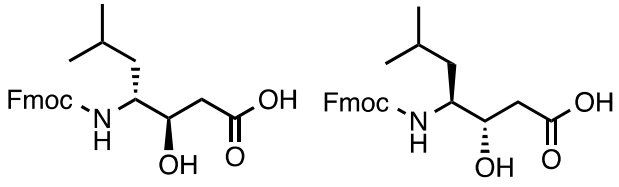

MW = 397.46

Synthesized as described by Cadicamo et al.[9]

^{1}H NMR (600 MHz, $CDCl_3$) δ 7.75 (d, *J* = 7.6 Hz, 2H), 7.58 (dd, *J* = 7.5, 4.4 Hz, 2H), 7.54 (dd, *J* = 15.9, 7.5 Hz, 1H), 7.38 (q, *J* = 9.6, 8.6 Hz, 2H), 7.30 (t, *J* = 7.6 Hz, 2H), 5.81 (d, *J* = 10.4 Hz, 0.3H), 5.13 (d, *J* = 9.7 Hz, 0.7H), 4.64 (ddd, *J* = 44.8, 10.7, 4.8 Hz, 0.8H), 4.49 - 4.39 (m, 1.7H), 4.19 (t, *J* = 6.6 Hz, 1H), 4.06 - 3.98 (m, 0.8H), 3.78 - 3.72 (m, 0.3H), 3.68 (tdd, *J* = 9.6, 5.1, 2.1 Hz, 0.8H), 3.09 (td, *J* = 9.9, 4.9 Hz, 0.3H), 2.51 (d, *J* = 6.3 Hz, 1.62H), 2.15 (d, *J* = 9.3 Hz, 0.2H), 2.12 (d, *J* = 9.2 Hz, 0.2H), 1.88 - 1.81 (m, 0.3H), 1.59 (ddt, *J* = 12.2, 8.5, 6.1 Hz, 0.8H), 1.52 (ddd, *J* = 14.7, 9.7, 5.4 Hz, 0.9H), 1.40 (dt, *J* = 13.5, 6.8 Hz, 0.4H), 1.31 (ddd, *J* = 13.7, 8.7, 4.7 Hz, 1.2H), 1.12 (ddd, *J* = 13.8, 8.5, 5.1 Hz, 0.3H), 0.90 (dd, *J* = 6.5, 3.3 Hz, 5H), 0.73 (d, *J* = 6.6 Hz, 1H), 0.55 (d, *J* = 6.6 Hz, 1H). Multiple conformations corroborated by Konno et al.[10]

(S,S): $[\alpha]_D^{25}$ = -24.43 (*c* 1.5, DCM), >98% ee Chiral RT = 6.71 min
(R,R): $[\alpha]_D^{25}$ = 35.12 (*c* 1.5, DCM), > 98% ee, Chiral RT = 7.97 min

LCMS (ESI) m/z: 397.82 (expected: 397.19 + H)

Macrocycle Synthesis

Resin Loading

Fmoc-NMe-Leu-OH was loaded onto 2-chlorotrityl chloride PS resin from Anaspec with 4.0 eq of DIPEA in dry DCM achieving calculated loading values of 0.9 mmol/gram of resin.

Linear SPPS

All cyclic peptides were synthesized on the solid phase using standard SPPS methods, starting from the appropriate Fmoc-protected *N*-methylated leucine

(position 6) linked to 2-chlorotrityl chloride resin through the carboxylic acid. Fmoc was deprotected with 2% DBU in DMF for 30 min at room temperature. The resin was washed with DMF (3x), DCM (3x), and DMF (3x) following deprotections as well as couplings. Peptide coupling was accomplished with incoming Fmoc-protected amino acid (1.5 eq), HOAT (1.5 eq), HATU (1.5 eq), DIPEA (2 eq) in DMF. The reactions were agitated 1 to 2 h at rt. Statine residues were coupled without hydroxyl protection[9].

Solution Phase Cyclization

Linear peptide was cleaved from the resin with 1% TFA in DCM then evaporated under reduced pressure. Linear peptide was diluted in a solution of 1:1 THF:ACN at a concentration of approximately 0.5 mg/mL to prevent polymerization. Cyclization was achieved with PyBOP (3 eq), HOAT (3 eq), and DIPEA (4 eq) overnight. Use of COMU[11] (1.2 eq) and DIPEA (1.5 eq) led to complete cyclization after 30 minutes, but side-products co-eluted with our desired macrocycles. Cyclic product was purified my reverse phase HPLC mass-directed fractionation.

Kinetic Solubility

Solubility was determined by titrating a 60 □M DMSO stock solution of peptide with PBS (pH = 7.4) while maintaining a DMSO concentration of < 1%. A 1 μL aliquot of stock solution was added to 100 μL PBS and sonicated. If solid was present, additional aliquots of 50 μL PBS were added and sonicated until no solid remained.

III. PERMEABILITY

Parallel artificial membrane permeability assay[12] to determine passive membrane diffusion rates of individual compounds. A 96-well donor plate with 0.45 μm hydrophobic Immobilon-P membrane supports (Millipore) and a 96-well Teflon acceptor plate were used in the PAMPA. A 1% (w/v) solution of lecithin in dodecane was prepared and sonicated for 5 minutes prior to use. The dodecane lecithin solution (5 μL) was carefully applied to the membrane supports in the wells of the donor plate, with care being taken not to touch the pipet tip to the membrane. The acceptor plate was prepared by adding 300 μL of 5% DMSO/PBS (pH 7.4) to each well. The donor wells were prepared by adding 150 μL of each cyclic peptide solution (10 μM in 5% DMSO/PBS at pH 7.4) to the wells in quadruplicate. The donor plate was then placed on top of the acceptor plate so the artificial membrane was in contact with the buffer solution below. A lid was placed on the donor well, and the system was covered with a glass evaporating dish and left for 5 hours at room temperature. A wet paper towel was placed on the inside of the chamber to prevent evaporation.

Once the assay was complete, a sample from each well (50 μL) was diluted in a 10 μM solution of H_2N-Tyr(O*t*-Bu)-CO_2H in 1:1 ACN:H_2O (50 μL), then 20 μL was injected into the LC-MS. Acceptor and donor well concentrations were measured by LC-MS (Thermo LTQ) using selected ion monitoring (SIM) mode to detect the parent masses of both the analyte and the internal standard. Analyte-to-standard peak area ratios from the TIC detector were calculated and used to determine relative concentrations in both donor and acceptor wells. These ratios were then used to calculate an equilibrium value adjusted for retention (E_R):

$$\mathbf{E_R = (R_A V_A + R_D V_D)/V_A + V_D}$$

Where R_A is the analyte-to-standard peak ratio of the acceptor, V_A is the volume of the acceptor (cm^3), R_D is the analyte-to-standard peak of the donor, and V_D is

the volume of the donor.

Transmittance percentage (%T) was then calculated for each sample:

$$\%T = (R_A/E_R) \times 100$$

The %T values were converted into time-independent P_e values:

$$P_e = [(V_A \times V_D)/(V_0 \times A \times t)] \times \ln(1-(\%T/100))$$

Where V_0 is the total volume (cm^3), A is accessible filter area of the membrane (0.24 cm^2), and t is the incubation time (s). Average %T and P_e values were calculated for each compound from at least three data points excluding extreme outlying permeability values. Standard deviations were calculated for the average values. Because percent recovery is accounted for in the E_R, we can assume no compound loss in the calculation and it holds true that apparent permeability (P_a) and effective permeability (P_e) values are equivalent.[13]

To calculate membrane/plate retention of each compound:

$$\%R = ([(R_A*V_A)+(R_D*V_D)]/(V_0*R_{D0}))*100)$$

Where %R is the percent recovery and R_{D0} is the initial analyte-to-standard ratio in the donor well.

***In Vitro* Permeability.** Cell permeability was determined using MDCK-LE cells (Pfizer, Inc., Groton, CT). MDCK-LE cells were generated in house as a subclone of Madin-Darby Canine Kidney wild-type (MDCK-WT) cells that displayed low expression of endogenous P-glycoprotein (approximately 1-2% of MDCK-WT cells, based on mRNA level). Cells were cultured in minimal essential medium □ with supplements and passaged when 70-80% confluent. Cell monolayer flux studies were conducted five days after seeding in 24-well transwell inserts (MDCK-LE in 1.0 □m pore size (Becton Dickinson, Cowley, UK)) at 4.2 x 10^4 cells/cm^2. In the MDCK-LE assay, donor and acceptor solutions

were prepared from HBSS containing HEPES at 20 mM, pH 7.4. Stock solutions of test compounds were prepared at 10 mM in DMSO and used to prepare donor solutions of 2 mM compound in 0.5% (v/v) DMSO. Apparent permeability (P_{app}) was determined in apical to basolateral (AB) direction in triplicate by incubating with compound for 2 h at 37 °C. Samples of the medium were analyzed using the LC-MS/MS method above. P_{app} values were calculated according to the equation $P_{app} = (Q/t) \times 1/C_o \times 1/A)$, where Q is the sampled concentration in the acceptor compartment, t is the incubation time, C_o is the initial concentration in the donor compartment, and A is the area of the filter of the trans-well plate.

For compound **6**, the initial MDCK-LE flux measured was 2.0×10^{-6} cm/s, which was significantly lower than the expected permeability based on its high PAMPA permeability. We re-assayed **1**, **4**, **5**, **6**, **12**, **13**, **14** in MDCK-LE cells using plates designed to minimize nonspecific binding, with 0.4% BSA and protease inhibitor, and low-binding tips, and found the permeability to be similar except for **6**, which showed a greater than 2-fold improvement in permeability. Compound **5**, which had low permeability in the MDCK-LE system (1.4×10^{-6} cm/s), had virtually identical permeability when the assay was re-run using low-binding plates (1.3×10^{-6} cm/s).

Rat Pharmacokinetic Studies. Rat studies were done at BioDuro, Pharmaceutical Product Development Inc. (Beijing, PRC); animal care and *in vivo* procedures were conducted according to guidelines from the BioDuro Institutional Animal Care and Use Committee. Jugular vein-cannulated male Wistar-Han rats (221-278 g), obtained from Vital River (Beijing, China) were used for these studies. All animals were housed individually. All orally dosed animals were fasted overnight before dosing and fed after collection of the 4 h blood samples, with access to food and water *ad libitium*. For intravenously dosed animals access to food and water was provided *ad libitium*. Compound **4** was administered intravenously (i.v.) via the tail vein of rats (n=3) over 30 s at 1.0 mg/kg, respectively, and serial blood samples were collected before dosing and

at 0.033, 0.083, 0.25, 0.5, 1.0, 2.0, 4.0, 7.0 and 24 h after dosing. For the i.v. study, **4** was administered as a solution in 10% propylene glycol:5% Tween 80:85% 20 mM sodium phosphate buffer (pH 7.4). For oral (p.o.) studies, male Wistar-Han rats (*n*=2) were administered compound **4** at 5 mg/kg as a suspension in 25% PEG400:75% water. Blood samples were taken before p.o. administration, and then serial samples were collected at 0.083, 0.25, 0.5, 1.0, 2.0, 4.0, 7.0 and 24 h after dosing. Blood samples from the pharmacokinetic studies were centrifuged at 3000 g for 10 min at 4 °C to generate plasma. All plasma samples were kept frozen until analysis. Aliquots of plasma (50 μL)) were transferred to 96-well plates, and acetonitrile:methanol (1:1) (200 μL) containing terfenadine as an internal standard (5 ng/mL) was added to each well. Samples were vortexed for 1 minute, followed by centrifugation for 15 minutes at ~2000 x *g*. Supernatants were removed and diluted in 2 volumes of water containing 0.1% formic acid. The samples were analyzed by liquid chromatography tandem mass spectrometry (LC-MS/MS), and concentrations of **4** in plasma were determined by interpolation from a standard curve.

LC-MS/MS Methodology. Plasma samples from the pharmacokinetic studies were prepared as described above, and 2 □L were injected into the LC-MS/MS for analysis. The HPLC system consisted of two Shimadzu LC-20AD pumps (Columbia, MD) and a CTC PAL autosampler (Leap Technologies, Switzerland). The column used was Kinetix C18 (30 x 3.0 mm, 2.6 □) (Phenomenex, Torrance, CA). Mobile phase A consisted of 5 mM ammonium acetate and 0.05% formic acid in water, and mobile phase B consisted of methanol with 0.1% formic acid. The flow rate was 0.7 mL/min. The initial mobile phase composition was 15% B and remained at 15% B for 0.4 min to equilibrate the column. The composition was ramped to 95% B over 2.0 min and held at 95% B for an additional 0.8 min. The mobile phase was then returned to initial conditions in 0.1 min. The total analysis time was 3.5 min.. The HPLC system was interfaced to a Sciex API 4000 mass spectrometer (Applied Biosystems, Foster City, CA), and was

equipped with a TurboIonspray ionization source operating in positive ion mode. Ultrahigh purity nitrogen gas was used as the nebulizing and turbo gas. The temperature of the turbo gas was set at 500 °C. The ion spray voltage was set at 4500 v. Multiple reaction monitoring (MRM) was utilized to monitor **4** (m/z 793.6 →100.2) and the internal standard, terfenadine (472.4 → 436.4).

Pharmacokinetic Data Analysis. Plasma concentration-time profiles were analyzed using non-compartmental method in Watson LIMS v7.4 (Thermo Fisher Scientific, Waltham, MA). Plasma clearance (CL_p) was calculated as the i.v. dose divided by the area under the plasma concentration-time curve from zero to infinity ($AUC_{0-\infty}$). $AUC_{0-Tlast}$ was calculated by the linear trapezoidal rule. The terminal slope (k_{el}) of the ln(concentration) versus time plot was calculated by linear least-squares regression and the $t_{1/2}$ was calculated as 0.693 divided by the absolute value of the slope. $AUC_{0-\infty}$ is the sum of $AUC_{0-Tlast}$ and C_{last}/k_{el}, where C_{last} is the concentration in the latest measurable time point. The steady state volume of distribution (V_{dss}) was determined using non-compartmental analysis as follows: V_{dss} = (i.v. dose x AUMC)/$(AUC)^2$, where AUMC is the total area under the first moment of the drug concentration-time curve from time zero to infinity. The maximum plasma concentration (C_{max}) observed after p.o. dosing and the time at which it was observed (T_{max}) were determined directly from the individual plasma time profiles. The relative bioavailability (F) of the p.o. dose was calculated by using the following equation: $F = AUC_{0-\infty}^{p.o.} / AUC_{0-\infty}^{i.v.} \times Dose^{i.v.} / Dose^{p.o.}$.

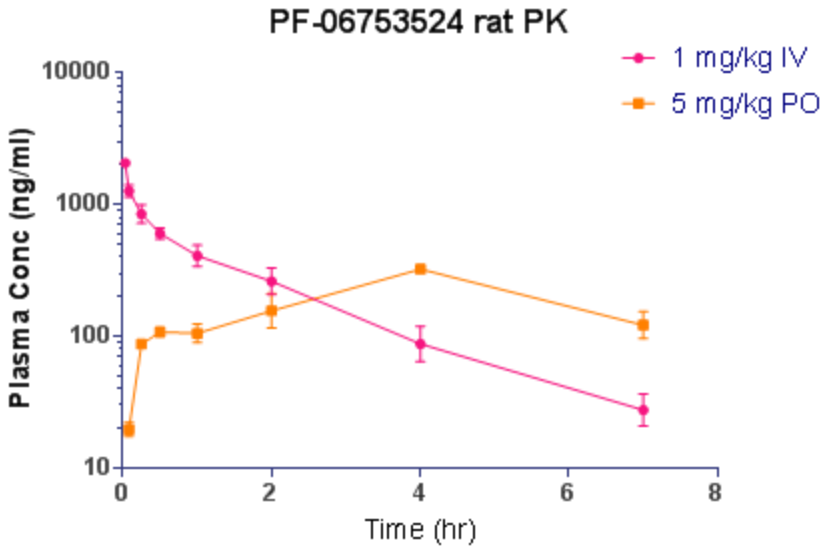

Figure S1. Plasma concentration-time profiles of **4** following i.v. (1 mg/kg, n=3) and p.o. (5 mg/kg, n=2) administration to male Wistar-Han rats. The error bars represent the range of values at each time point.

IV. NMR SPECTROSCOPY AND STRUCTURE DETERMINATION

All NMR spectra were recorded at 298 K on a 600 MHz Varian spectrometer equipped with a 5 mm inverse detection probe. Spectra were referenced to residual solvent proton and carbon signals (δH 7.26, δC 77.16 for $CDCl_3$), and were processed and analyzed using MestReNova (Mestrelab) on a Macbook Pro laptop computer. CP-PKs **1, 4, 5, 6** and **14** were fully assigned. Assignment of resonances for each amino acid residue was accomplished by employing ^{1}H, ^{13}C, gCOSY, HSQC, HMBC, and TOCSY experiments. Each residue was assigned using ^{1}H and TOCSY chemical shifts and confirmed through COSY and HSQC cross-peaks. Assembly of these residues to assign the final cyclic structure was accomplished by considering long-range HMBC correlations from α-protons and NMe-protons of NMe-amino acids to adjacent carbonyl carbons; NH protons, α-protons, and γ-protons of γ-amino acids to adjacent carbonyl

carbons; and α-proton, γ-proton, and NH proton NOESY correlations between adjacent amino acid residues. NOESY experiments were performed with a mixing time of 600 ms, d1 of 1.5 s, nt of 8, ni of 200, and ss of 32. NOE build-up curves were constructed for **4** and **14** to verify that the NOEs were in the linear range. NOESY correlations were documented for all available signals, and converted to interproton distances. This was accomplished by first normalizing the 2D-NOESY crosspeak volume integrals to the average volumes of their respective diagonal cross-peaks in both dimensions. Then the diagonal-normalized volumes were converted to interproton distances using the following formula:

$$\mathbf{R_x = R_{ref}\,(I_{ref}/I_x)^{1/6}}$$

Where R_x is the variable interproton distance, I_x is the variable integration, R_{ref} is a reference interproton distance, and I_{ref} is a reference integration. The geminal α-protons of the statine monomer were used as a distance reference of 1.73 Å.

V. COMPUTATIONAL MODELING

For the 14 members of the virtual library selected for synthesis, the potential energy landscape in both implicit water and chloroform was exhaustively sampled with the macrocycle sampling module in PLOP[15]. Each CP-PK was built from its sequence six times, each time starting from a different residue. For each of these starting sequences, 36 independent PLOP runs were performed, where each run corresponded to a different selection of the midpoint atom along the macrocycle backbone. During a single PLOP simulation, the CP-PK was cleaved at the midpoint, yielding two branches that were independently sampled along all backbone torsions. The resolution for dihedral sampling scaled adaptively from 120° to 5°, as required for satisfying closure conditions. Standard phi and psi torsions were sampled based on allowed Ramachandran populations. Branch

conformations that met closure conditions at the midpoint were retained. These structures were clustered by k-means according to backbone torsion; the lowest energy representative was retained for each cluster. Side chains were sampled along all freely rotatable bonds using a 10° resolution. Finally, the retained conformations were subjected to a Truncated Newton minimization. A minimum output of 50 unique conformations was required from each run. Conformations within 5 kcal/mol and 10 kcal/mol of the lowest energy structure in chloroform were retained for comparison to NMR data.

Solution Structures

DISCON 3.0a[16], an implementation of the NAMFIS[17] methodology using the Janocchio software platform[18], was used to fit the low-energy conformations (5 or 10 kcal/mol from the global minima) generated by PLOP to the NMR data. 100 runs were performed for cluster levels between 1 and 20 to identify the relative contribution of each conformation to the NMR data (**Table S4**). Clusters with the lowest total error were selected as the representative population ensemble for each compound. Except for **14**, the resulting conformer clusters were consistent with the *cis*/*trans* rotamers about all amides observed by NOE crosspeaks and proline $^{13}C\beta$-$^{13}C\gamma$ shift differences[14] (**Table S3**). Filtering of conformations generated by PLOP for compounds **1**, **4**, **5**, **6**, and **14** using a 5-kcal/mol energy cut-off from the global minimum yielded initial sets of 11, 32, 15, 18, and 10 structures, respectively. Hierarchical clustering in DISCON was used to select representative conformations with a maximal cluster number of 15. Clustering analyses demonstrated that binning conformations into more than 15 clusters did not improve discrimination of additional conformers with high reproduction of the NMR variables. In order to satisfy the *cis*-amide restraint about the MeLeu3-MeLeu4 amide bond of **14**, we employed a cutoff of 10-kcal/mol, resulting in 244 structures and up to 50 clusters. The solution total error for the ensemble of **4** had lower error than either of its individual conformers.

Table S2. DISCON Best-fit Conformer Output

Conformer	RMS error (Å)	Population of Conformer
1	1.3	100%
4a	1.1	48%
4b	1.1	52%
5	0.9	100%
6	2.6	100%
14	1.1	100%

Table S3. NMR-derived Amide Conformational Restraints

	Amide Isomers			
	L3-L4$_{(NOE)}$		L6-P1$_{(Pro\ ^{13}C\beta,\ ^{13}C\gamma)}$	
cpd				
1	1.61 Å	*cis*	27.4, 24.5	*trans*
4	-	*trans*	25.0, 26.9	*trans*
5	-	*trans*	24.6, 27.5	*trans*
6	1.49 Å	*cis*	28.9, 24.8	*trans*
14	1.68 Å	*cis*	25.3, 24.9	*trans*

	^{1}H NMR $J_{(HN\text{-}C\alpha H)}$		DISCON Conformer $J_{(HN\text{-}C\alpha H)}$	
cpd	NH2	NH5	NH2	NH5
1	9.4	8.9	10.9	5.6
4a	9.7	8.2	10.9	10.9
4b	“ “	“ “	5.3	10.9
5	9.4	8.8	10.9	4.1
6	7.5	9.8	5.3	10.4
14	10	9.8	5.9	10.8

NMR-derived conformational restraints. *J*-coupling was observed in ^{1}H NMR and *cis*/*trans* amides were observed via NOESY and proline ^{13}Cβ-^{13}Cγ shifts[14].

Table S4. Comparison of NOESY Crosspeak-generated input and Computational Model output Interproton Distances

Macrocycle 1				
Reference	pair	NOE-Calculated Distance (Å)	**1** Distance (Å)	Difference (Å)
Sta5NH	L4b'	3.09	3.72	0.63
	L4Nme	3.13	2.7	-0.43
	L4a	2.16	3.35	1.19
	L3a	2.63	4.28	1.65
Sta2NH	L6b'	2.68	5.33	2.65
	P1y'	3.45	3.56	0.11
	P1d'	3.1	3.14	0.04
L3a	L4a	1.61	2.03	0.42
L4a	Sta2y	3.54	4.81	1.27
L6a	P1d''	2.03	2.34	0.31
	P1d'	2.02	2.34	0.32
L6Nme	L6b	2.47	2.33	-0.14
	Sta5a'	2.28	4.08	1.8
L3Nme	L3b'	2.69	2.52	-0.17
	Sta2a'	2.2	2.87	0.67
L4Nme	L4b'	1.1	2.39	1.29
	Sta2a'	4.7	7.16	2.46
	Sta5a'	3.59	7.09	3.5
P1b'	P1b''	1.72	1.76	0.04

Macrocycle 4						
Reference	Pair	NOE Distance (Å)	**4a** Distance (Å)	Difference (Å)	**4b** Distance (Å)	Difference (Å)
Sta2NH	L6Nme	3.51	5.0	1.49	4.7	1.19
	P1d	3.61	3.3	-0.31	5.0	1.39
	P1a	2.41	3.4	0.99	2.3	-0.11
	L6a	4.66	3.4	-1.26	5.1	0.44
	P1b'	3.97	4.0	0.03	4.4	0.43
	Sta2a'	4.15	3.1	-1.05	2.4	-1.75
	P1y''	4.01	3.1	-0.91	5.0	0.99
Sta5NH	L6Nme	3.25	4.6	1.35	4.3	1.05
	L4a	2.17	2.7	0.53	2.7	0.53
L4a	Sta5a''	4.92	4.8	-0.12	5.0	0.08
L3a	L4Nme	2.1	2.4	0.3	2.4	0.3
	Sta2a''	4.21	4.7	0.49	4.6	0.39
	Sta2a'	4.64	4.8	0.16	5.3	0.66

	Sta2b	4.44	6.1	1.66	5.5	1.06
L6a	P1d'	2.14	2.0	-0.14	2.3	0.16
	P1d''	2.25	2.2	-0.05	2.5	0.25
	L6Nme	3	3.7	0.7	3.7	0.7
P1a	Sta2a''	4.96	4.1	-0.86	4.4	-0.56
	Sta2y	5.2	5.2	0	2.6	-2.6
L4Nme	L4b''	2.46	2.1	-0.36	2.2	-0.26
L6Nme	Sta5a'	2.51	2.1	-0.41	2.7	0.19
L3Nme	P1b'	3.47	7.4	3.93	8.1	4.63
	Sta2a'	2.45	2.4	-0.05	2.4	-0.05
Sta5a'	Sta5a''	1.71	1.7	-0.01	1.7	-0.01
Sta2a'	Sta2''	1.72	1.7	-0.02	1.7	-0.02

Macrocycle 5

Reference	Pair	NOE Distance (Å)	**5** Distance (Å)	Difference (Å)
Sta2NH	Pro1b	3.19	3.1	-0.09
	sta2a	2.54	2.7	0.16
	pro1a	2.09	3.5	1.41
Sta5NH	Sta5a	2.67	2.3	-0.37
	Leu4a	1.96	2.1	0.14
Leu3a	Sta2a	3.64	4.6	0.96
Leu6a	sta5a	2.52	4.4	1.88
	Pro1d	2.04	2.4	0.36
Pro1a	P1y	2.02	3.2	1.18
	P1y'	2.45	4.0	1.55
P1y	P1y'	1.73	1.8	0.07

Macrocycle 6

Reference	Pair	NOE Distance (Å)	**6** Distance (Å)	Difference (Å)
Sta5NH	Sta5b	2	3.6	1.6
	Sta5a	2.64	5.1	2.46
	sta5a'	2.39	5.0	2.61
	L6NMe	2.99	7.1	4.11
	L4NMe	3.3	2.9	-0.4
	Pro1d	3.3	7.3	4
	Sta2b	3.12	2.8	-0.32

	Leu4a	1.84	2.7	0.86
	Leu3a	2.58	3.4	0.82
Sta2NH	Sta2b	1.9	2.7	0.8
	sta5a	2.44	4.1	1.66
	sta2a	2.68	4.4	1.72
	sta2a'	2.34	4.3	1.96
	L6NMe	2.88	4.8	1.92
	Sta2y	2	2.9	0.9
Leu3a	Leu3b	2.42	2.4	-0.02
	Leu4NMe	3.14	4.6	1.46
	Leu3NMe	2.7	3.6	0.9
	Pro1d	2.67	9.4	6.73
	Leu4a	1.49	2.0	0.51
Leu6a	Leu6NMe	2.89	3.4	0.51
	Pro1d	1.97	3.2	1.23
	Pro1d'	1.87	2.5	0.63
Leu4a	L4NMe	2.54	4.1	1.56
Sta2b	Sta2d	2.08	2.5	0.42
	Sta2a	2.86	2.7	-0.16
	sta2a'	2.16	2.5	0.34
	sta2y	1.95	3.0	1.05
Pro1a	Pro1b	1.81	2.4	0.59
Pro1d	Pro1d	1.66	1.8	0.14
Sta5b	sta5d	2.02	3.2	1.18
	sta5a	2.16	2.4	0.24
sta5y	sta5d	2.14	2.5	0.36
	sta5a	2.61	3.4	0.79
sta2y	sta2a	3.13	2.9	-0.23
	sta2a'	2.51	2.4	-0.11
Leu3NMe	Leu3b	2.46	2.5	0.04
	Sta2a	2.45	2.3	-0.15
	Leu6Nme	2.68	10.4	7.72
Leu4Nme	Pro1b	2.61	10.1	7.49
	sta5a	3.79	7.1	3.31
Leu6Nme	Sta5a	3.46	3.0	-0.46
	sta5a'	2.4	2.3	-0.1
Sta2a	Sta2a'	1.96	1.7	-0.26
Sta5a	Sta5a'	1.61	1.7	0.09

Macrocycle 14				
Reference	pair	NOE Distance (Å)	**14** Distance (Å)	Difference (Å)
Vin2NH	L6Nme	2.96	5.1	2.14
	P1d'	3.53	4.0	0.47
	P1a	2.14	2.7	0.56
Sta5NH	L4Nme	3.88	3.5	-0.38
	L4a	2.12	2.6	0.48
	L3a	2.19	3.5	1.31
	L3Nme	5.21	4.7	-0.51
L6a	Sta5a"	4.62	5.3	0.68
	Sta5a'	4.5	4.8	0.3
	P1d"	1.91	2.4	0.49
	P1d'	2.43	2.9	0.47
L3a	L4Nme	4.72	4.5	-0.22
	L4a	1.68	2.1	0.42
Vin2b	Sta5a'	3.71	2.4	-1.31
	L6Nme	2.53	4.1	1.57
	L3Nme	2.6	5.1	2.5
Vin2y	P1b'	4.02	5.0	0.98
L3Nme	L3b'	2.55	2.2	-0.35
L6Nme	L6b'	3.11	4.2	1.09
	Sta5a'	2.71	2.7	-0.01
Sta5a"	Sta5a'	1.71	1.7	-0.01
P1b'	P1b"	1.73	1.8	0.07

VI. NMR SPECTRA

^{1}H Macrocycles

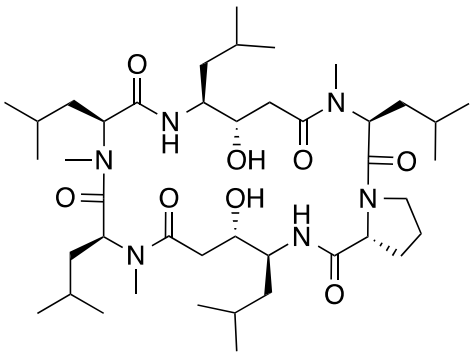

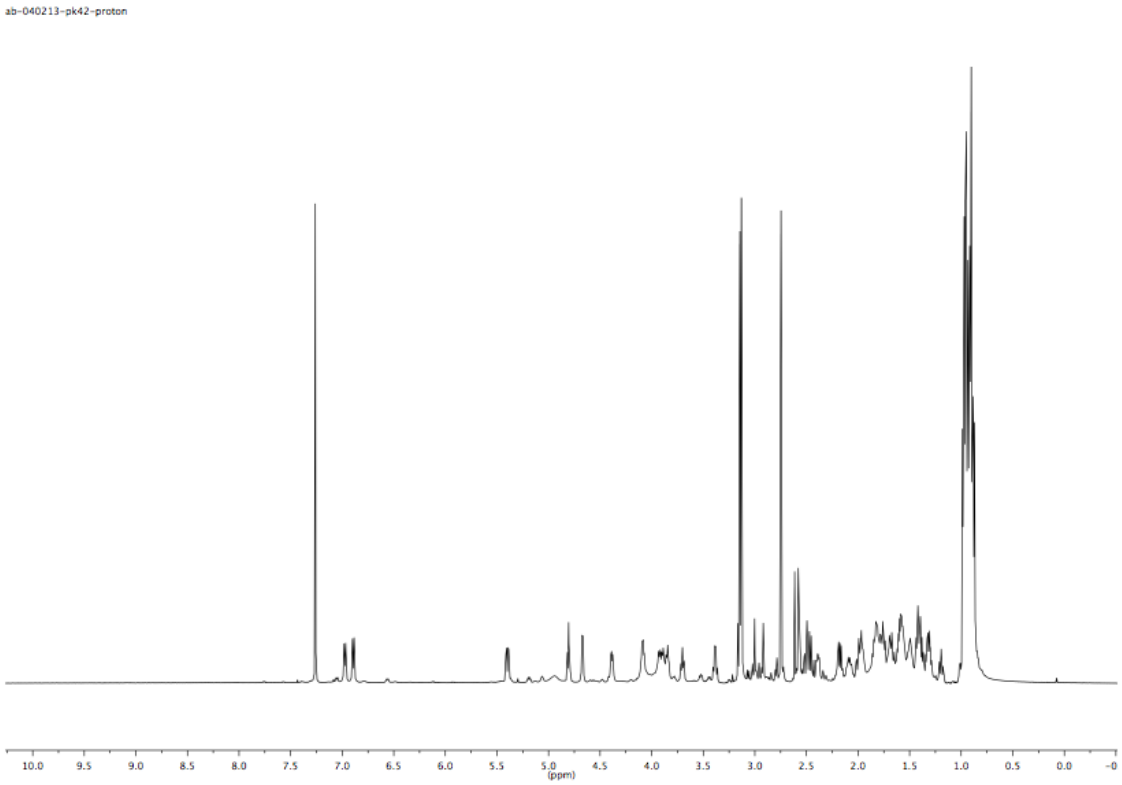

Figure S3. Macrocycle **1** ^{1}H in $CDCl_3$

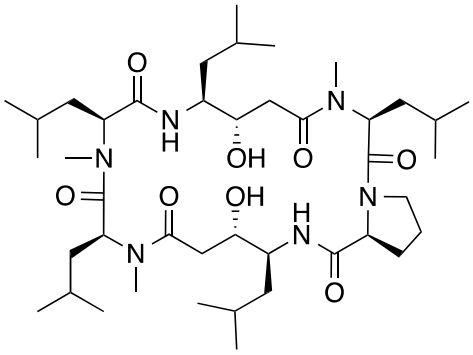

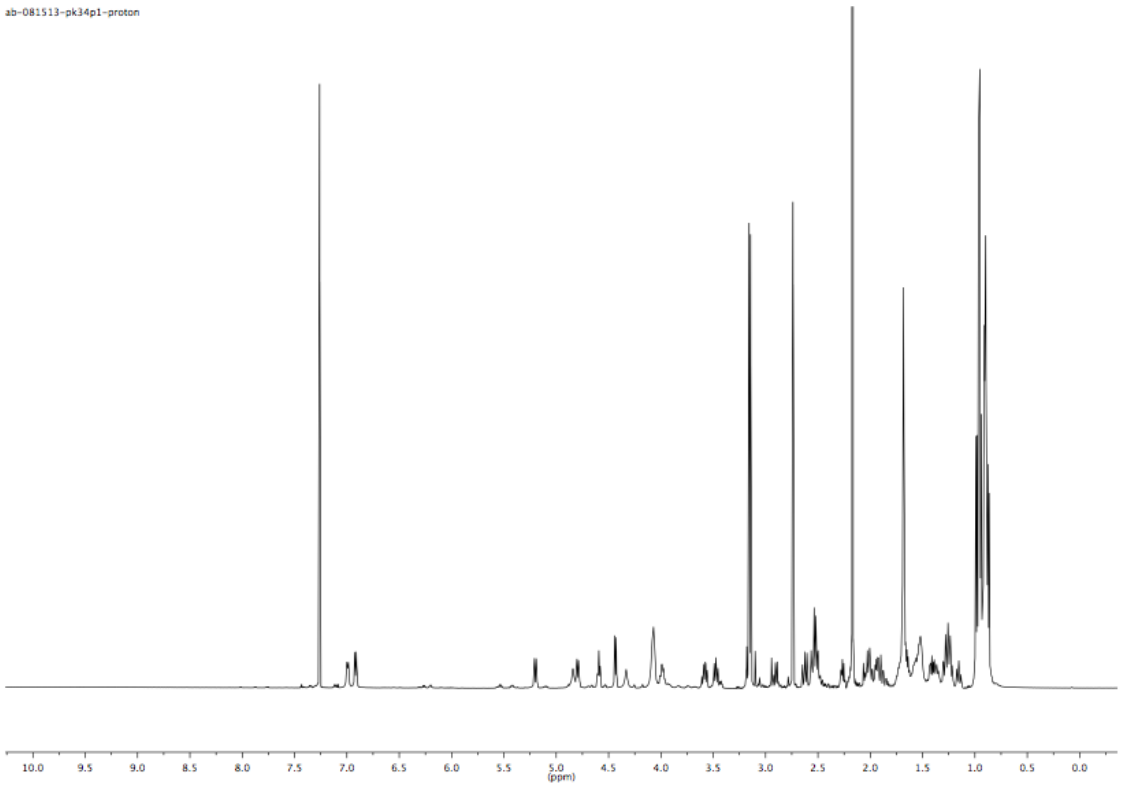

Figure S4. Macrocycle **2** ^{1}H in $CDCl_3$

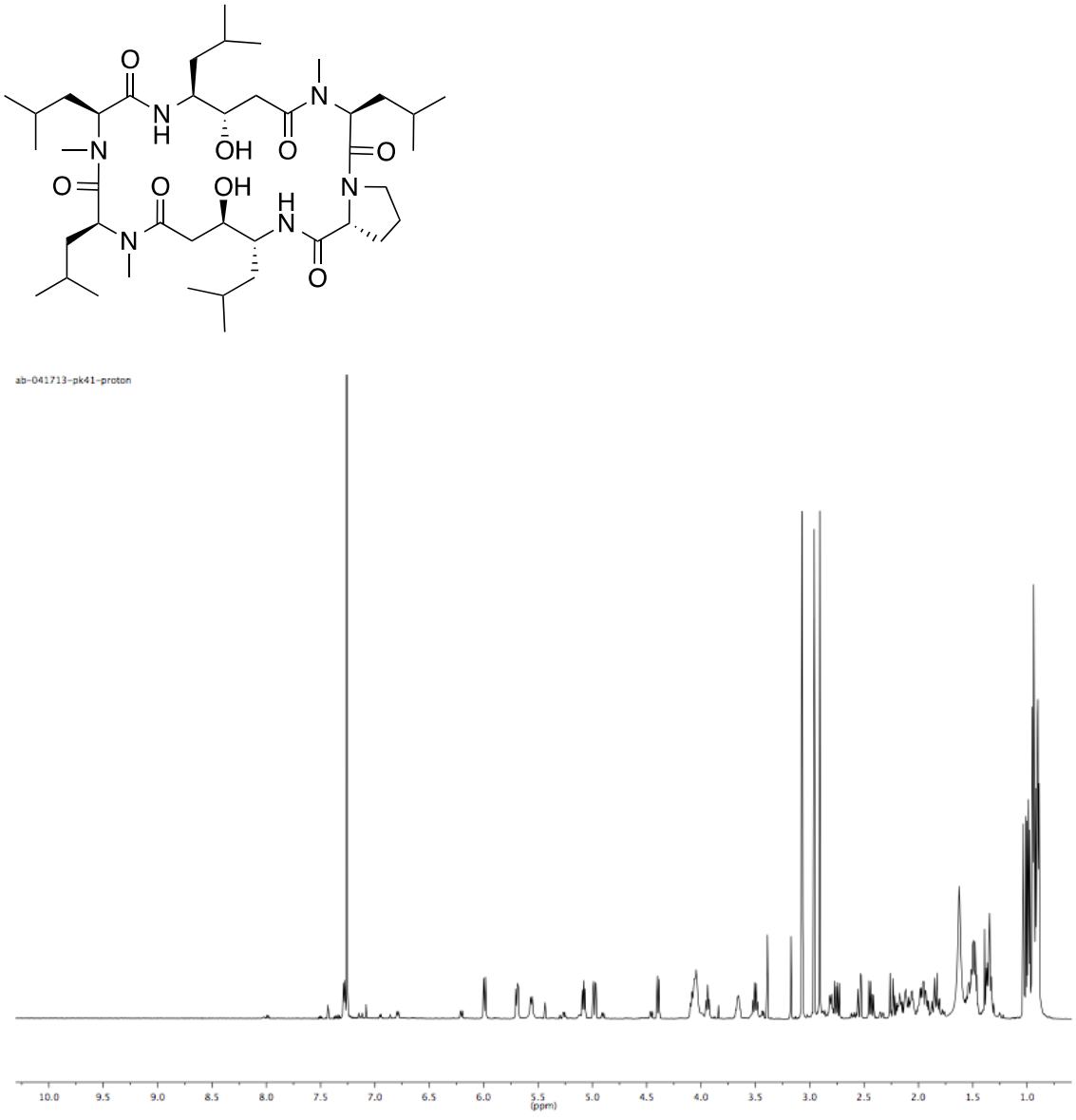

Figure S5. Macrocycle **3** ^{1}H in $CDCl_3$

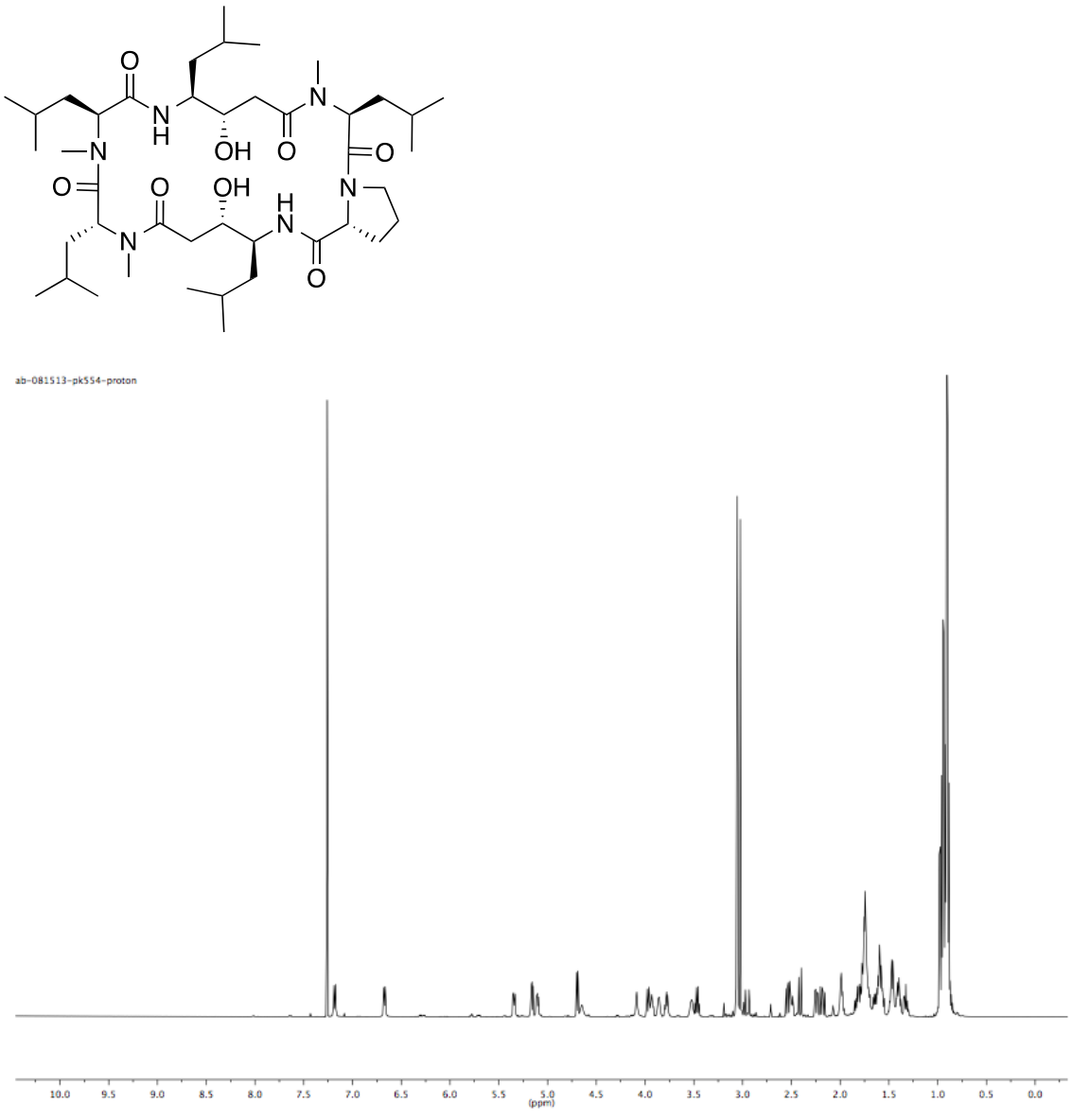

Figure S6. Macrocycle **4** ^{1}H in $CDCl_3$

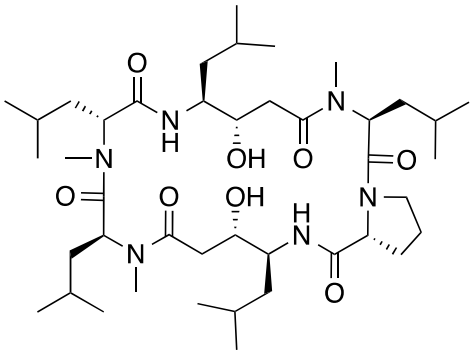

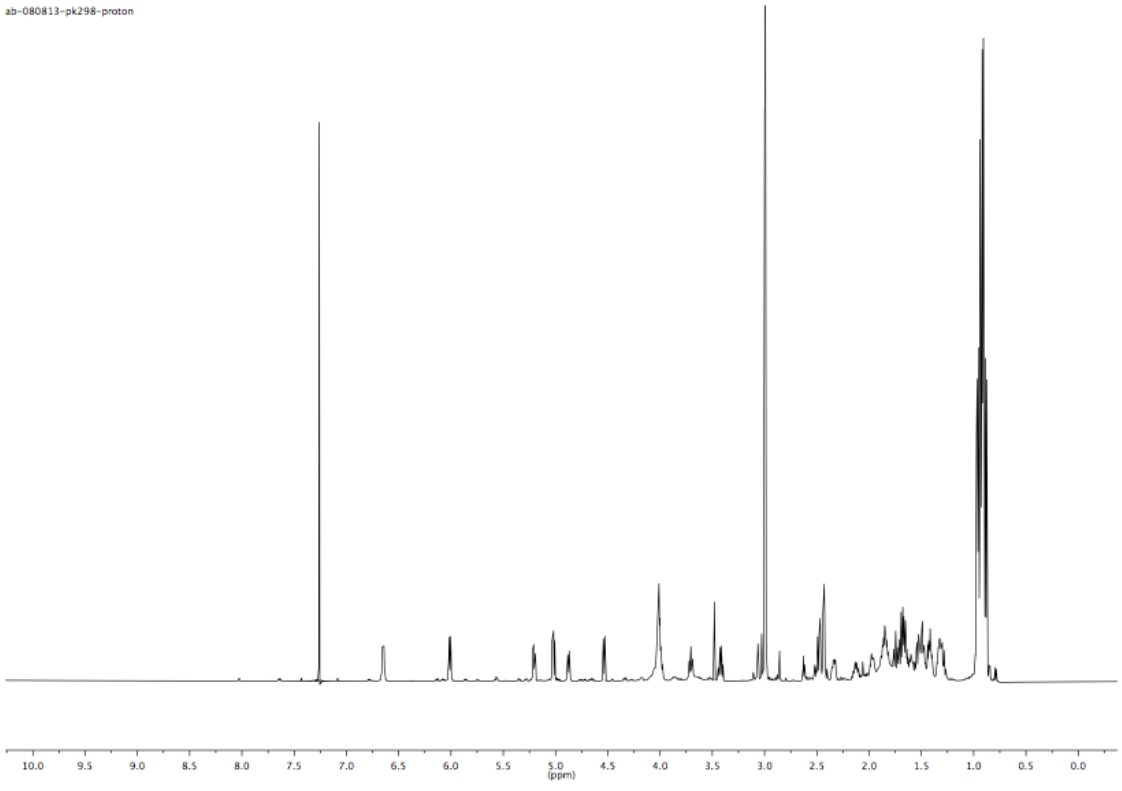

Figure S7. Macrocycle **5** ^{1}H in $CDCl_3$

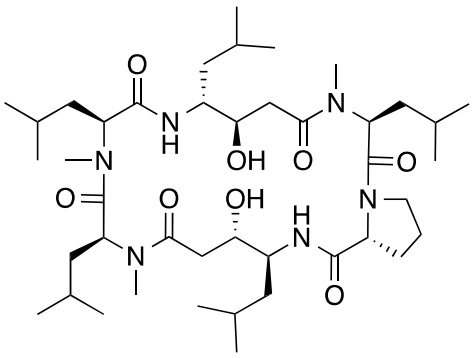

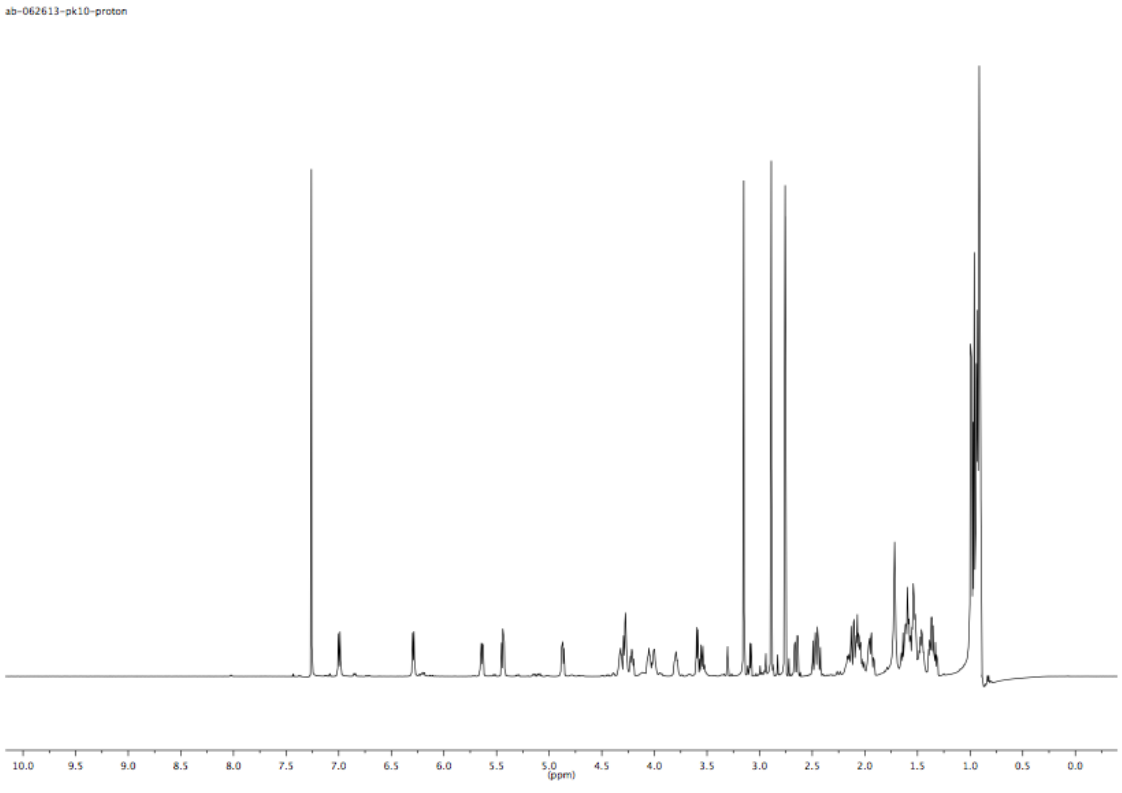

Figure S8. Macrocycle **6** ^{1}H in $CDCl_3$

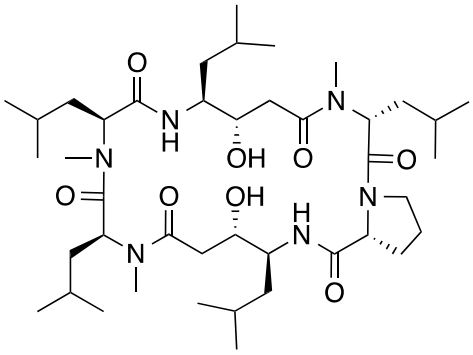

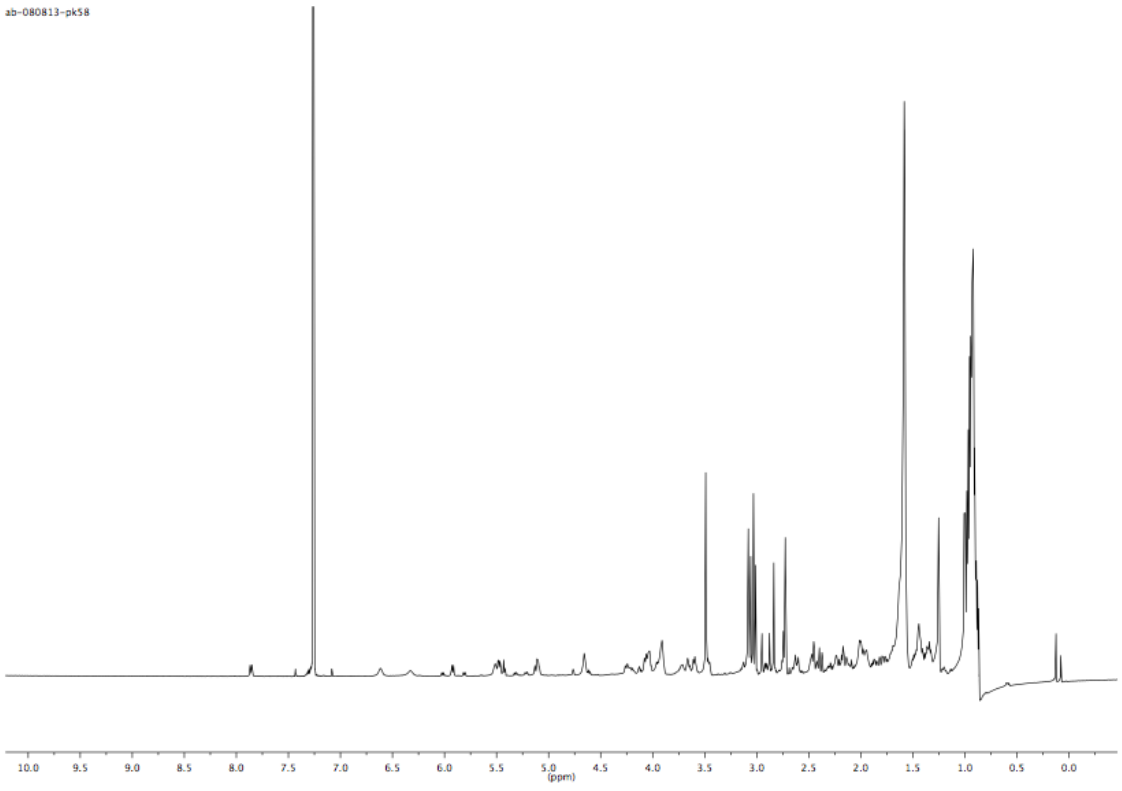

Figure S9. Macrocycle **7** ^{1}H in $CDCl_3$

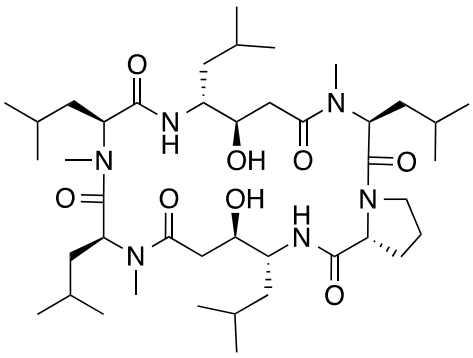

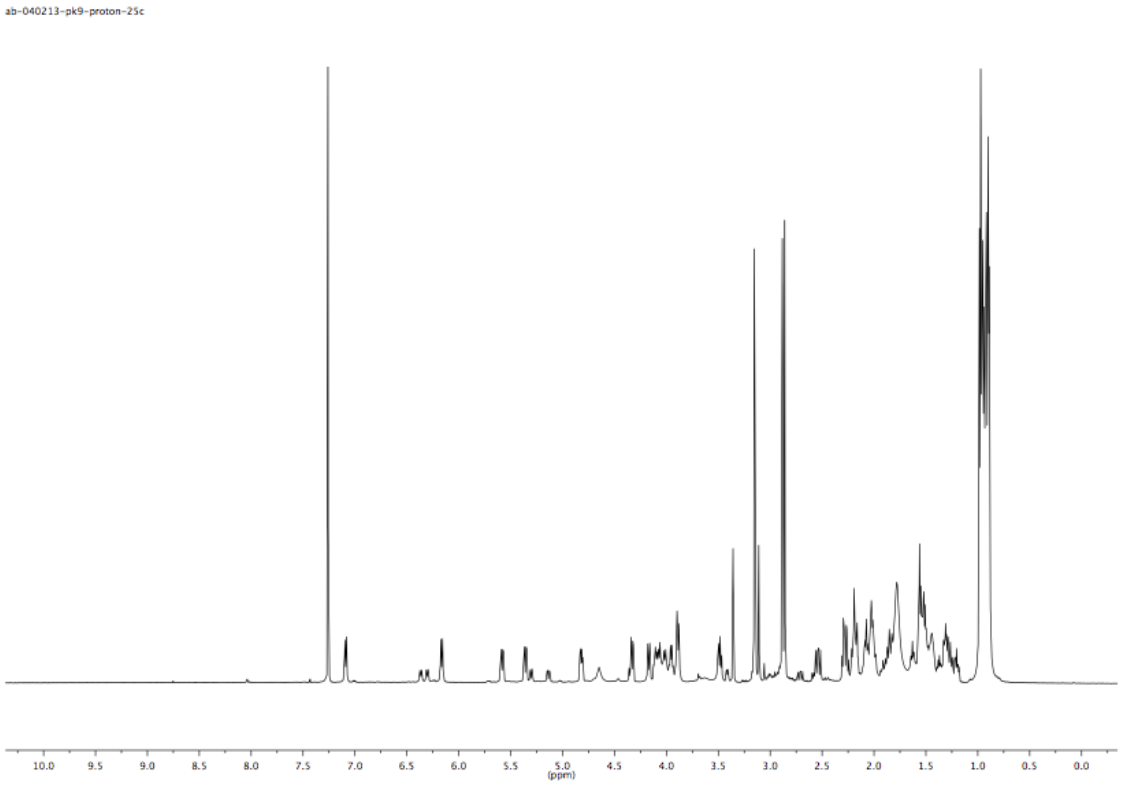

Figure S10. Macrocycle **8** ^{1}H in $CDCl_3$

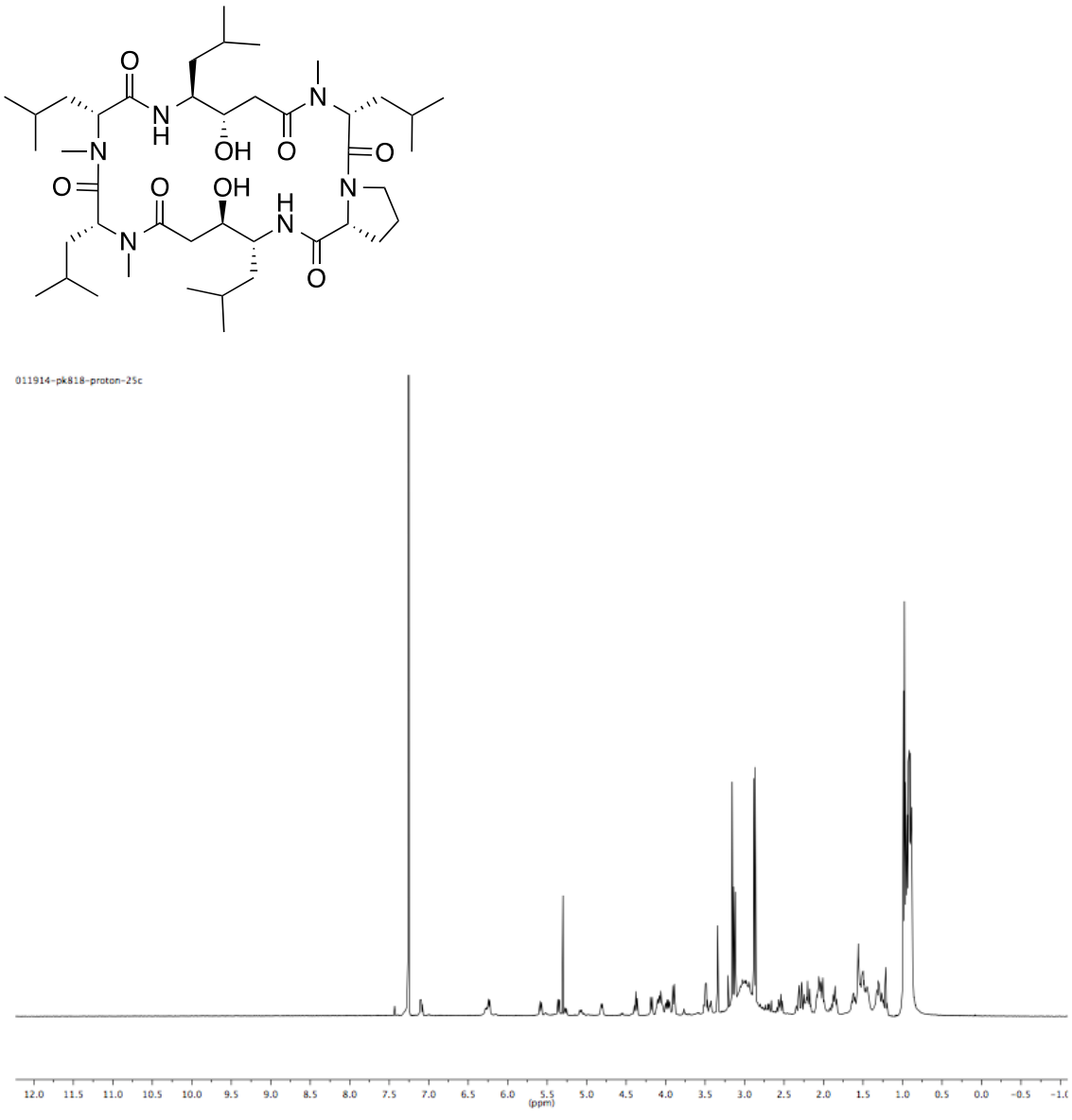

Figure S11. Macrocycle **9** ^{1}H in $CDCl_3$

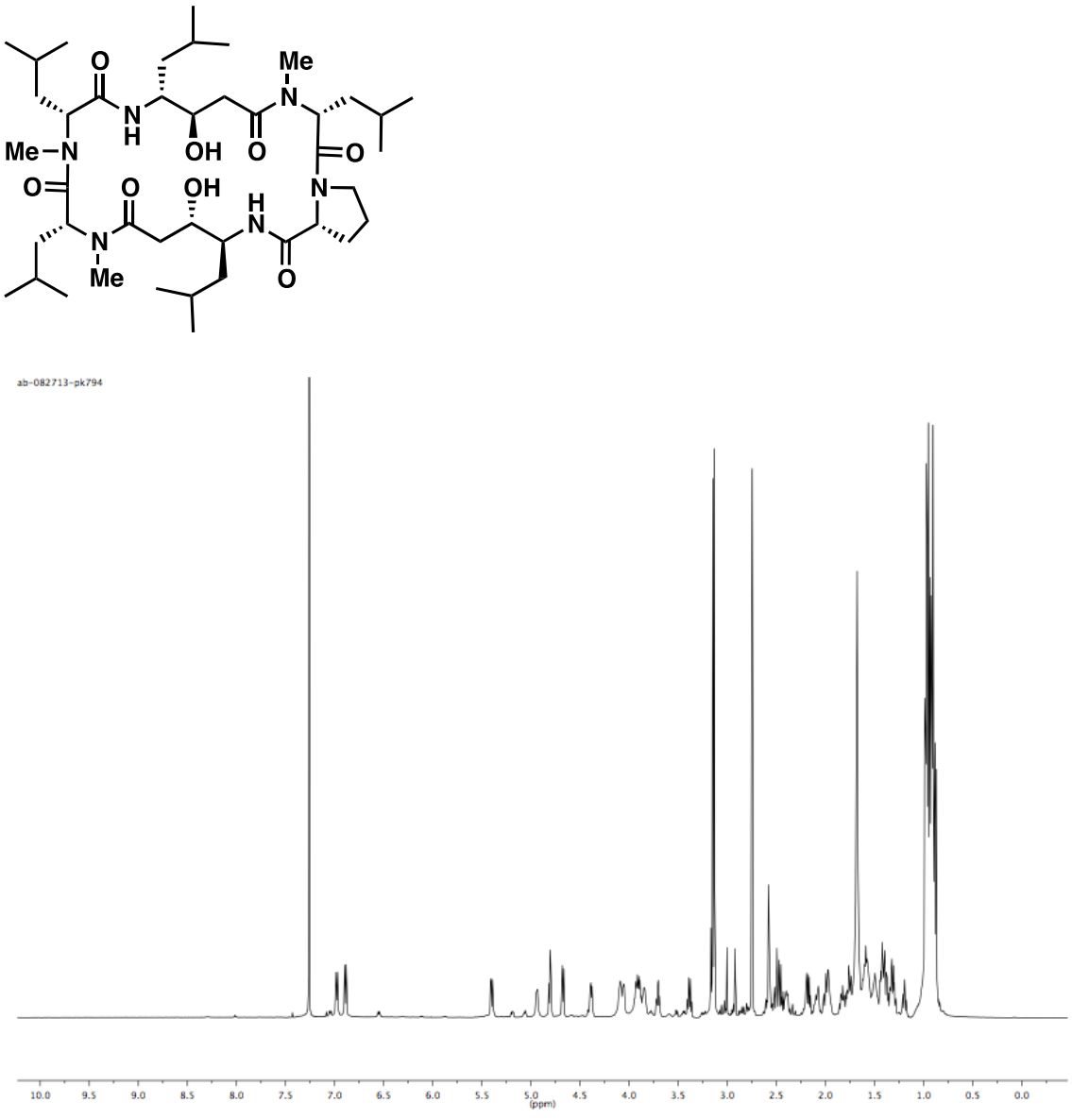

Figure S12. Macrocycle **10** ^{1}H in $CDCl_3$

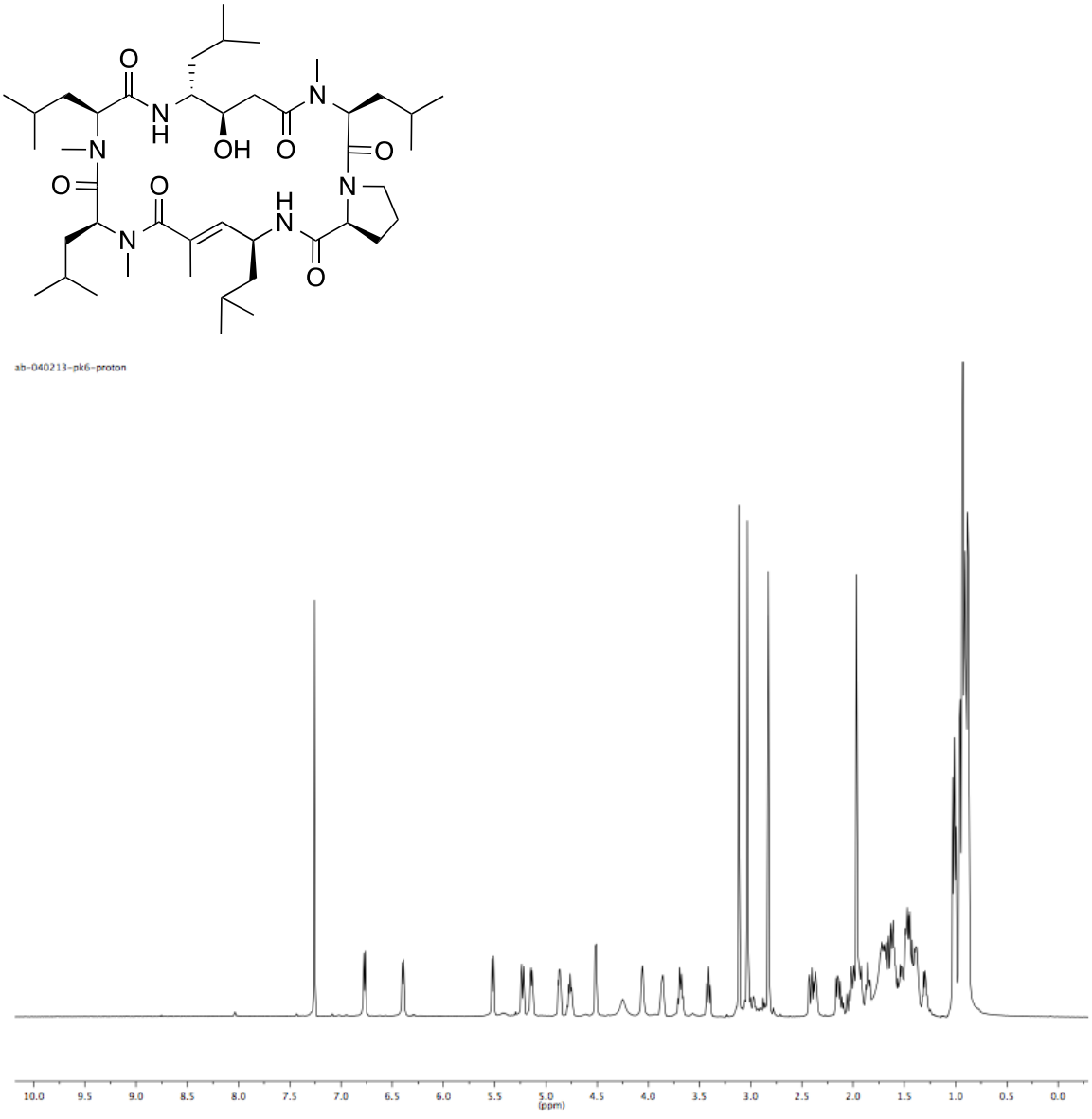

Figure S13. Macrocycle **11** ^{1}H in $CDCl_3$

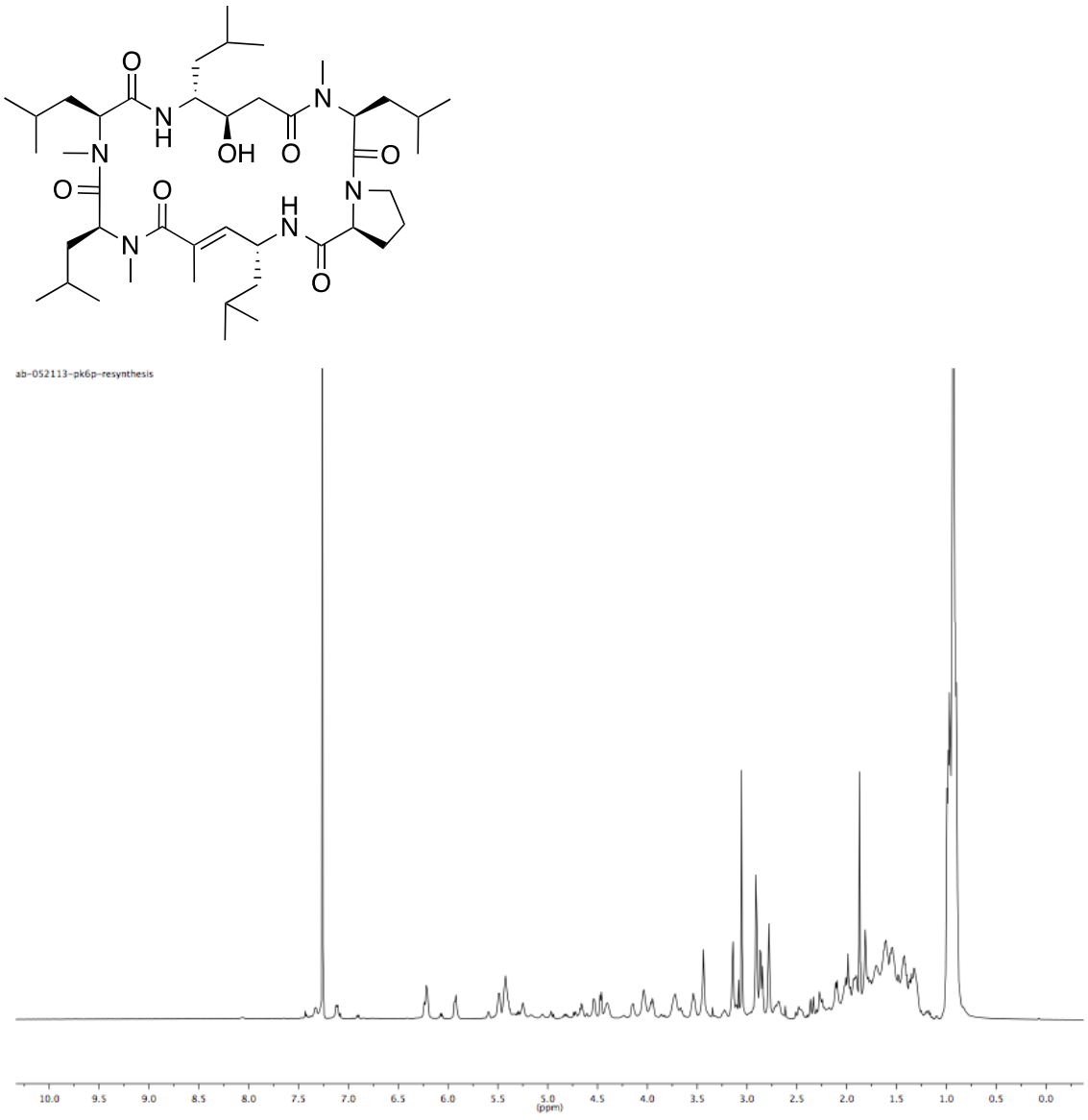

Figure S14. Macrocycle **12** ^{1}H in $CDCl_3$

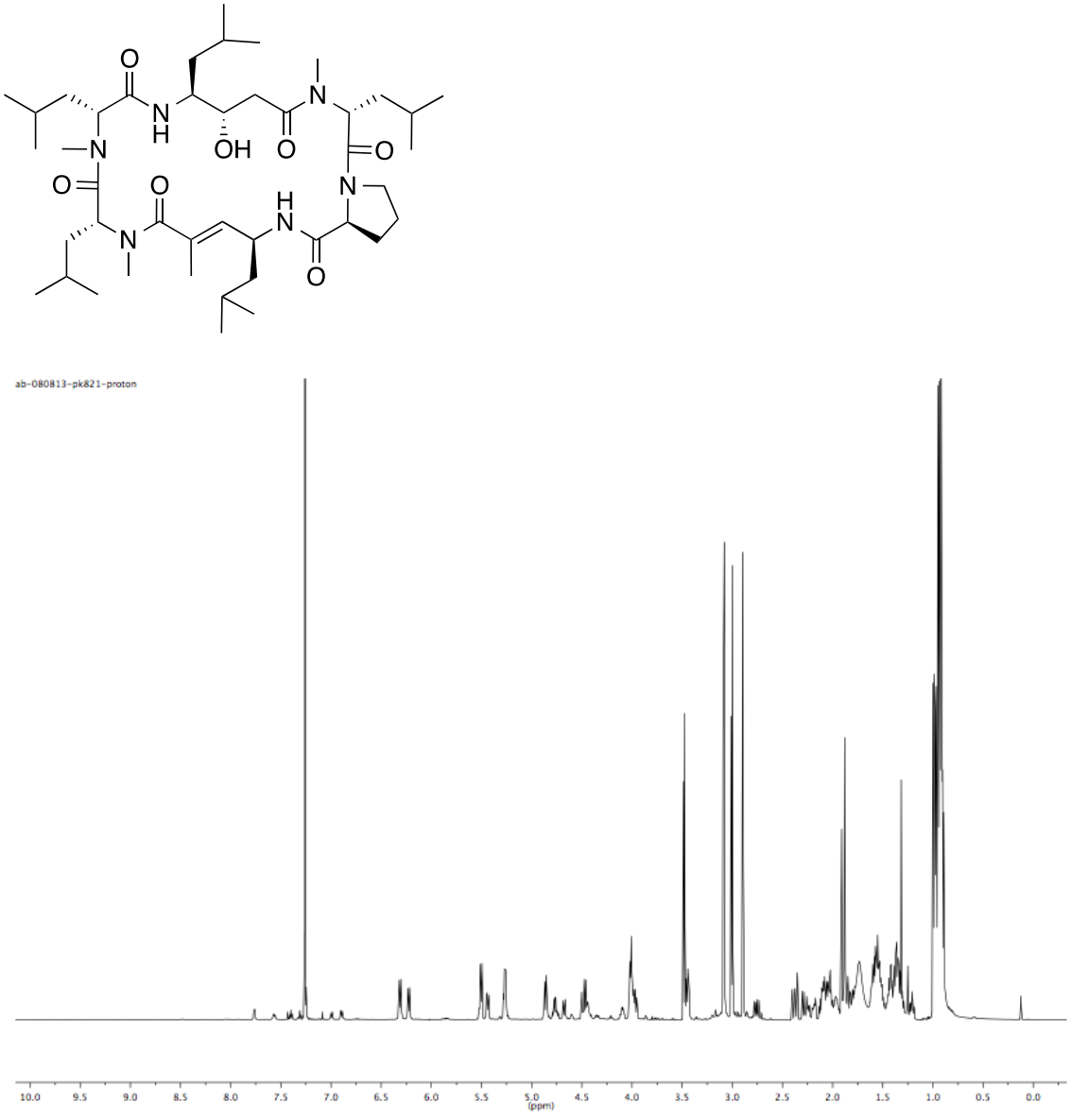

Figure S15. Macrocycle **13** ^{1}H in $CDCl_3$

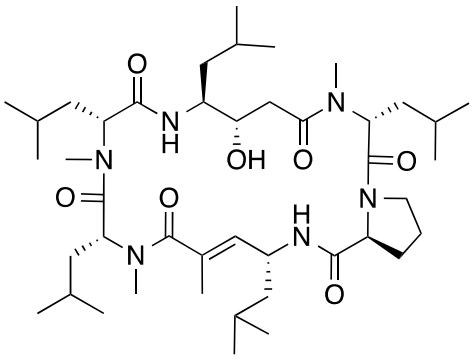

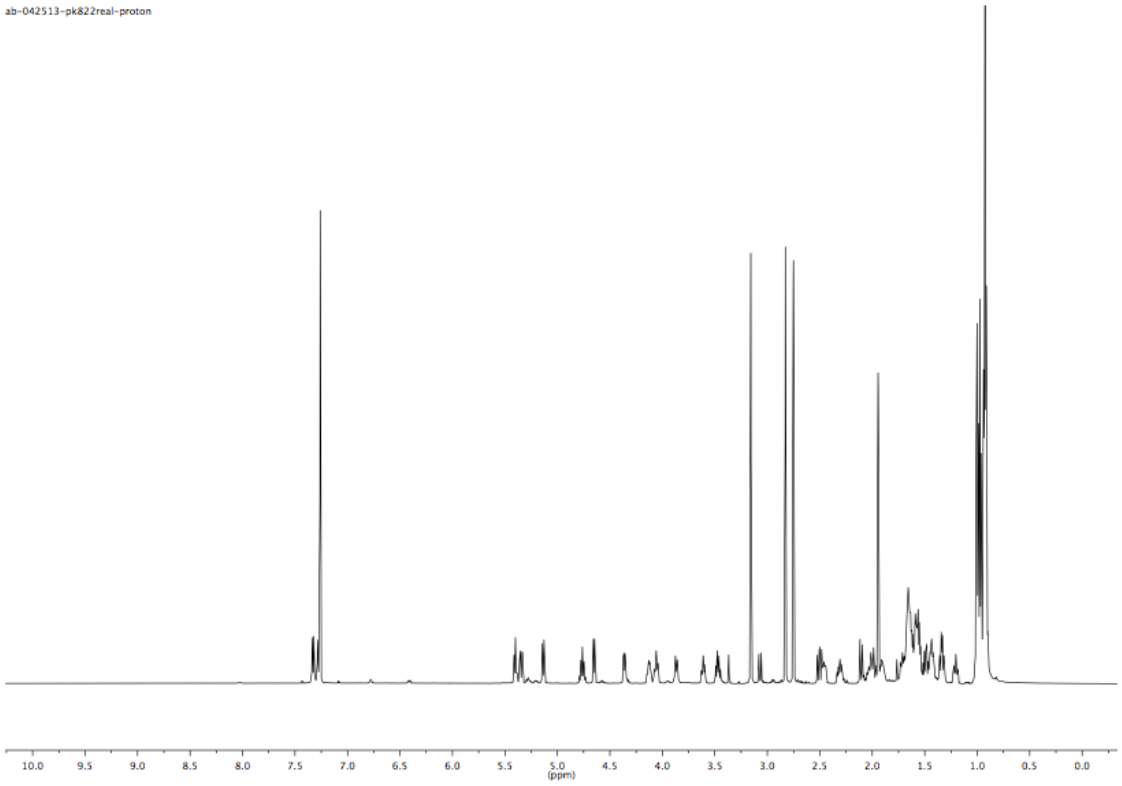

Figure S16. Macrocycle **14** ^{1}H in $CDCl_3$

2D Macrocycles

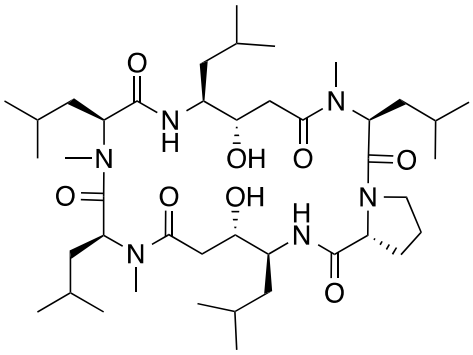

Figure S17. Macrocycle **1** COSY in $CDCl_3$

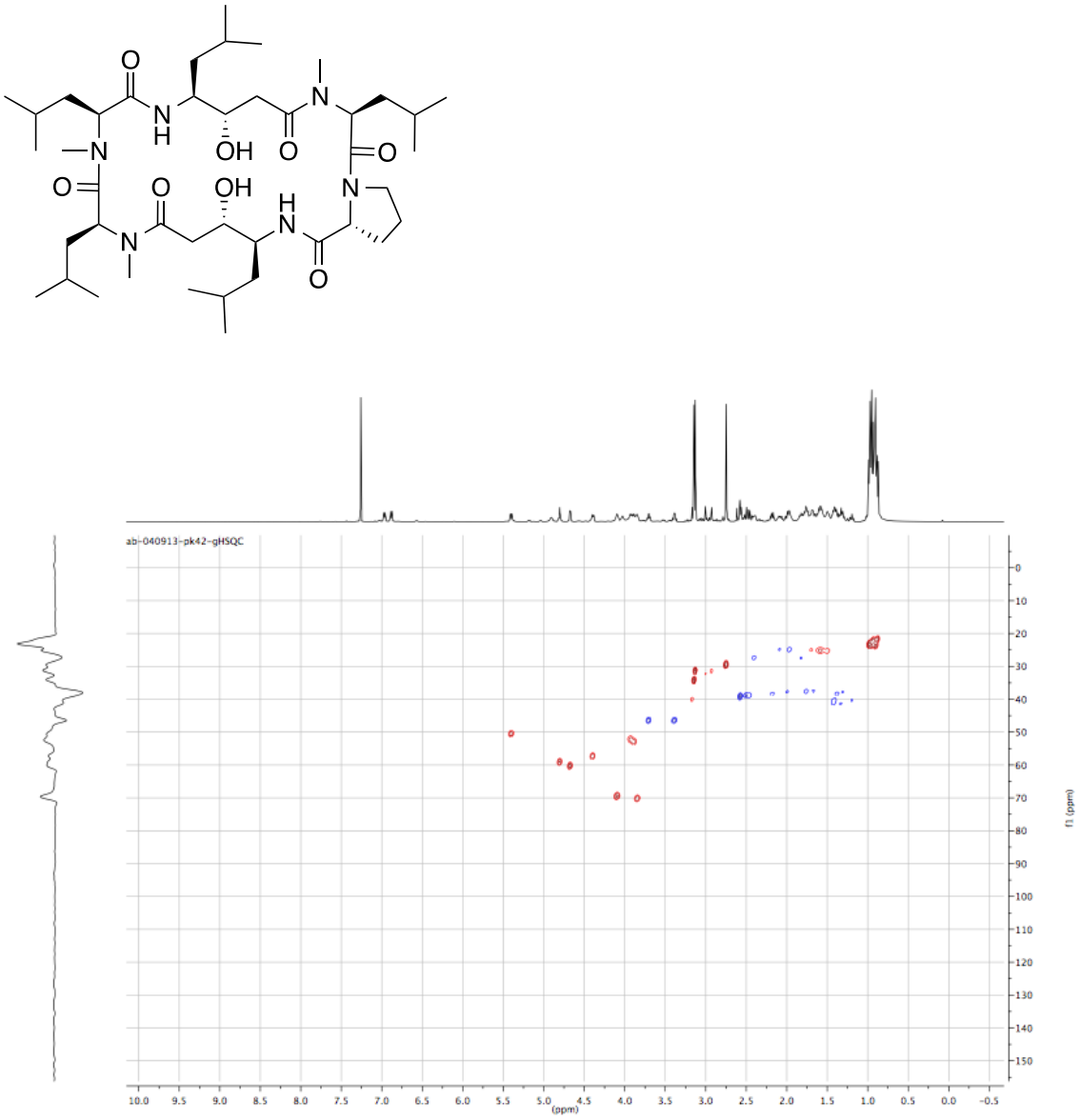

Figure S18. Macrocycle **1** HSQC in $CDCl_3$

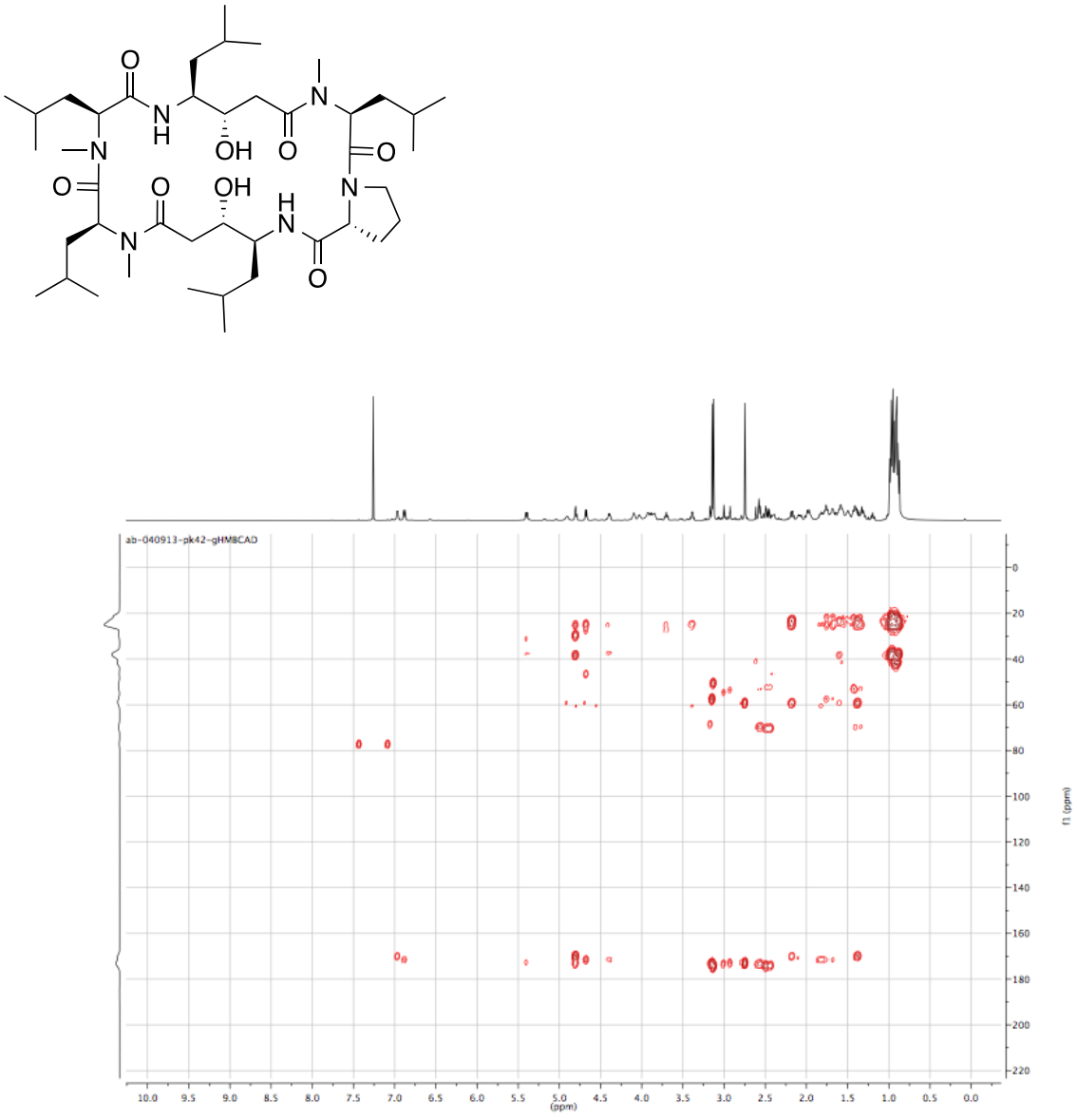

Figure S19. Macrocycle **1** HMBC in $CDCl_3$

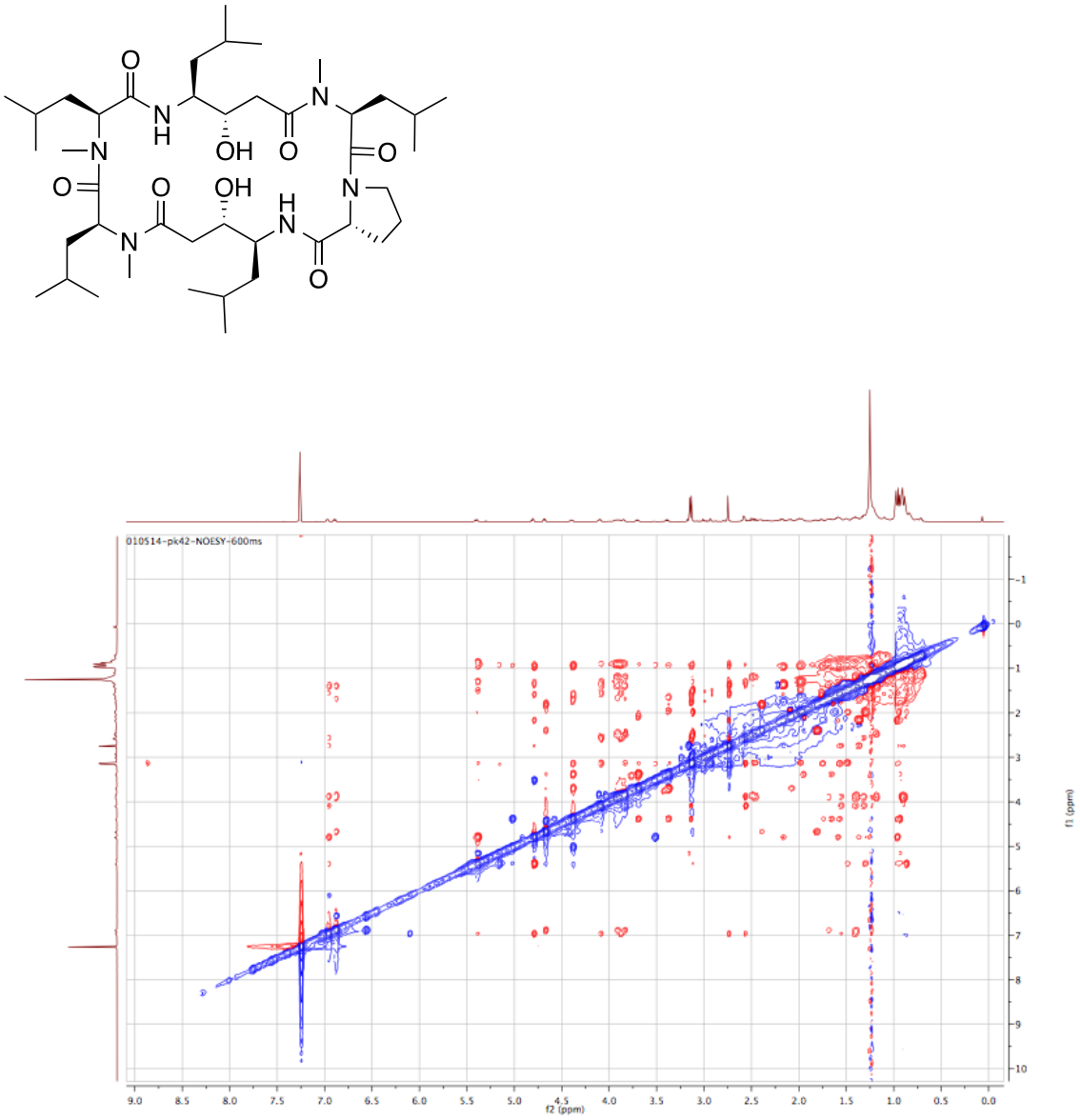

Figure S20. Macrocycle **1** NOESY in $CDCl_3$

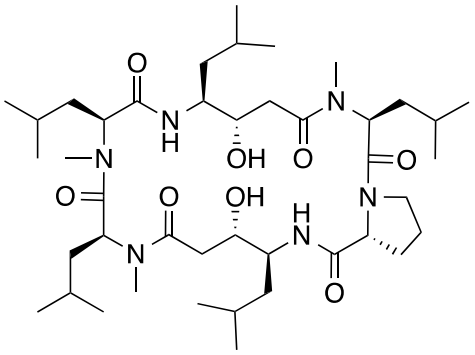

Table S5. Macrocycle **1** in $CDCl_3$

Residue	Resonance	δ H	δ C, mult.	COSY	NOESY	HMBC
Pro1	CO	-	171.43			
	α	4.67	60.32, CH	P1β	P1β, P1δ	P1γ, P1β, P1δ, L6CO
	β	2.40, 1.82	27.37, CH_2		P1γ, P1δ	
	γ	2.08, 1.96	24.49, CH_2			
	δ	3.70, 3.38	46.44, CH_2	P1γ	L6α, Sta2NH	P1α
Sta2	CO	-	174.12			
	α	2.47	38.48. CH_2		L4NMe	
	β	3.84	70.23, CH			
	OH	4.03				
	γ	3.92	51.84, CH			
	δ	1.19. 1.42	40.4, CH_2			
	NH	6.88		Sta5γ	Sta5γ, P1γ, P1δ	Sta5γ, P1CO
Leu3	CO	-	172.9			
	α	5.41	50.53, CH	L3β	L3β, L4α	L3NMe, L3β, L3CO
	β	1.31, 1.99	37.61. CH_2			
	NMe	3.13	31.38, CH_3			L3α, Sta2CO
Leu4	CO	-	169.8			
	α	4.80	59.09, CH	L4β	L4β, L4Nme	L4NMe, L4β, L4CO, L3CO
	β	1.40, 2.18	38.16			
	NMe	2.75	29.6, CH_3		L4β, L4α	L4α, L3CO
Sta5	CO	-	173.1			
	α	2.57	38.84, CH_2		L4NMe	
	β	4.09	69.52, CH	Sta5OH, Sta5α	Sta5NH	
	OH	4.91				
	γ	3.88,	53.02, CH_2	Sta5δ	Sta2NH, Sta5NH	Sta5δ, Sta5β
	δ	1.33, 1.42	41.15. CH_2			
	NH	6.96		Sta5α	Sta5α, L4α, L4Nme, L3α	Sta5α, Sta5β, L4CO
Leu6	CO	-	171.3			
	α	4.39	57.35, CH	L6β	P1δ	L6NMe, L6β, L6CO
	β	1.73. 1.67	37.21, CH_2			
	NMe	3.14	34.21, CH_3			L6α, P1CO, Sta5CO

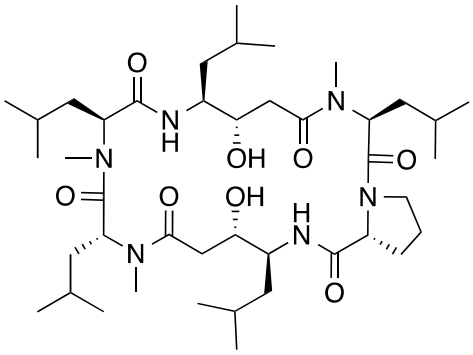

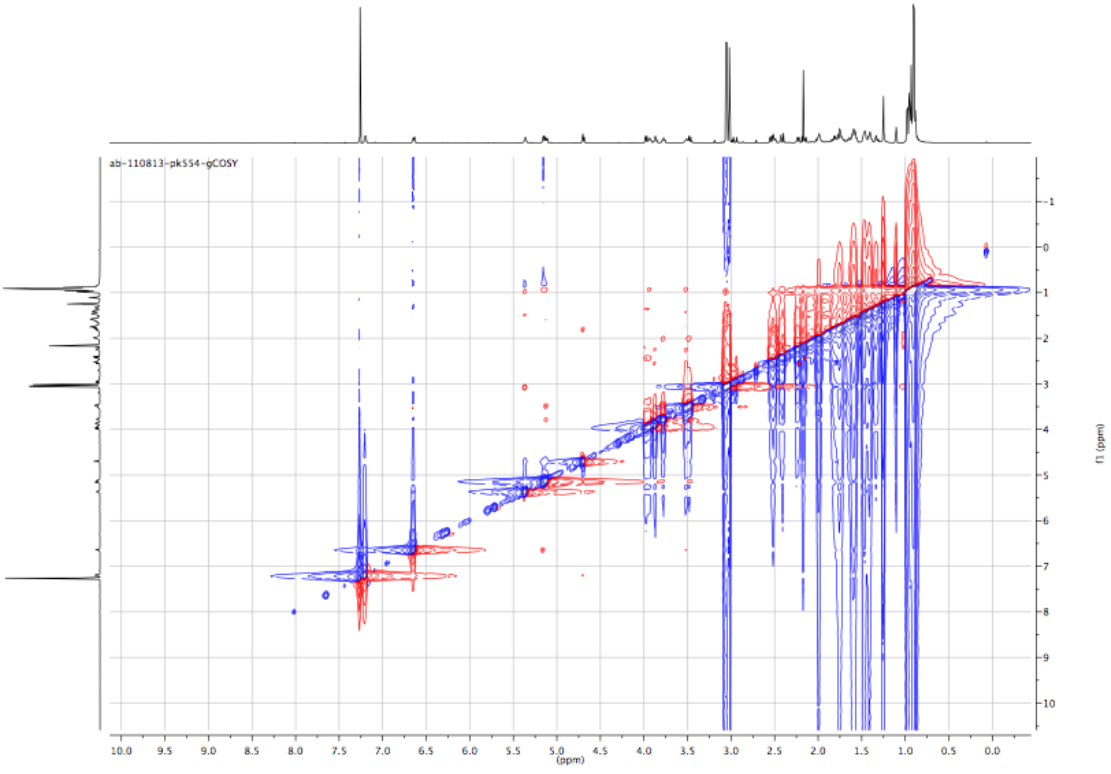

Figure S21. Macrocycle **4** COSY in $CDCl_3$

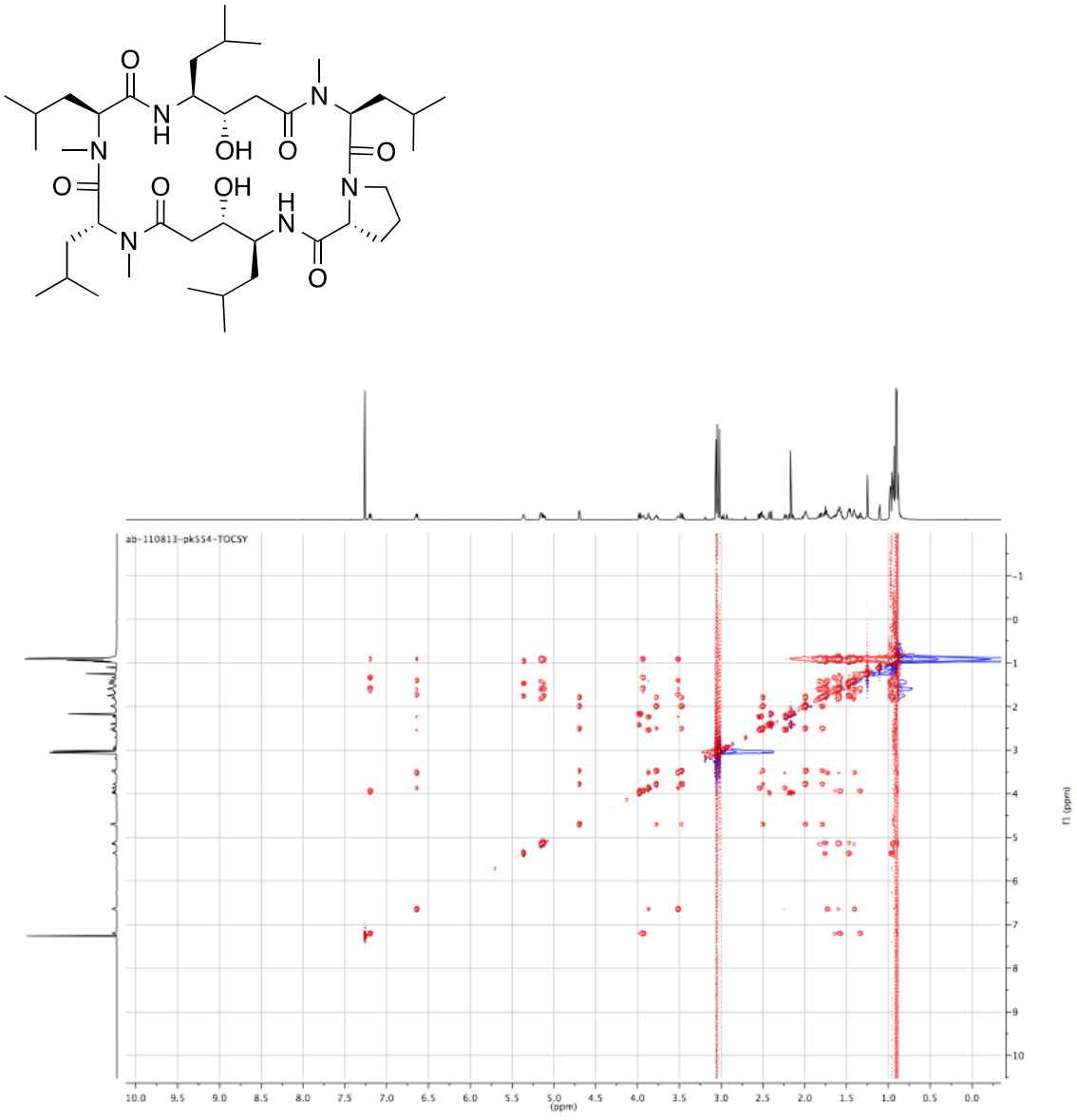

Figure S22. Macrocycle **4** TOCSY in $CDCl_3$

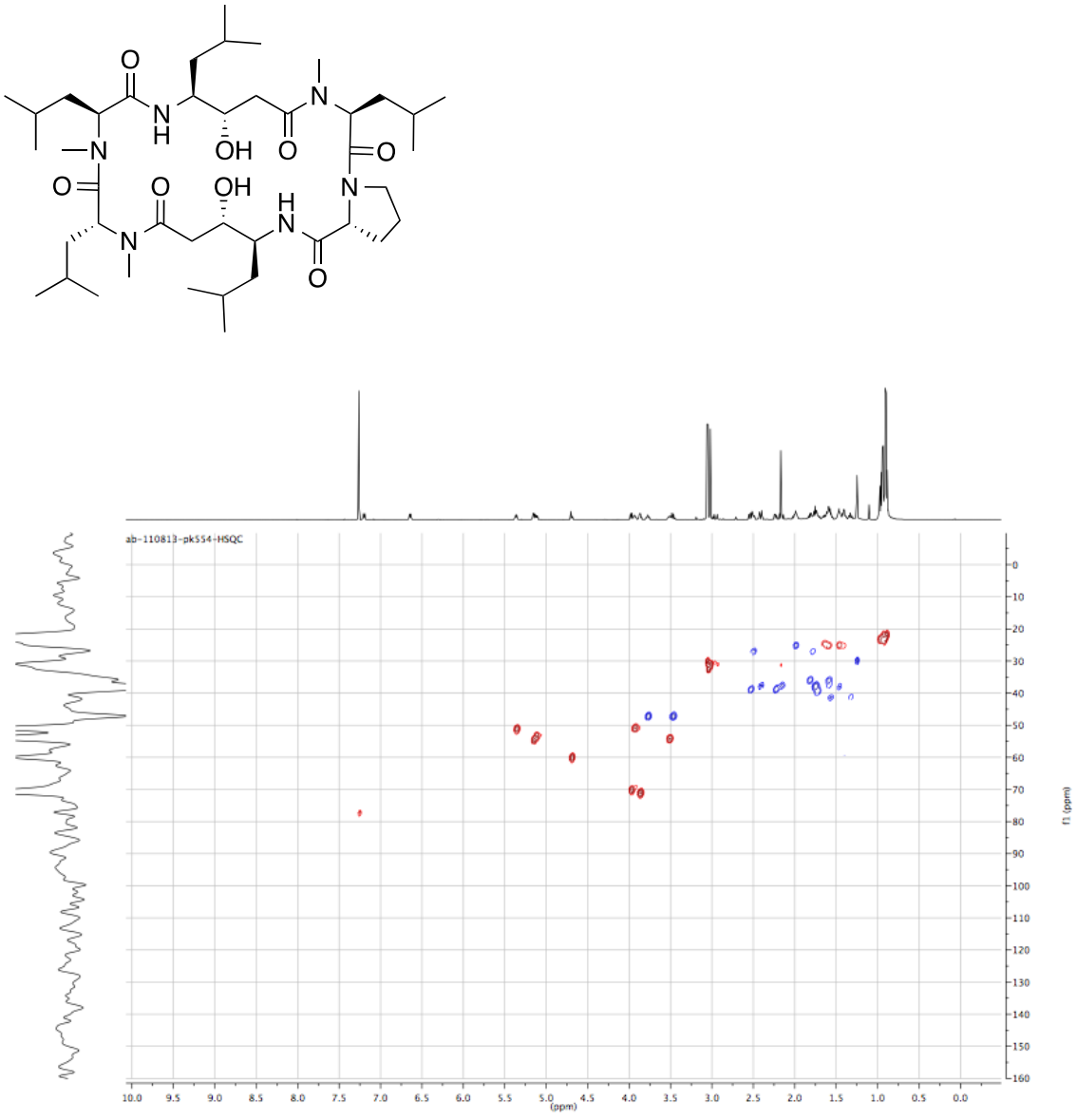

Figure S23. Macrocycle **4** HSQC in $CDCl_3$

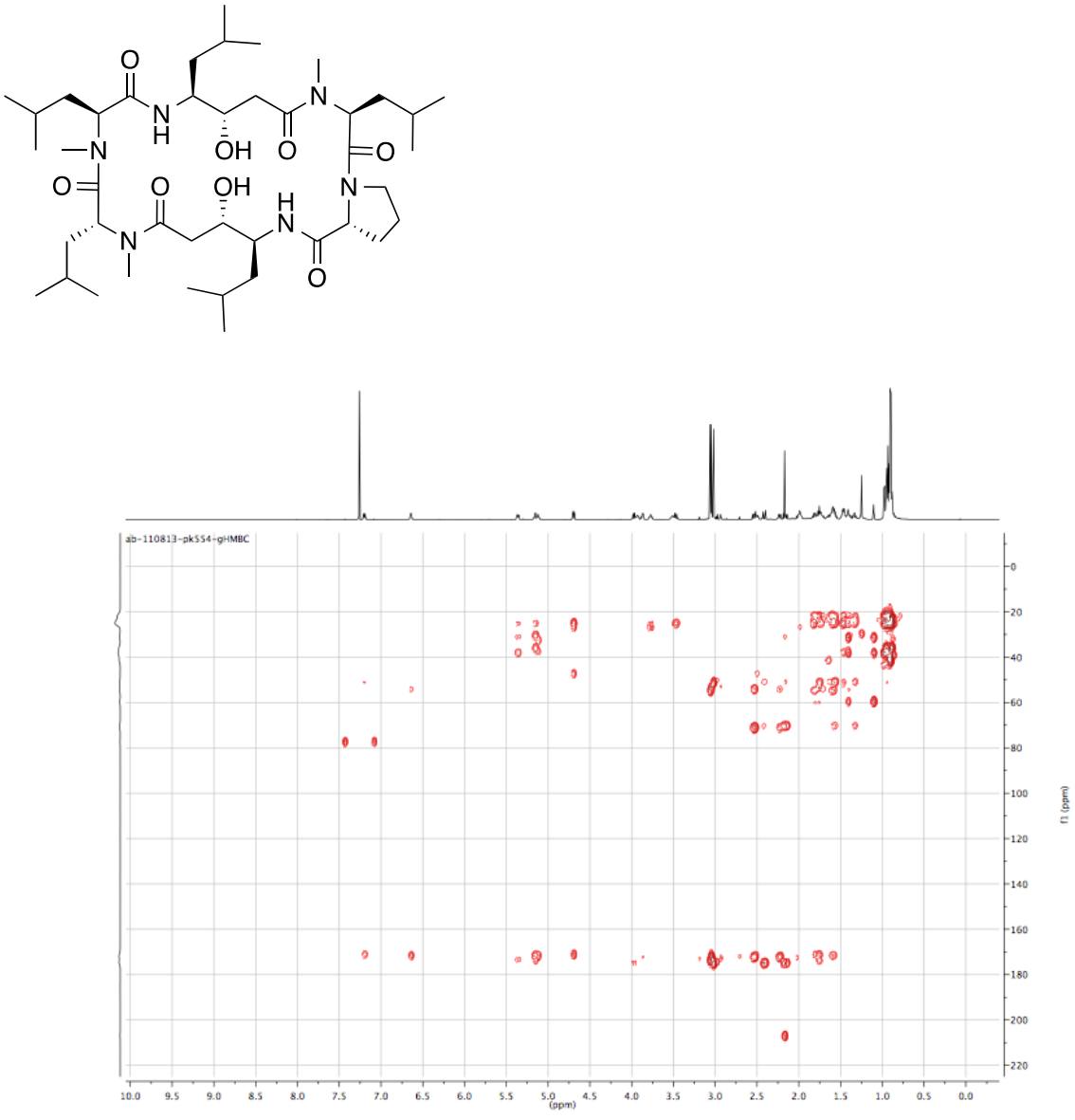

Figure S24. Macrocycle **4** TOCSY in $CDCl_3$

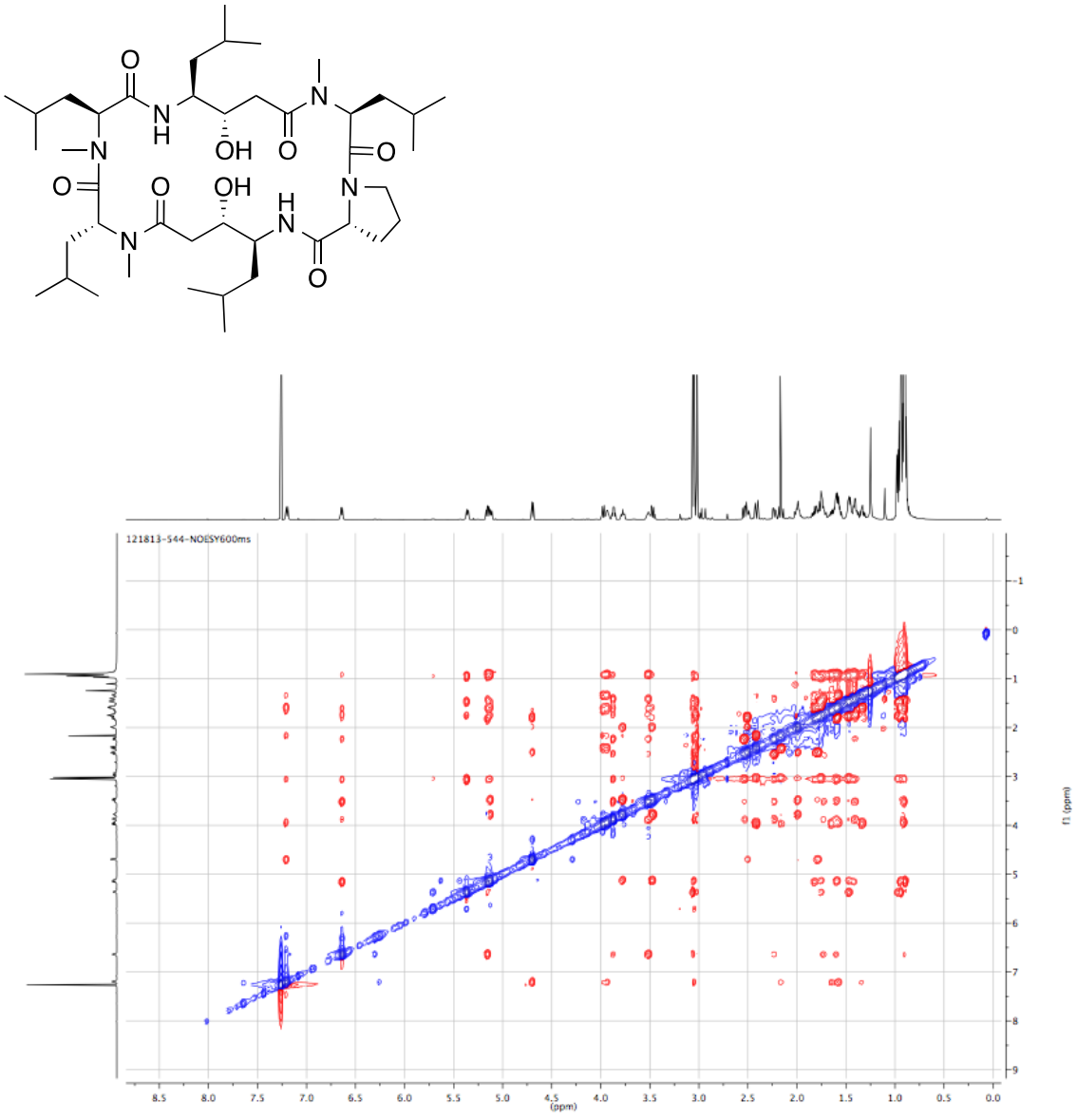

Figure S25. Macrocycle **4** NOESY in $CDCl_3$ 600 ms Mix Time

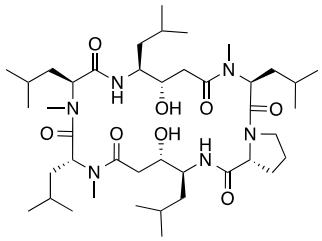

Table S6. Macrocycle **4** in $CDCl_3$

Residue	Resonance	δ H	δ C, mult.	NOESY	TOCSY	HMBC
Pro1	CO	-	170.89			
	α	4.69	59.87, CH	Sta2NH, Sta2α, Sta2γ	P1γ, P1β, P1δ	P1β, P1δ, P1CO
	β	1.99	25.02, CH_2	Sta2NH, L3NMe	P1γ, P1δ, P1α	L6CO
	γ	2.49, 1.79	26.9, CH_2	Sta2NH	P1β, P1γ, P1δ	P1δ
	δ	3.78, 3.47	47.1, CH_2	P1β, P1δ, L6α, Sta2NH	P1β, P1γ, P1δ, P1α	P1γ, P1α, L6CO
Sta2	CO	-	174.60			
	α	2.41, 2.18	37.77, CH_2	Sta2α, L3α, P1α, L3NMe	Sta2α, Sta2β	Sta2γ, Sta2β, Sta2CO
	β	3.99	70.05, CH	L3α	Sta2α	Sta2α, Sta2δ, Sta2CO
	γ	3.93	50.81, CH	Sta2α, P1α	Sta2δ Sta2NH	Sta2ε Sta2δ, P1CO
	δ	1.57, 1.33	41.45, CH_2		Sta2γ, Sta2ε, Sta2NH	
	ε	1.64	24.45, CH			
	NH	7.20		Sta2α, Sta2γ, P1α, L6α, P1δ, P1γ	Sta2δ, Sta2γ	Sta2γ, P1CO
Leu3	CO	-	173.11			
	α	5.36	50.93, CH		L3β	L3NMe, L3β, L3CO
	β	1.76, 1.47	37.68, CH_2		L3α	L3CO
	NMe	3.02	31.07, CH_3	Sta2α		L3α, Sta2CO,
Leu4	CO	-	171.31			
	α	5.15	54.45, CH	L4β, L4NMe	L4β	L4NMe, L4β, L4CO, L3CO
	β	1.59, 1.82	35.93, CH_2	L4NMe		
	NMe	3.06	30.29, CH_3	L4β		L4α, L3CO
Sta5	CO	-	171.71			
	α	2.53, 2.23	38.81, CH_2	Sta5α	Sta5α, Sta5β, Sta5γ	Sta5γ, Sta5β, Sta5CO
	β	3.87	70.95, CH	Sta5α, L4α	Sta5α, Sta5NH	Sta5CO
	γ	3.52	54.03, CH	Sta5NH	Sta5δ, Sta5α, Sta5β, Sta5NH	L4CO
	δ	1.73, 1.60				
	NH	6.64		Sta5δ, Sta5α, Sta5γ, L6NMe, L4α	Sta5δ, Sta5α, Sta5γ, Sta5β	Sta5α, Sta5γ, Sta5β, L4CO
Leu6	CO	-	172.01			
	α	5.12	53.36, CH	P1δ	L6β	L6NMe, L6β, L6CO
	β	1.76. 1.59	37.39, CH_2			
	NMe	3.05	32.57, CH_3			L6α, P1CO, L6CO

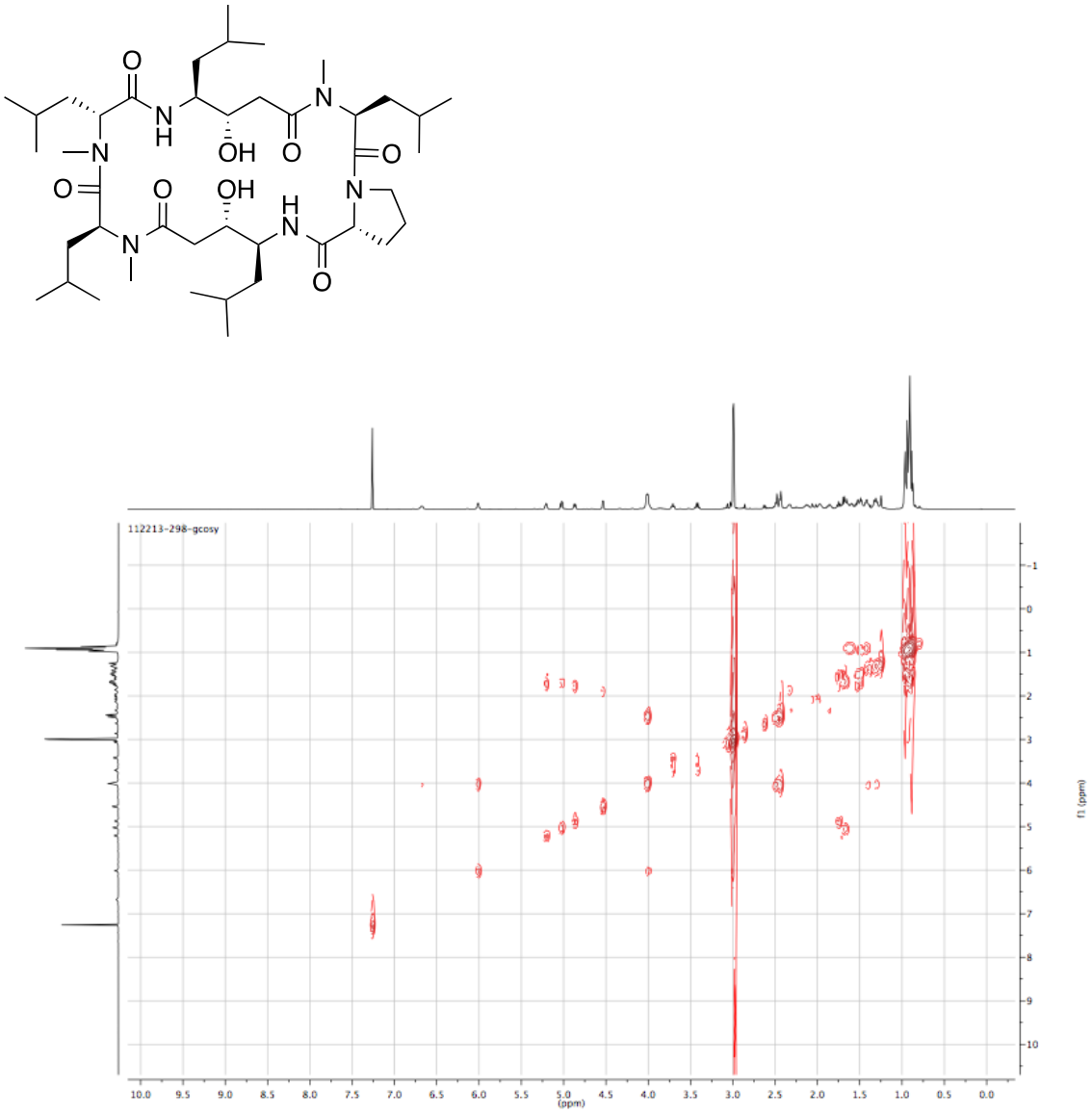

Figure S26. Macrocycle **5** COSY in $CDCl_3$

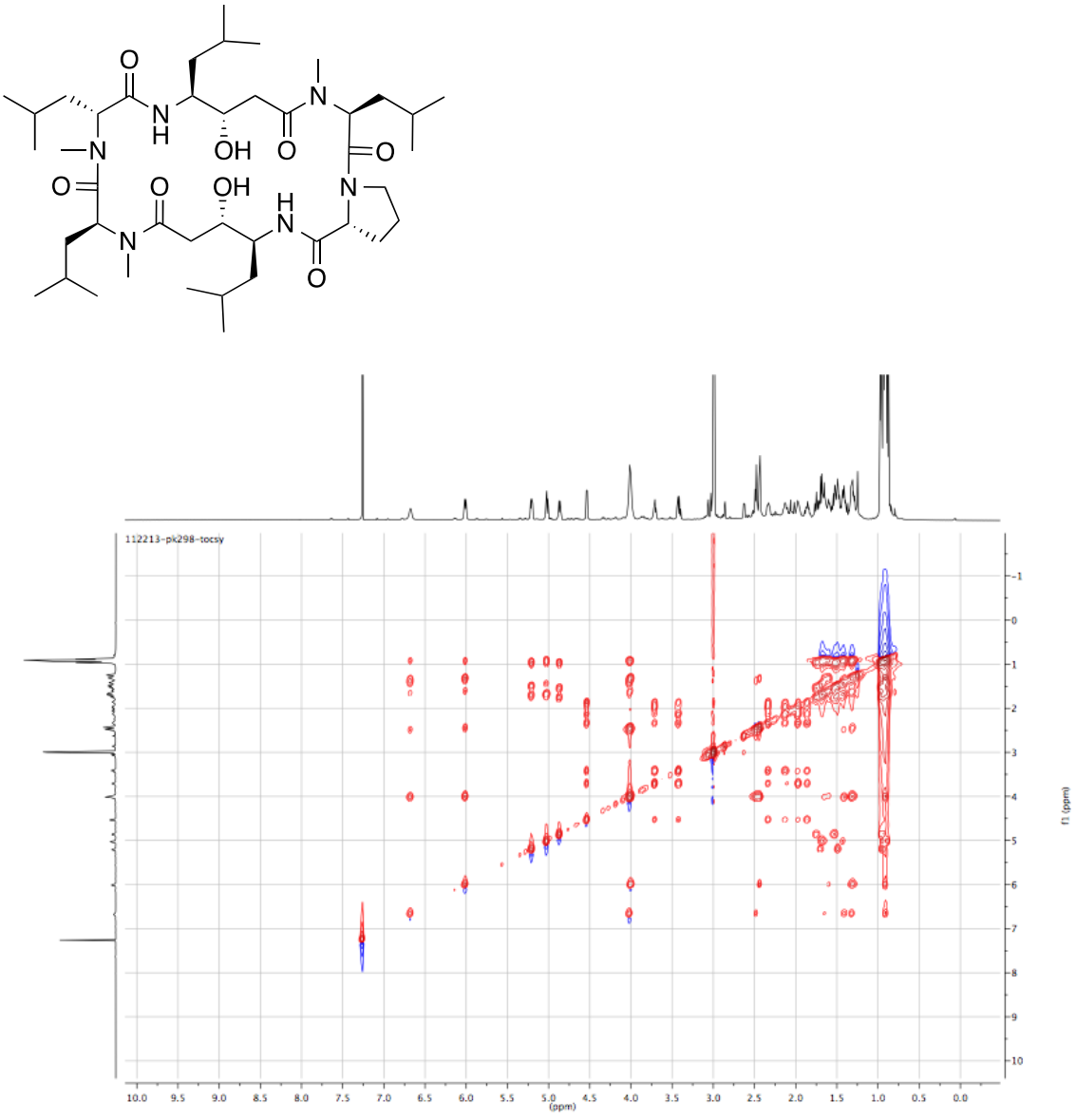

Figure S27. Macrocycle **5** TOCSY in $CDCl_3$

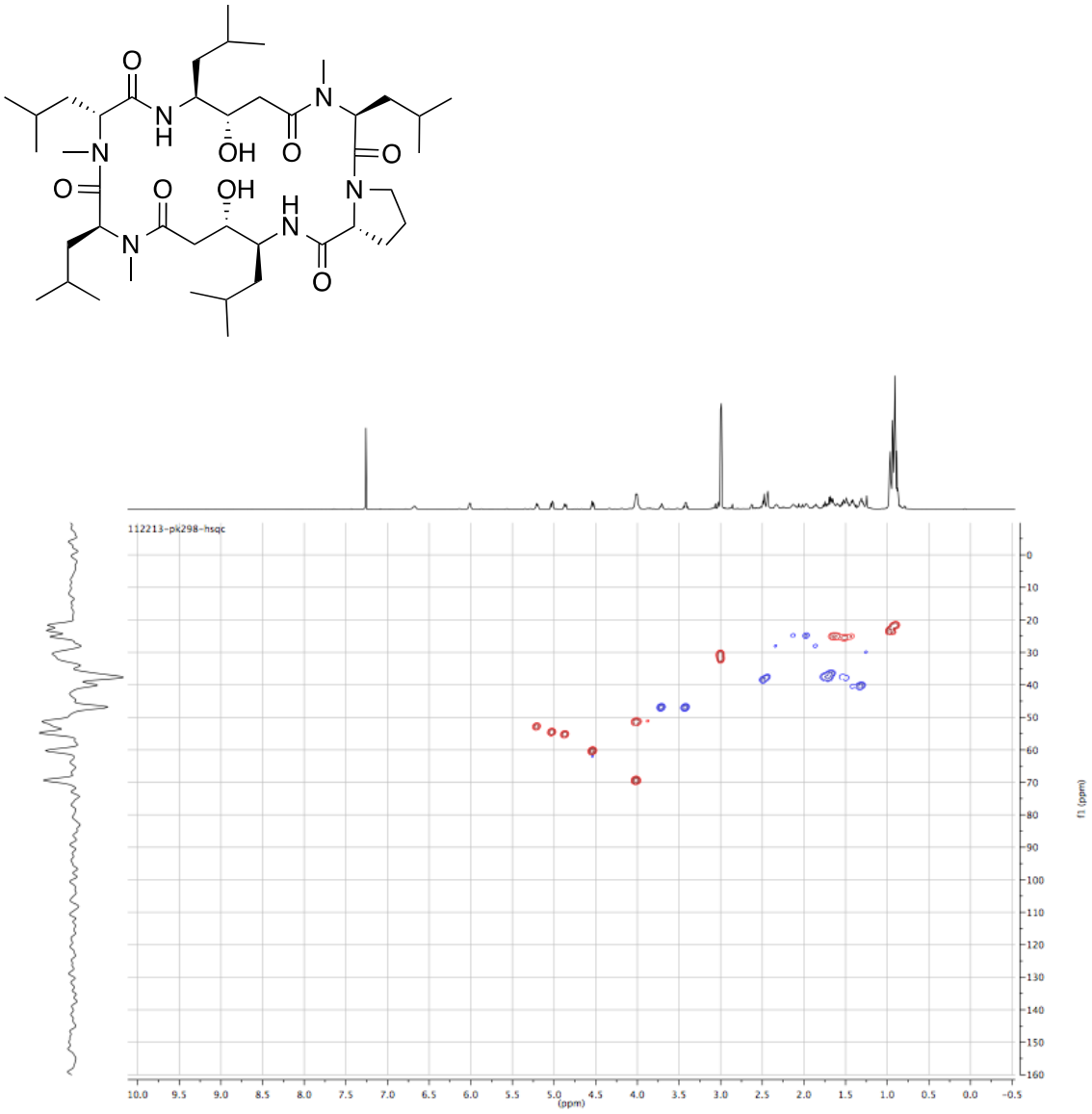

Figure S28. Macrocycle **5** HSQC in $CDCl_3$

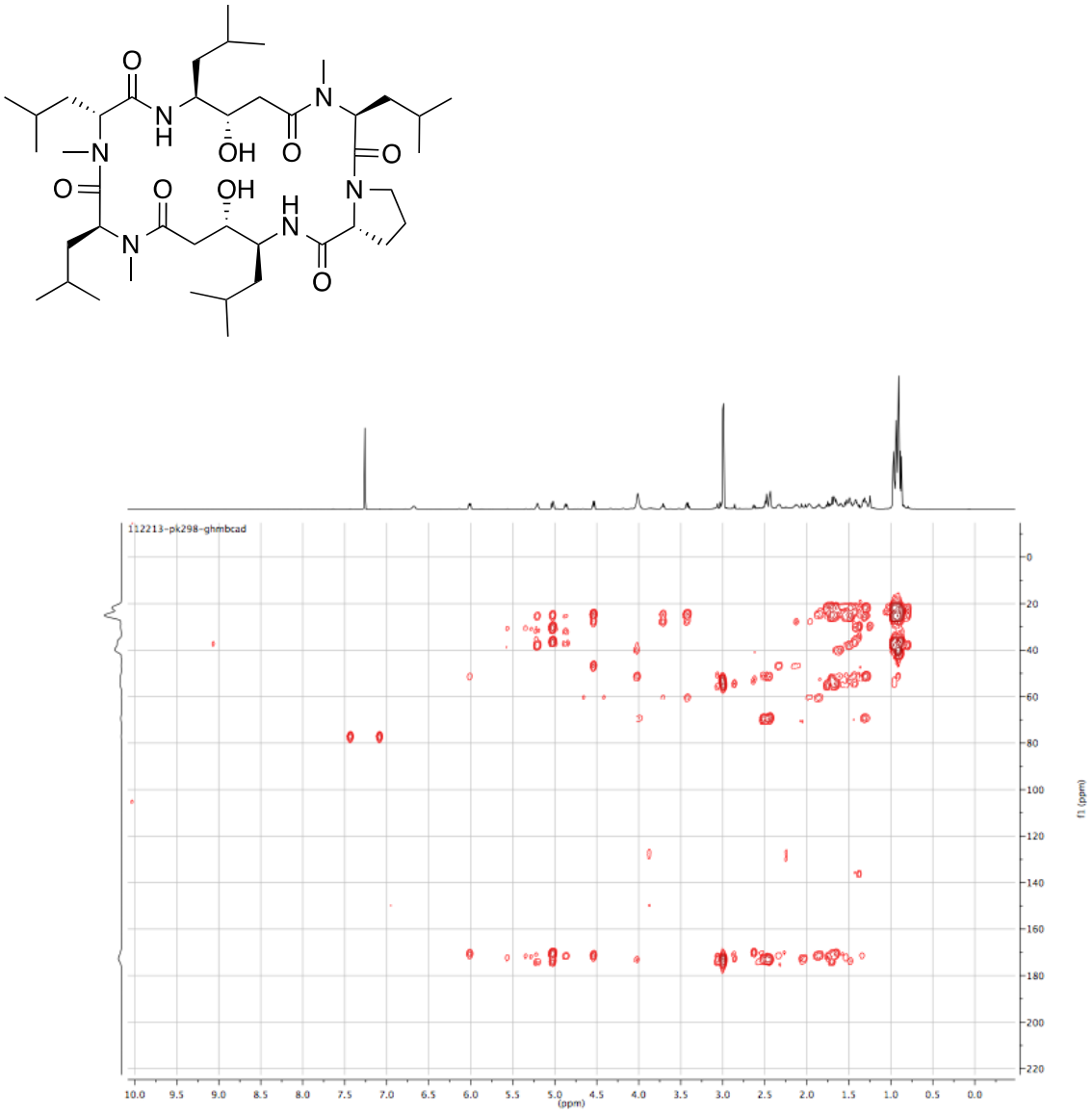

Figure S29. Macrocycle **5** HMBC in $CDCl_3$

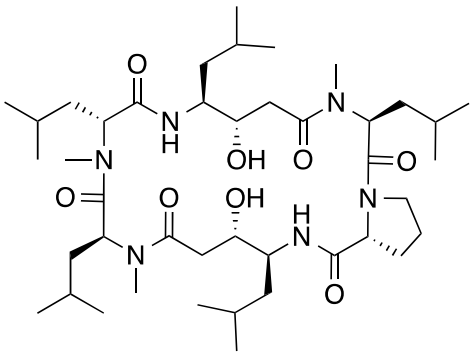

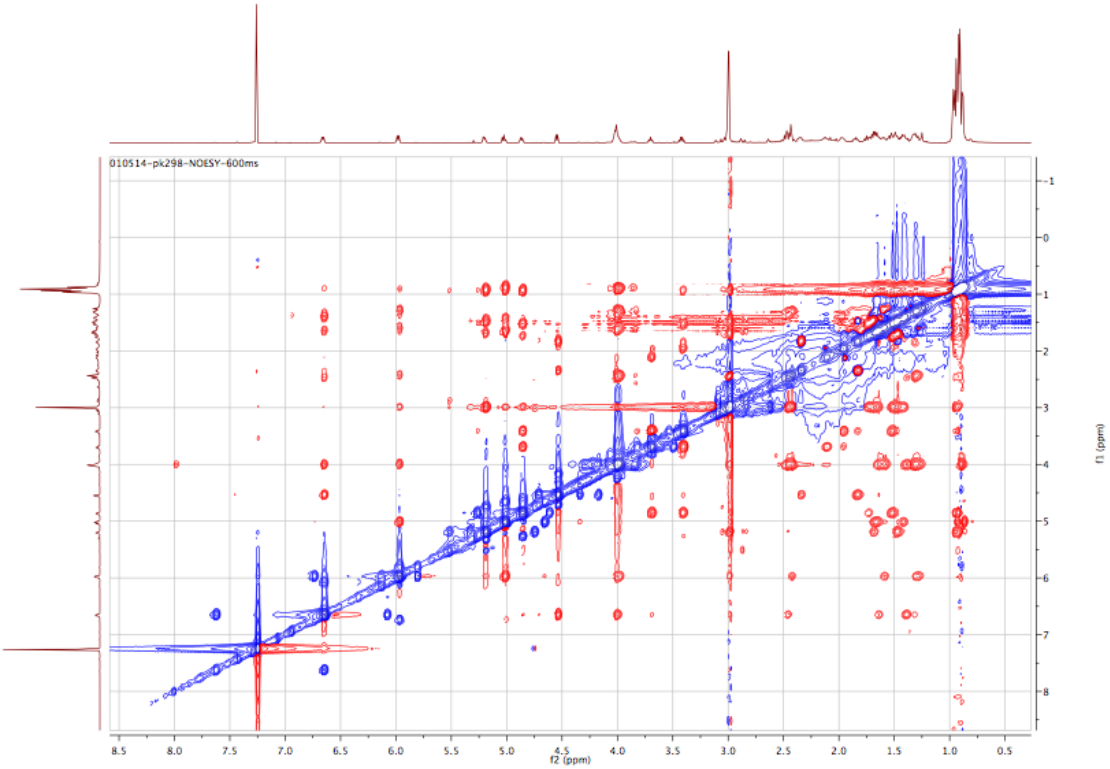

Figure S30. Macrocycle **5** NOESY in $CDCl_3$ 600 ms Mix time

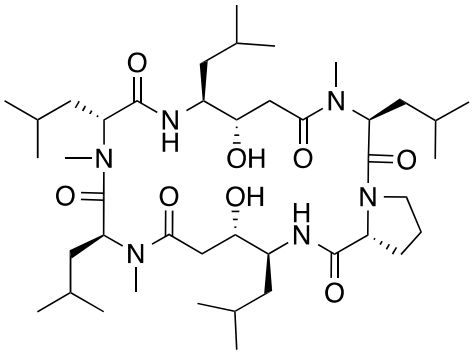

Table S7. Macrocycle **5** in $CDCl_3$

Residue	Resonance	δ H	δ C, mult.	NOESY	TOCSY	HMBC
Pro1	CO	-	171.23			
	α	4.54	60.18, CH	P1γ, Sta2NH	P1β, P1γ, P1δ	P1β, P1γ, P1δ, P1CO
	β	1.97, 2.11	24.57, CH_2			
	γ	1.85, 2.33	27.46, CH_2	P1γ, Sta2NH		
	δ	3.71, 3.42	46.75, CH_2	P1β, P1δ	P1β, P1γ, P1δ	P1α, P1β, P1γ
Sta2	CO	-	170.88			
	α	2.48				
	β	4.02	69.31, CH		Sta2α, Sta2δ	
	γ	4.01	51.18, CH		Sta2α, Sta2δ	
	δ	1.64				
	NH	6.68		P1β, P1γ, P1δ, P1α	Sta2α, Sta2δ, Sta2γ	
Leu3	CO	-	174.18			
	α	5.20	52.70, CH	Sta2α	L3β	L3β, L3CO, Sta2CO
	β	1.72	37.22, CH_2			
	NMe	3.01	31.03, CH_3			
Leu4	CO	-	170.56			
	α	5.02	54.14, CH	Sta5NH	L4β	L4β, L4CO, L3CO
	β	1.72	36.13, CH_2			
	NMe	3.00	30.24, CH_3			
Sta5	CO	-	173.82			
	α	2.44, 1.70	37.50, CH_2			
	β	4.02	69.31, CH		Sta5δ, Sta5α	
	γ	4.01	51.18, CH		Sta5δ, Sta5α	
	δ	1.64				
	NH	6.01		Sta5α, L4α	Sta5δ, Sta5α, Sta5β, Sta5γ	L4CO, Sta5γ
Leu6	CO	-	171.48			
	α	4.87	55.09, CH	P1δ	L6β	L6CO
	β	1.78	37.29, CH_2			
	NMe	2.99	32.09, CH_3			

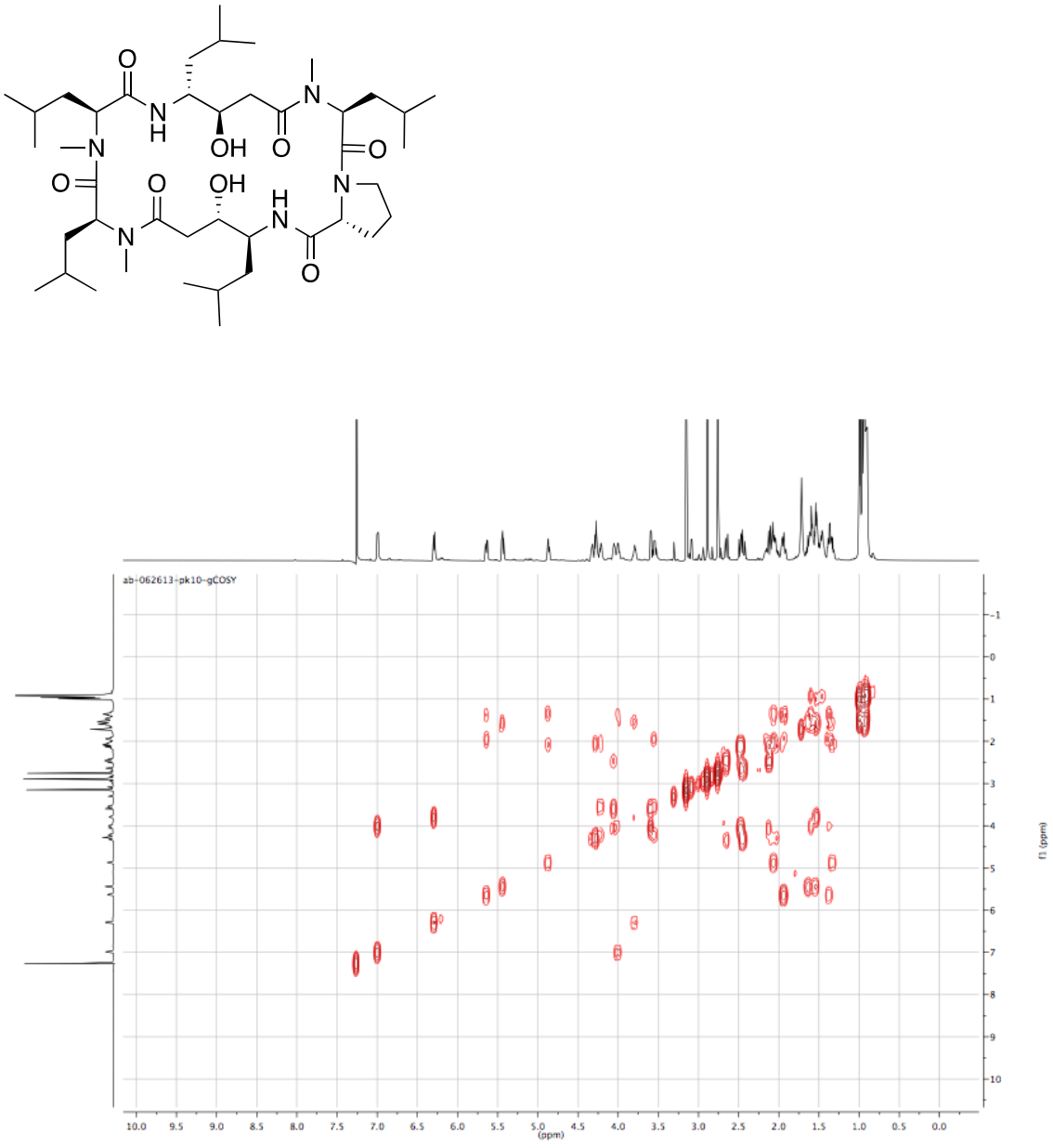

Figure S31. Macrocycle **6** COSY in $CDCl_3$

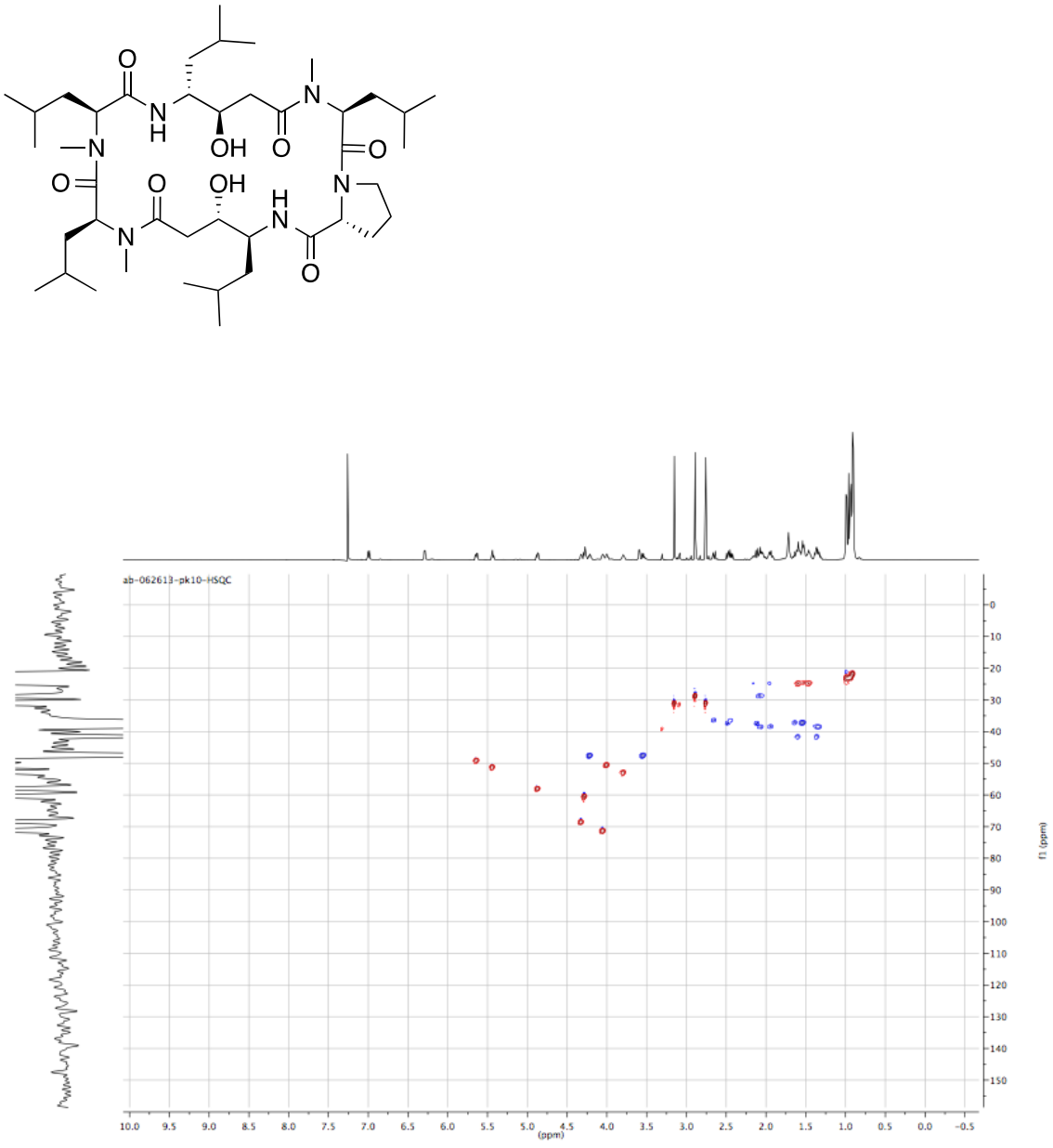

Figure S32. Macrocycle **6** HSQC in $CDCl_3$

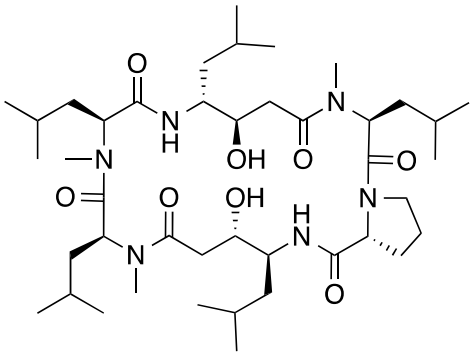

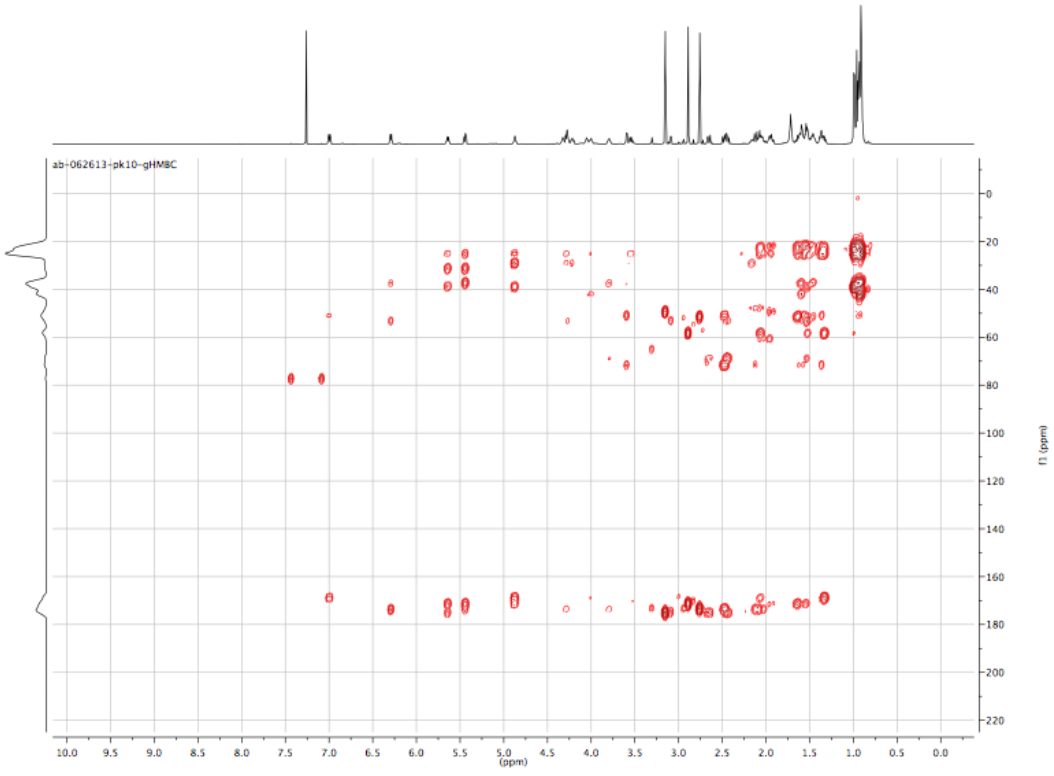

Figure S33. Macrocycle **6** HMBC in $CDCl_3$

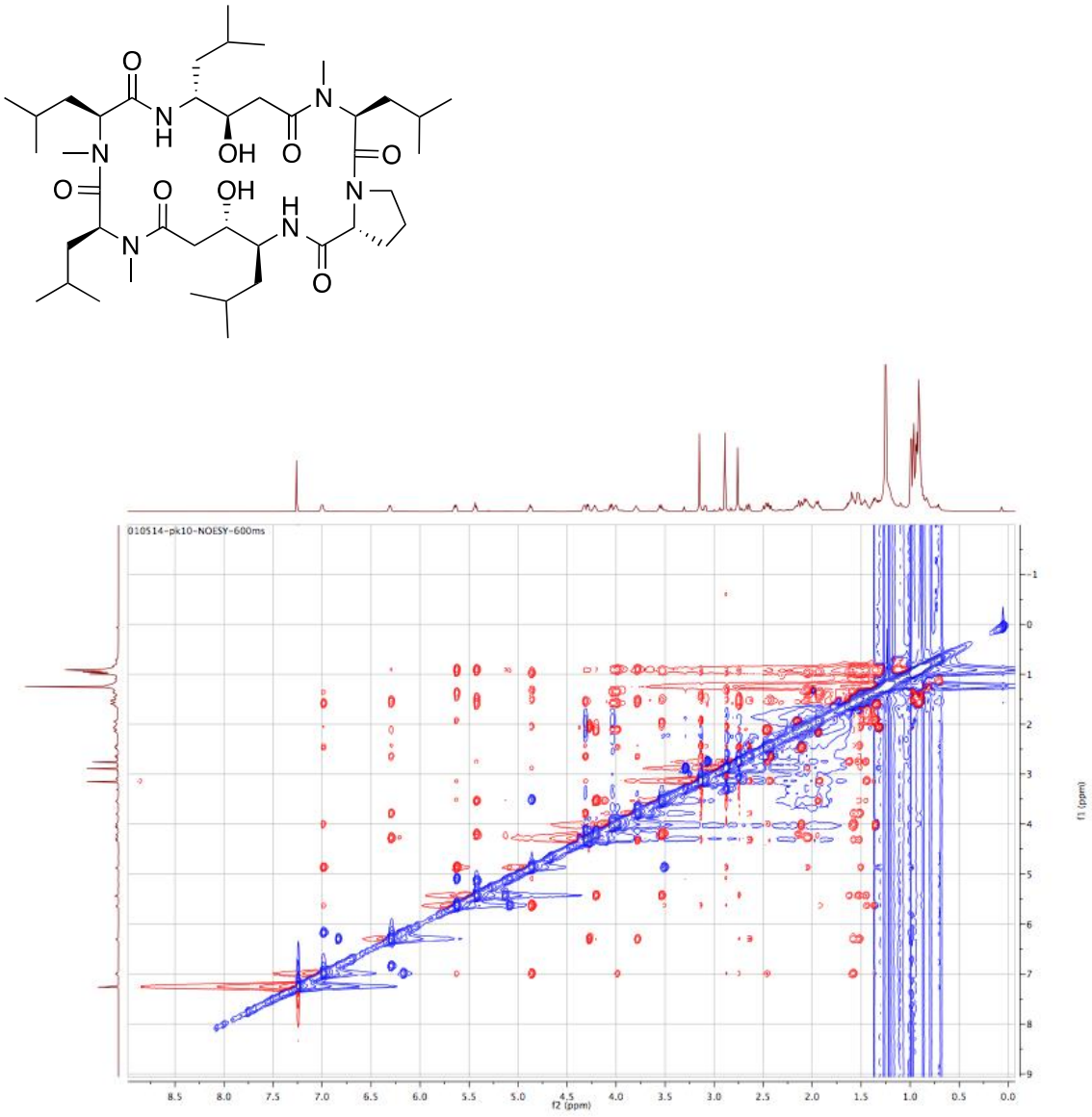

Figure S34. Macrocycle **6** NOESY in $CDCl_3$

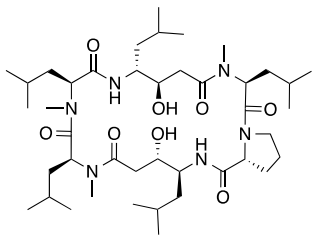

Table S8. Macrocycle **6** in $CDCl_3$

Residue	Resonance	δ H	δ C, mult.	COSY	NOESY	HMBC
Pro1	CO	-	173.1			
	α	4.28	60.36, CH	P1β	Sta2α, P1β	P1γ, P1β, P1δ, P1CO, L6CO
	β	2.07,	28.86, CH_2		P1α	
	γ	1.99, 2.15	24.76, CH_2		P1γ	
	δ	4.22, 3.55	47.34, CH_2	P1γ, P1δ	P1δ, Sta5NH	P1β, Pro1α, Pro1γ
Sta2	CO	-	174.95			
	α	2.43, 2.67	36.31, CH_2	Sta2β	Sta2NH, Sta2β	Sta2β, Sta2CO
	β	4.33	68.45, CH	Sta2α, Sta2γ	Sta2NH	
	OH	4.27			Sta2NH	Sta2γ, Sta2β
	γ	3.80	52.66, CH	Sta2δ	Sta2NH	Sta2δ, Sta2β, P1CO
	δ	1.53	37.31, CH_2			
	NH	6.29		Sta2γ	Sta2OH, L6Nme, Sta2γ	Sta2δ, Sta2γ, P1CO
Leu3	CO	-	171.07			
	α	5.64	49.06, CH	L3β	L4α, L4Nme, L3Nme	L3NMe, L3β, L3CO, Sta2CO
	β	1.94 , 1.38	38.28, CH_2			
	NMe	3.15	30.81, CH_3		Sta2α	L3α, Sta2CO
Leu4	CO	-	168.69			
	α	4.87	58.00, CH	L4β	L4β	L4NMe, L4β, L3CO, L4CO
	β	1.33, 2.06	38.77, CH_2		L4α	
	NMe	2.89	28.73, CH_3		Sta2α, L4β	L4α, L4CO
Sta5	CO	-	173.31			
	α	2.11, 2.48	37.22, CH_2	Sta5β		
	β	4.05	71.20, CH	Sta5α, Sta5OH	P1γ	
	OH	3.59				Sta5γ. Sta5β
	γ	4.00	50.47, CH	Sta5δ		Sta5δ, Leu4CO
	δ	1.36, 1.59	41.50, CH_2			
	NH	6.99		Sta5γ	L4α, L6Nme, L4Nme, P1δ, L3α, Sta5γ	Sta5γ, Leu4CO
Leu6	CO	-	171.2			
	α	5.44	51.06, CH	L6β	P1δ, L6Nme	L6NMe, L6β, L6CO
	β	2.12, 1.54	37.27, CH_2			
	NMe	2.76	30.92, CH_3		Sta2α, L6β	L6α, Sta5CO

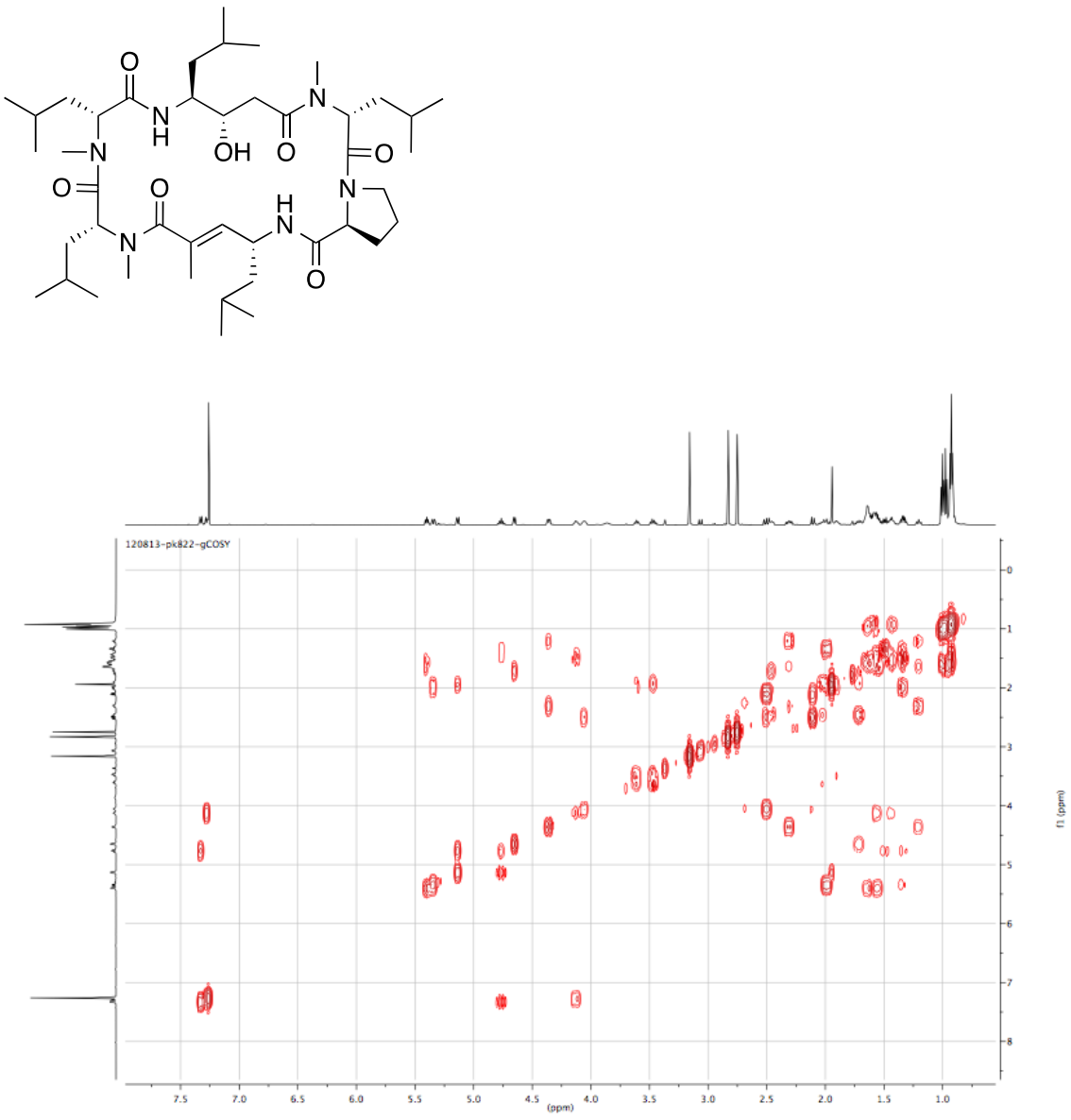

Figure S35. Macrocycle **14** COSY in $CDCl_3$

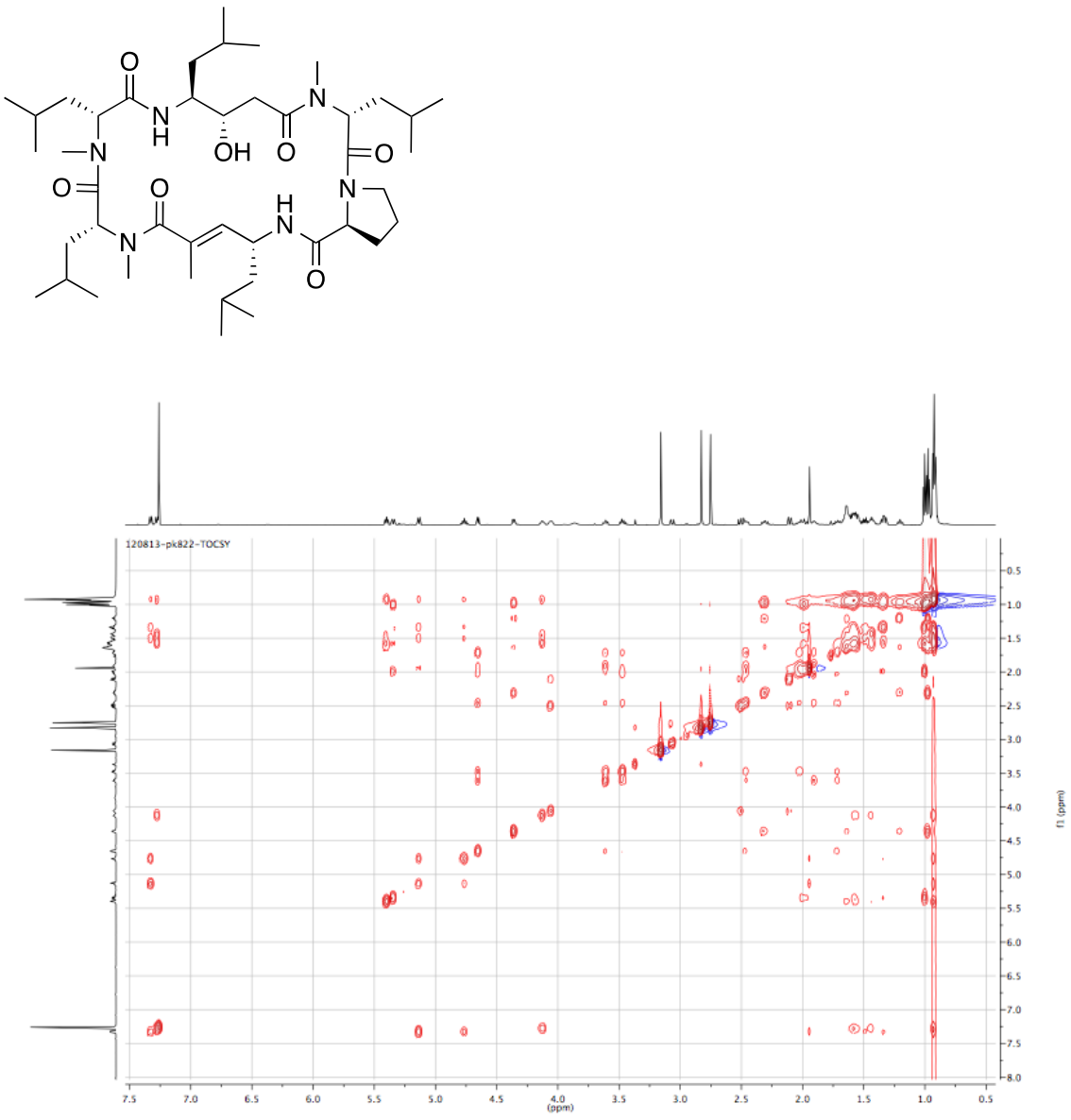

Figure S36. Macrocycle **14** TOCSY in $CDCl_3$

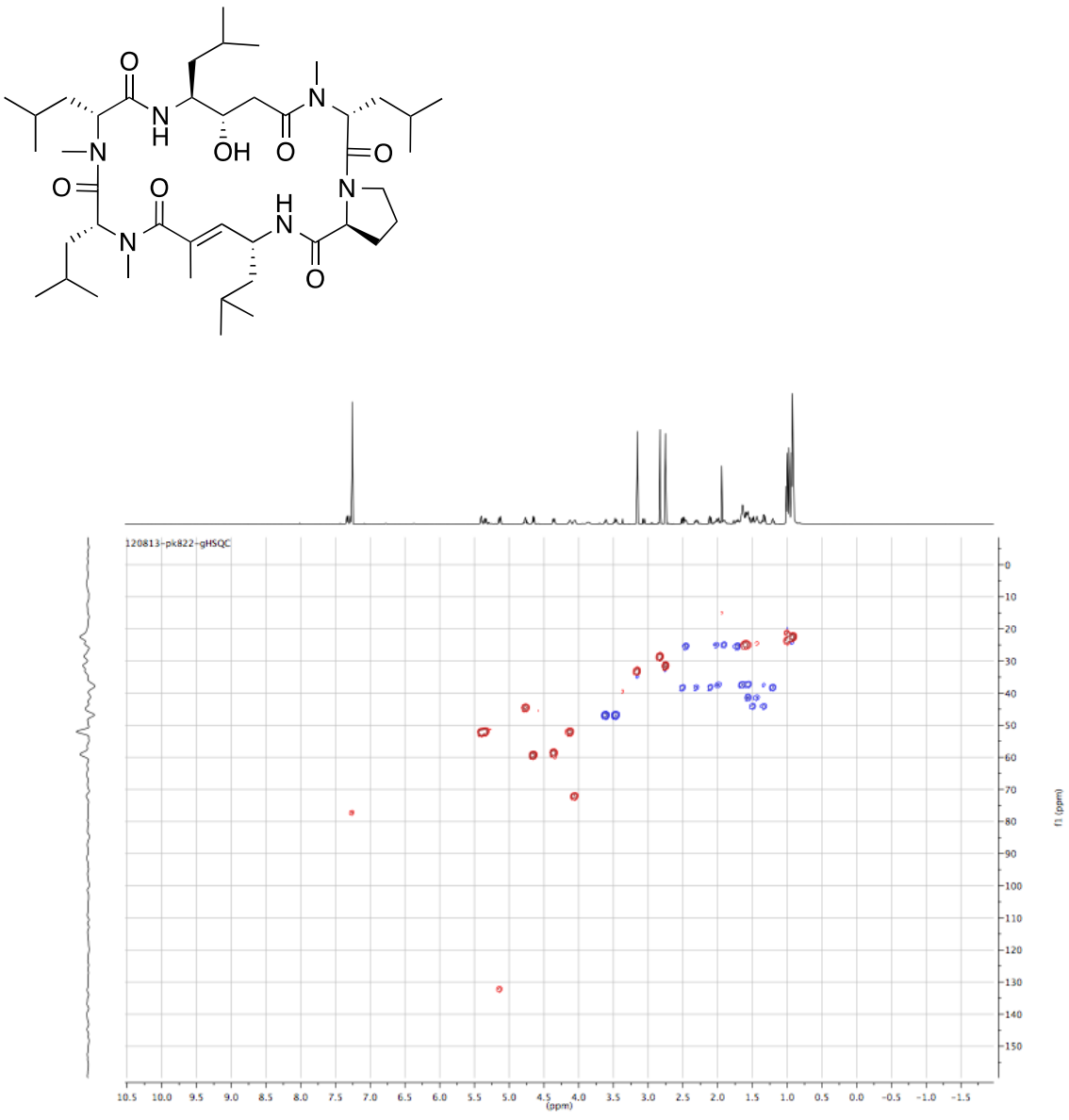

Figure S37. Macrocycle **14** HSQC in $CDCl_3$

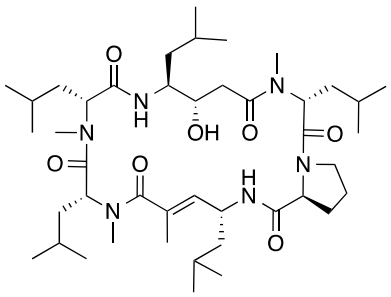

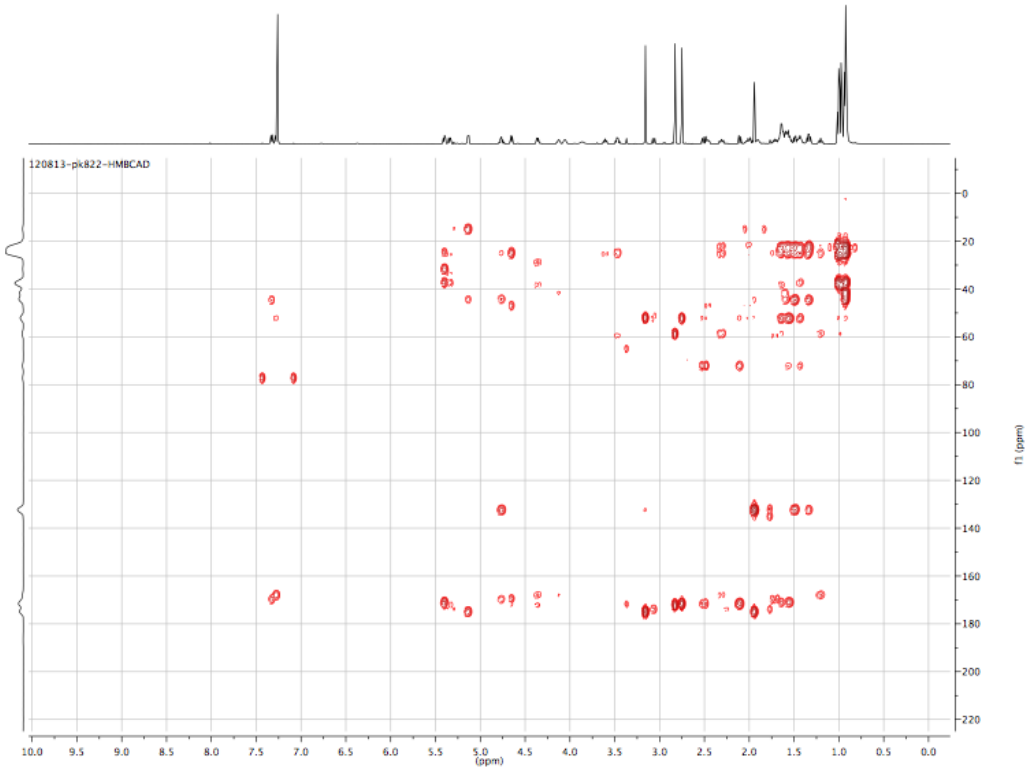

Figure S38. Macrocycle **14** HMBC in $CDCl_3$

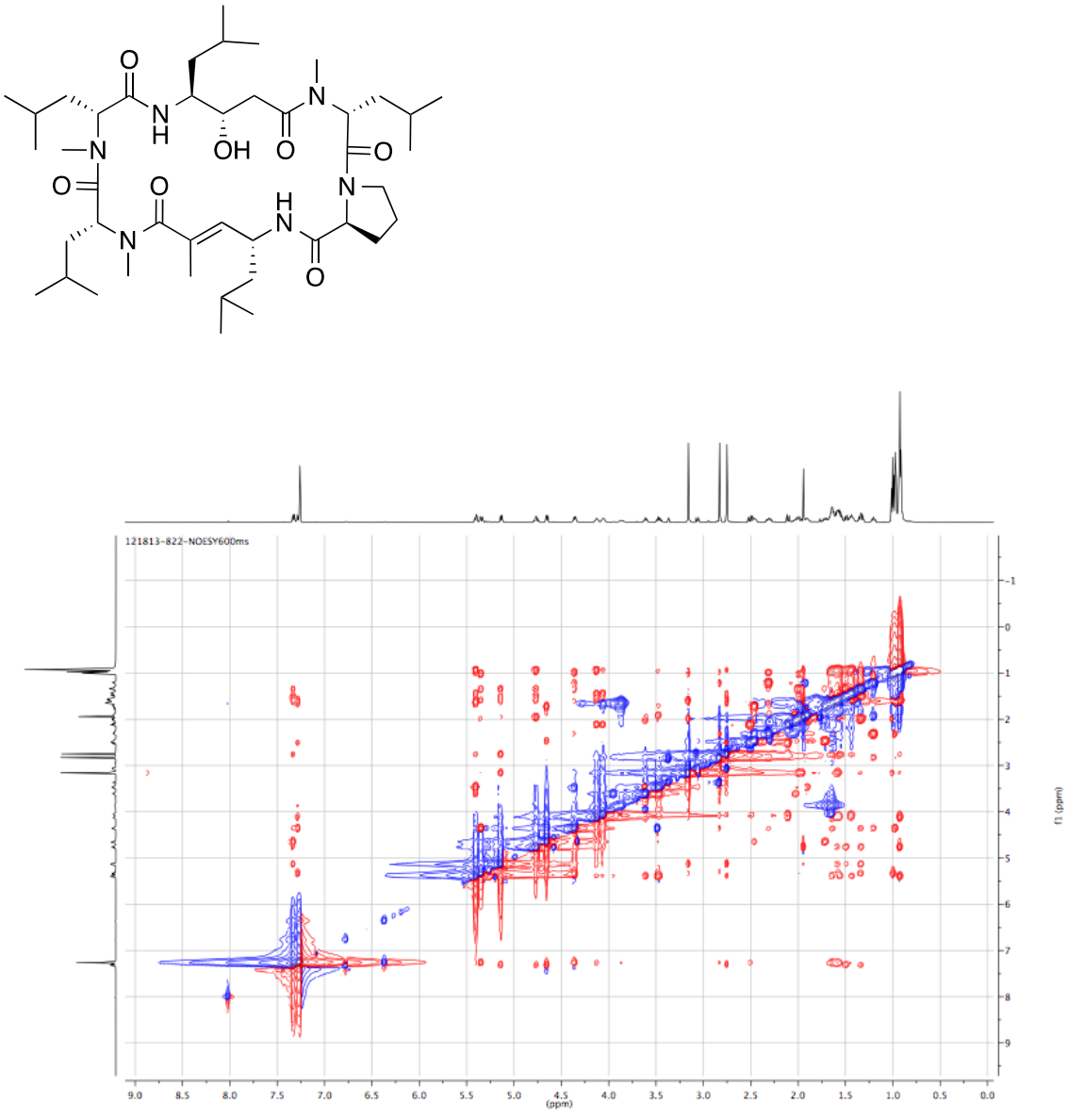

Figure S39. Macrocycle **14** NOESY in $CDCl_3$ 600 ms Mix Time

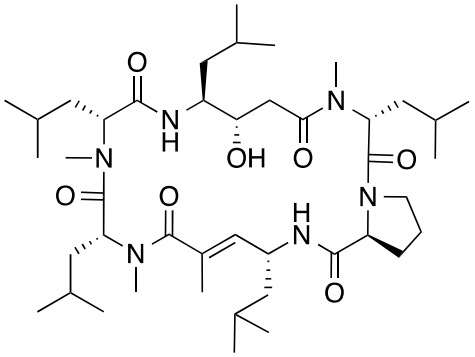

Table S9. Macrocycle **14** in $CDCl_3$

Residue	Resonance	δ H	δ C, mult.	COSY	TOCSY	NOESY	HMBC
Pro1	CO	-	169.56				
	α	4.66	59.42, CH	P1β	P1β, P1γ, P1δ	Vin2NH	P1δ, P1CO
	β	1.71, 2.46	25.33, CH_2	P1α		Vin2γ	
	γ	2.02, 1.91	24.86, CH_2	P1β, P1δ, P1δ			
	δ	3.61, 3.47	46.78, CH_2	P1γ	P1β	Vin2NH, Sta5NH, L6α	P1β, P1γ, P1α
Vin2	CO	-	174.90				
	α	-	116.12, C				
	αMe	1.94	14.89, CH_3			Vin2NH	
	β	5.13	132.13, CH		Vin2δ, Vin2γ, VinαMe	Sta5α, L6NMe, L3NMe	Vin2δ
	γ	4.76	44.47, CH	Vin2NH, Vin2β, Vin2δ	P1β	P1β	Vin2δ, Vin2β, P1CO
	δ	1.33, 1.49	44.21, CH_2			L3α, L3NMe	
	NH	7.33		Vin2γ	Vin2δ, Vin2γ, Vin2β	L6NMe, P1δ, P1α	Vin2γ, P1CO
Leu3	CO	-	171.87				
	α	5.34	51.99, CH	L3β	L3β	Sta5NH, L4α	
	β	1.96, 1.64	37.52, CH_2			L3NMe	
	NMe	3.16	33.16, CH_3			Vin2δ, L3β	L3α, Vin2CO
Leu4	CO	-	167.92				
	α	4.36	58.65, CH	L4β	L4β	Sta5NH, L3α	L4β, L4CO, L3CO
	β	2.31, 1.2	38.22, CH_2				
	NMe	2.83	28.57, CH_3			L3α	L4α, L3CO
Sta5	CO	-	171.5				
	α	2.11, 2.50	38.22, CH_2			Vin2β, L6α, L6NMe	
	β	4.05	72.18, CH	Sta5α	Sta5α,		
	γ	4.13	52.07, CH	Sta5δ, Sta5NH	Sta5δ, Sta5NH		Sta5δ, Sta4CO
	δ	1.46, 1.54	41.49, CH_2			P1α, L6NMe	
	NH	7.28			Sta5δ, Sta5γ	L4NMe, P1δ, L4α, L3α, L3NMe	Sta5γ, L4CO
Leu6	CO	-	171.1				
	α	5.40	52.21, CH	L6β	L6β	Sta5α, P1δ	L6β, L6NMe, L6CO
	β	1.66	37.43, CH_2				
	NMe	2.75	31.45, CH_3			Sta5δ, L6β, Sta5α, Vin2β, Vin2NH	L6α, Sta5CO

Monomers

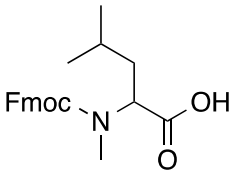

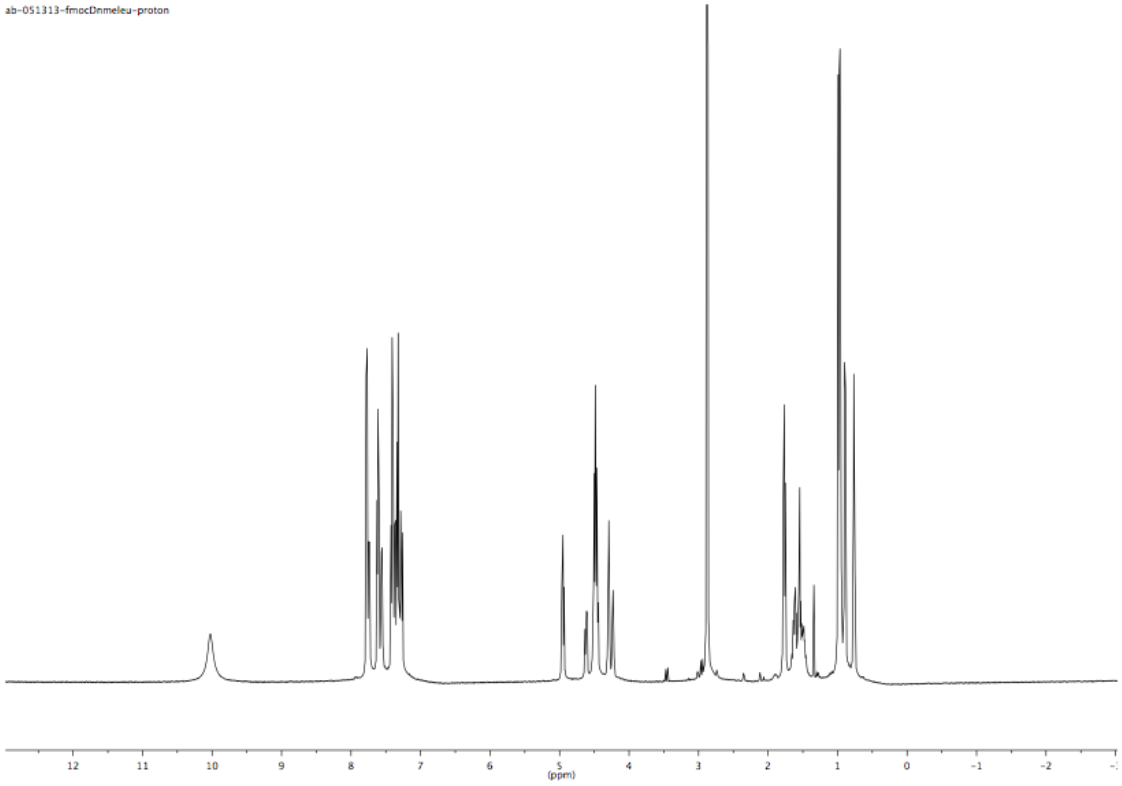

Figure S40. Fmoc-Nme-Leu Proton in $CDCl_3$

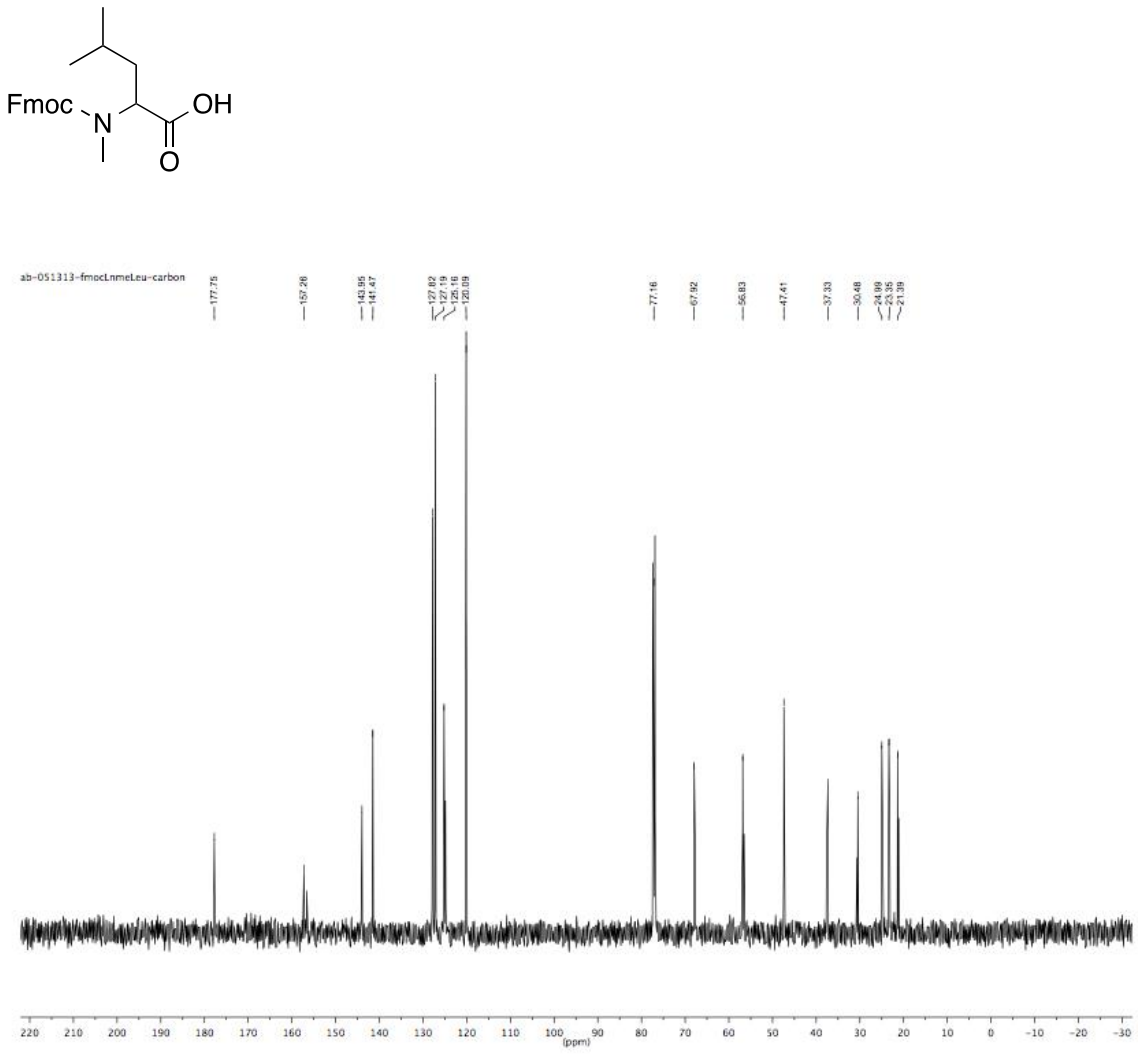

Figure S41. Fmoc-Nme-Leu Carbon in $CDCl_3$

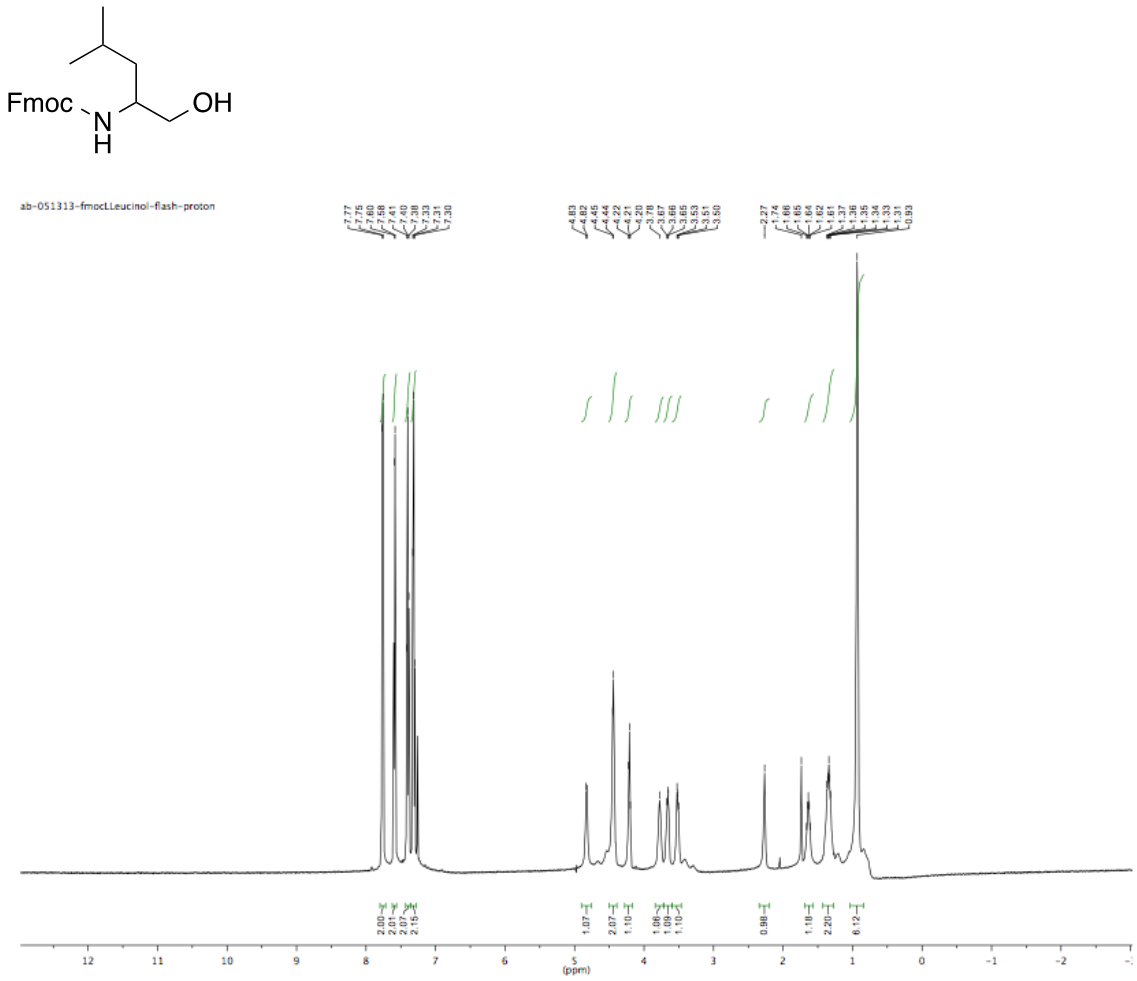

Figure S42. Fmoc-Leucinol Proton in $CDCl_3$

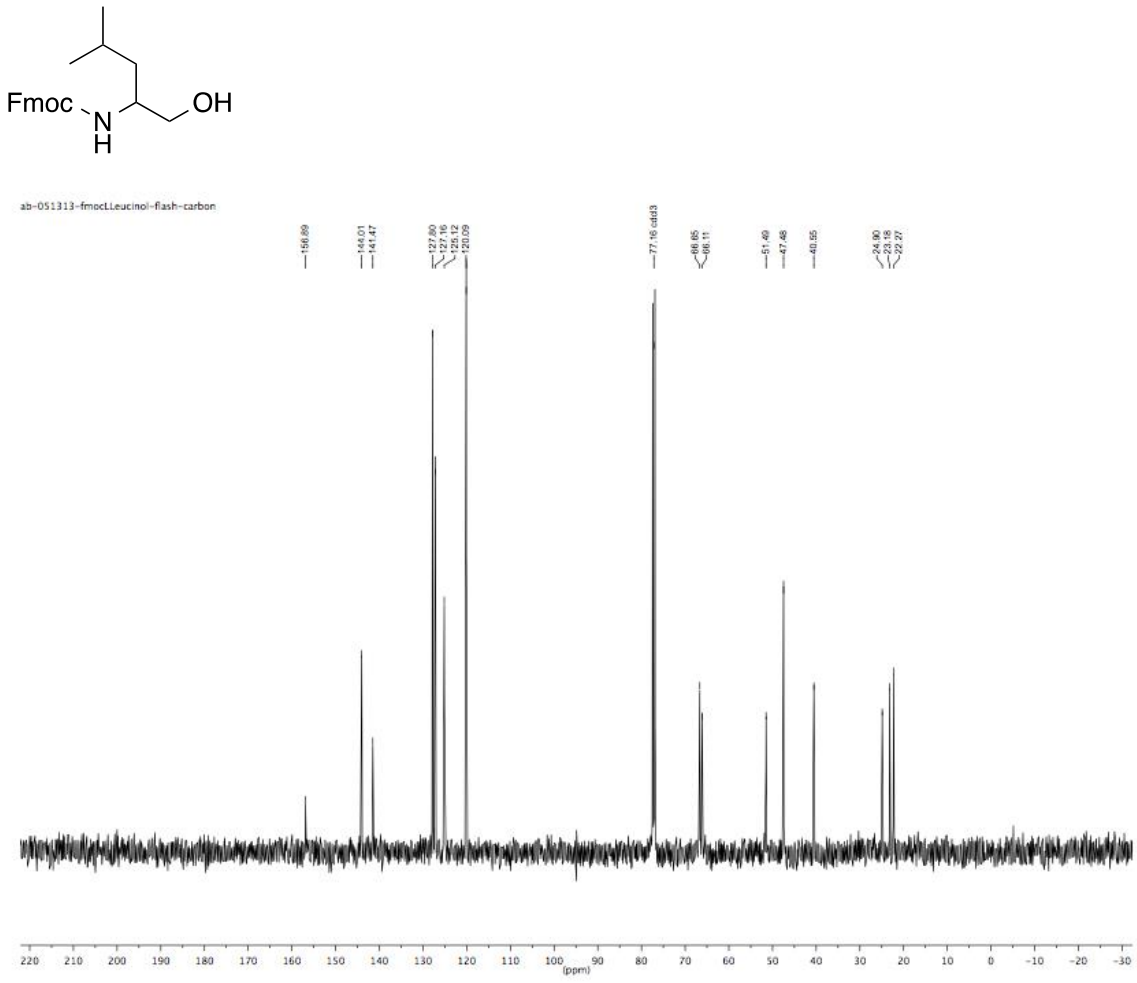

Figure S43. Fmoc-Leucinol Carbon in $CDCl_3$

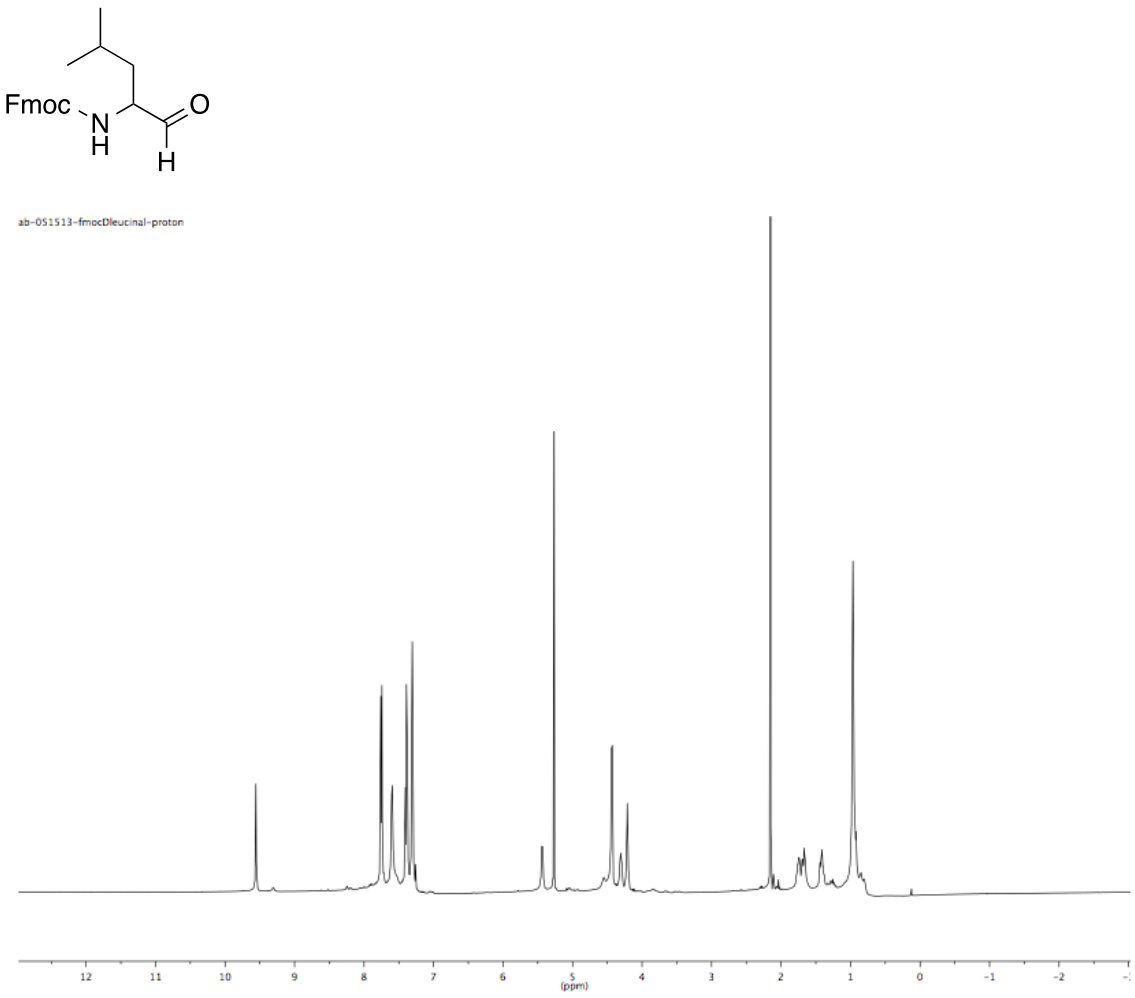

Figure S44. Fmoc-Leucinal Proton in $CDCl_3$

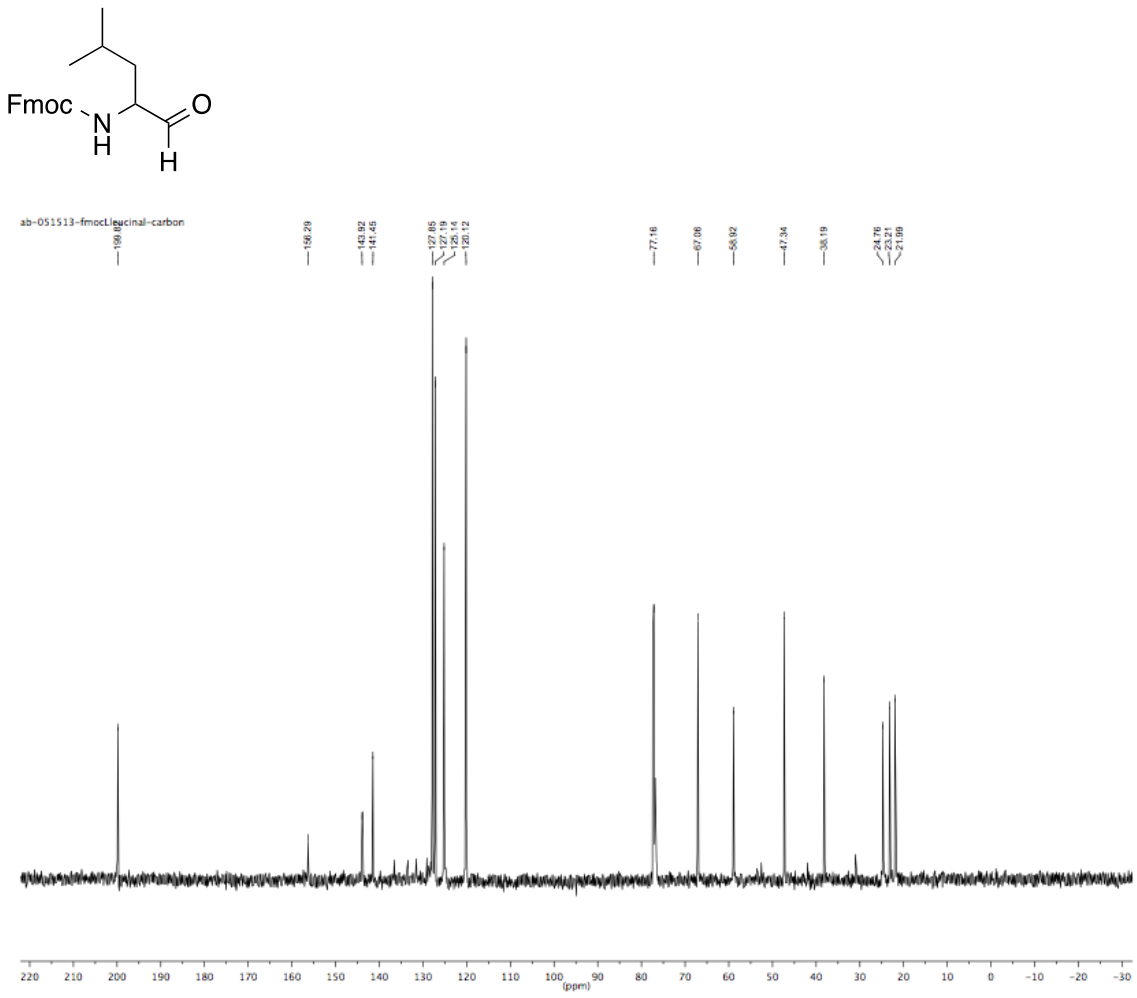

Figure S45. Fmoc-Leucinal Carbon in $CDCl_3$

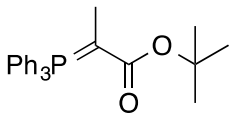

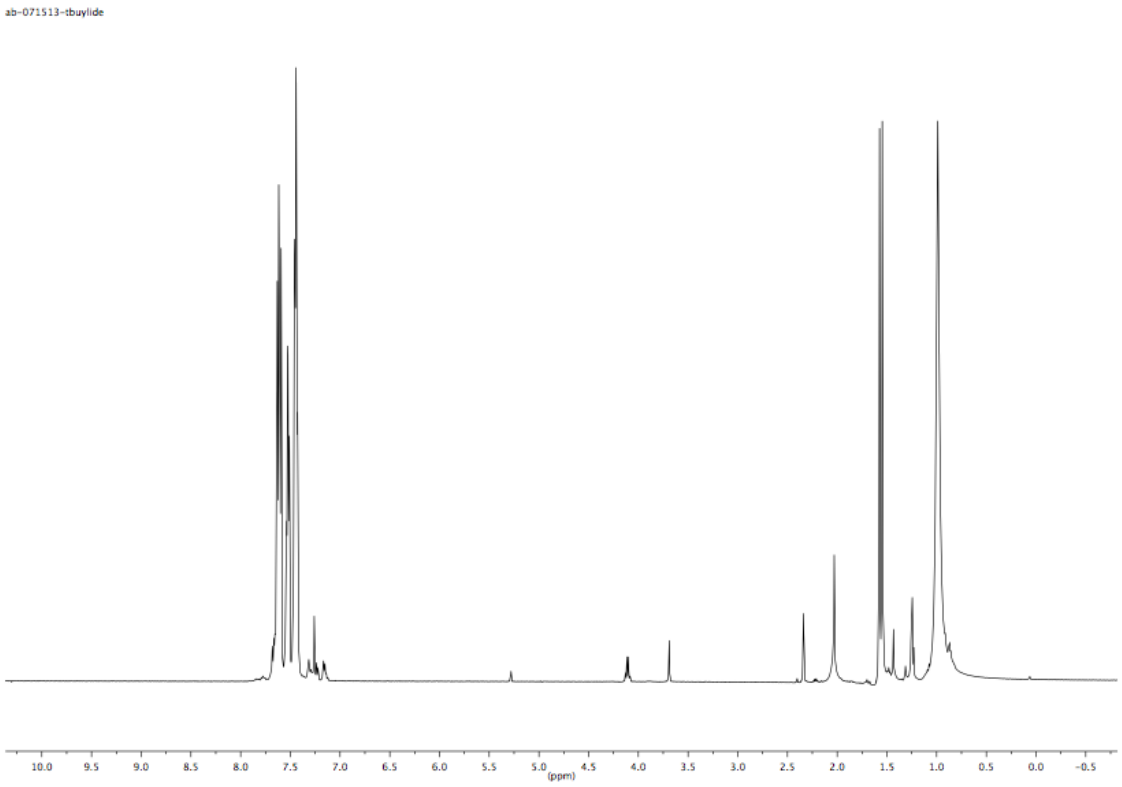

Figure S46. *tert*-butyl ylide Proton in $CDCl_3$

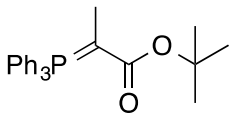

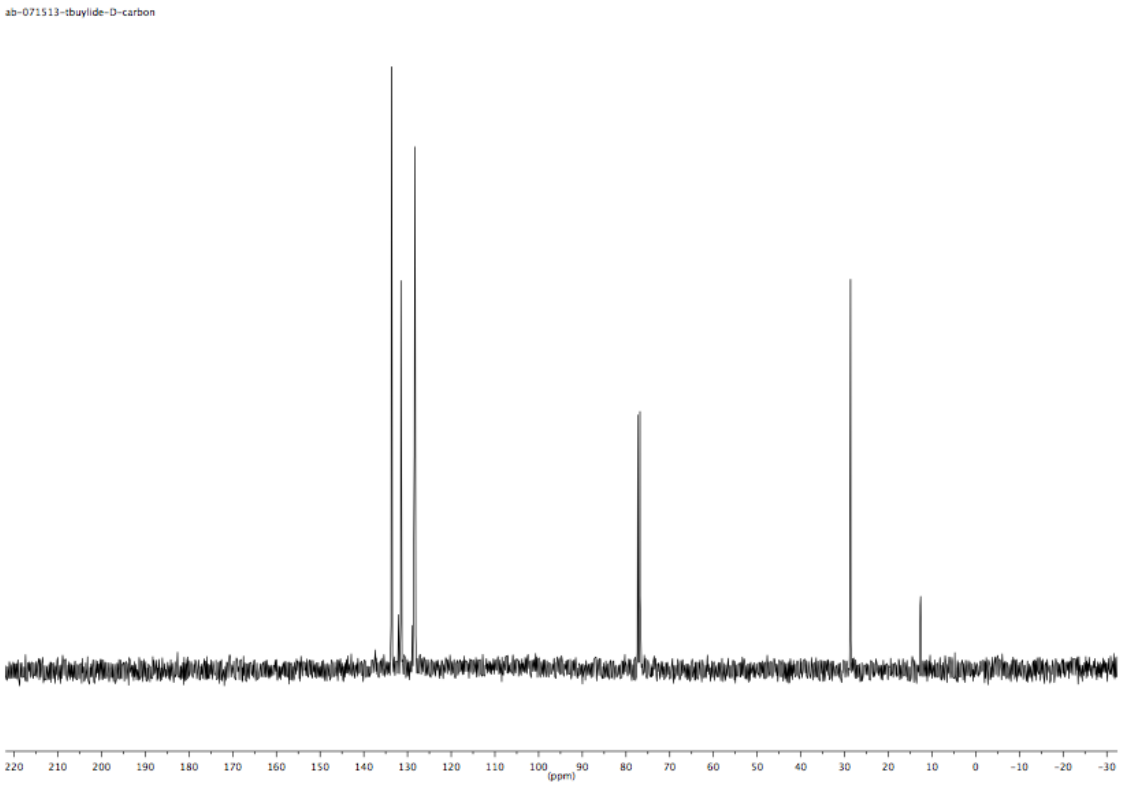

Figure S47. *tert*-butyl ylide Carbon in $CDCl_3$

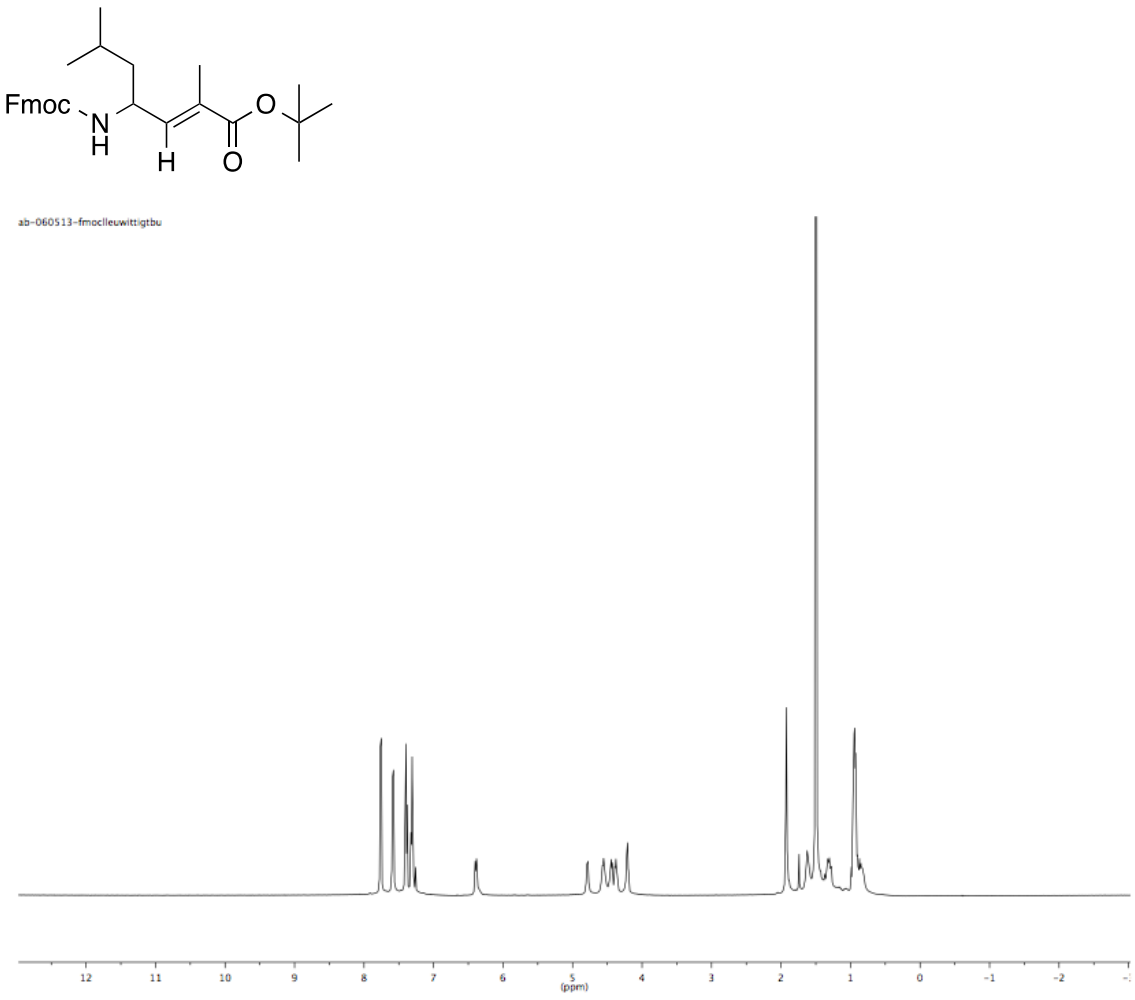

Figure S48. Fmoc-Leu-vinylogue tBu ester Proton in $CDCl_3$

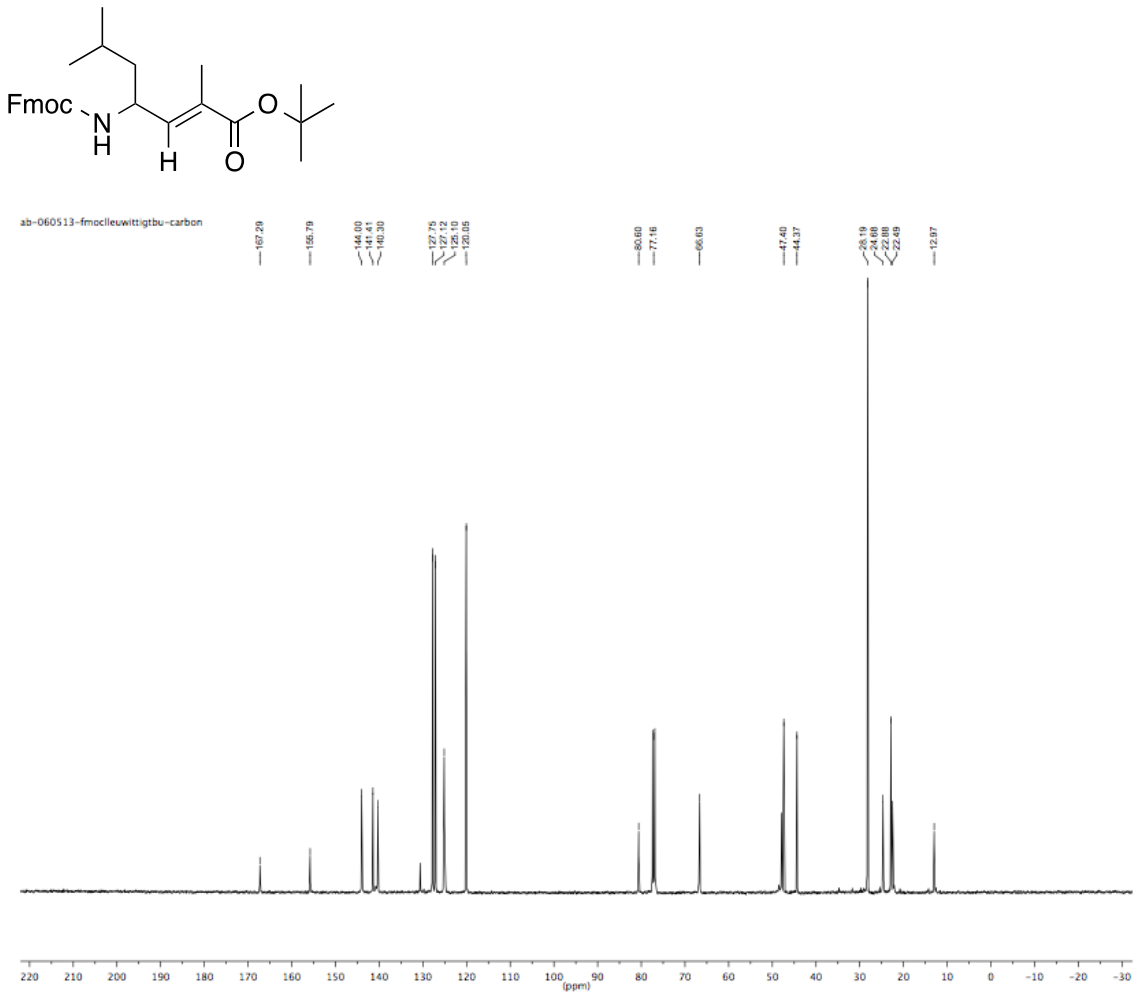

Figure S49. Fmoc-Leu-vinylogue tBu ester Carbon in $CDCl_3$

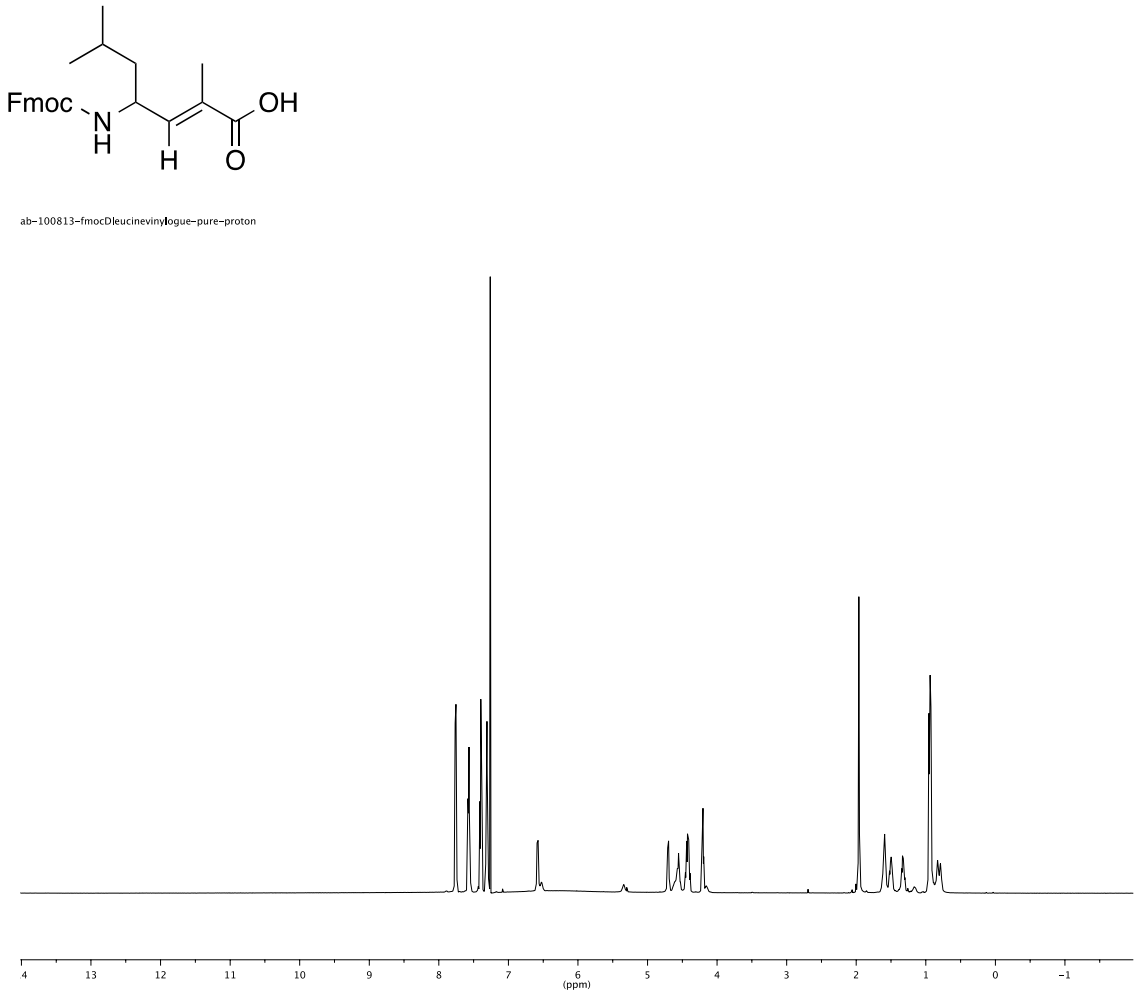

Figure S50. Fmoc-Leu-vinylogue acid Proton in $CDCl_3$

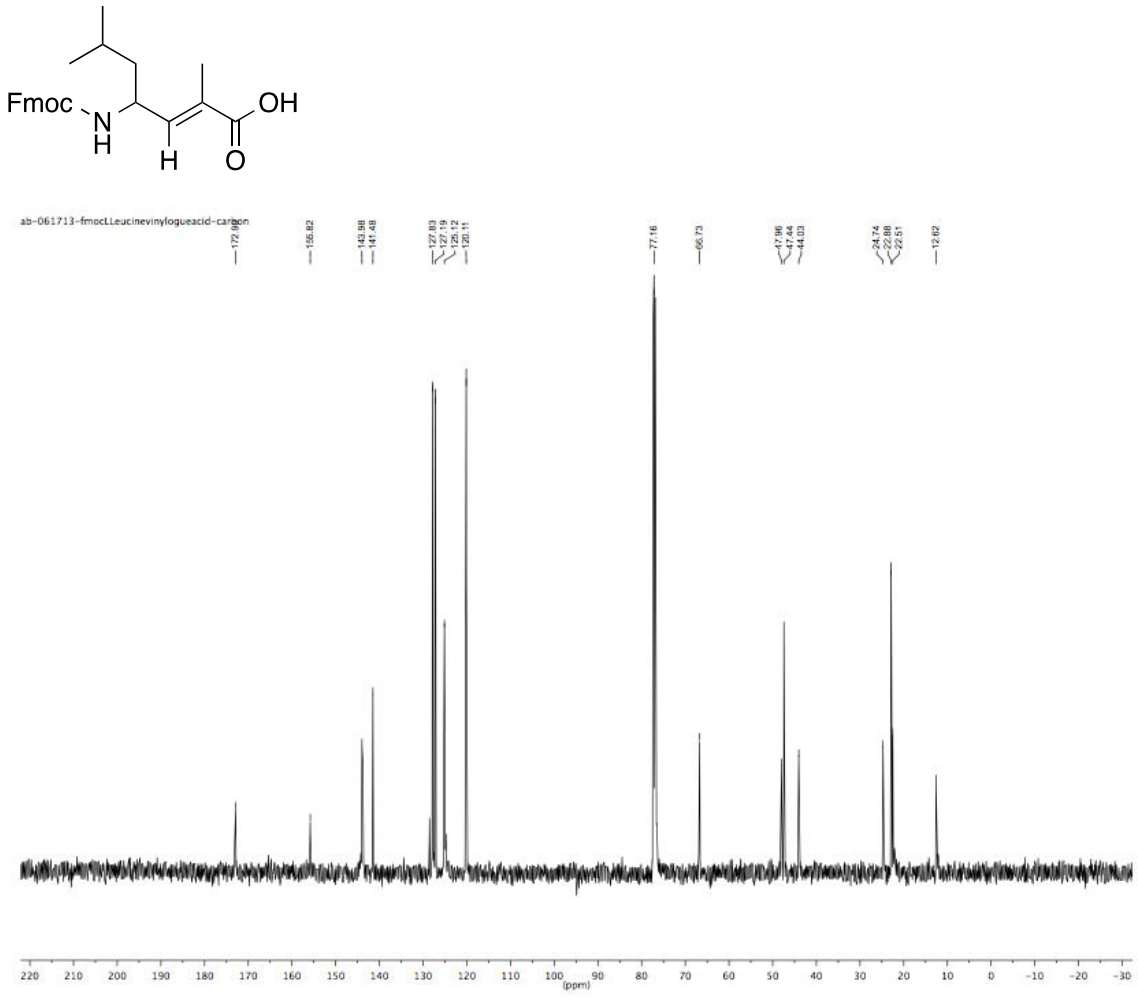

Figure S51. Fmoc-Leu-vinylogue acid Carbon in $CDCl_3$

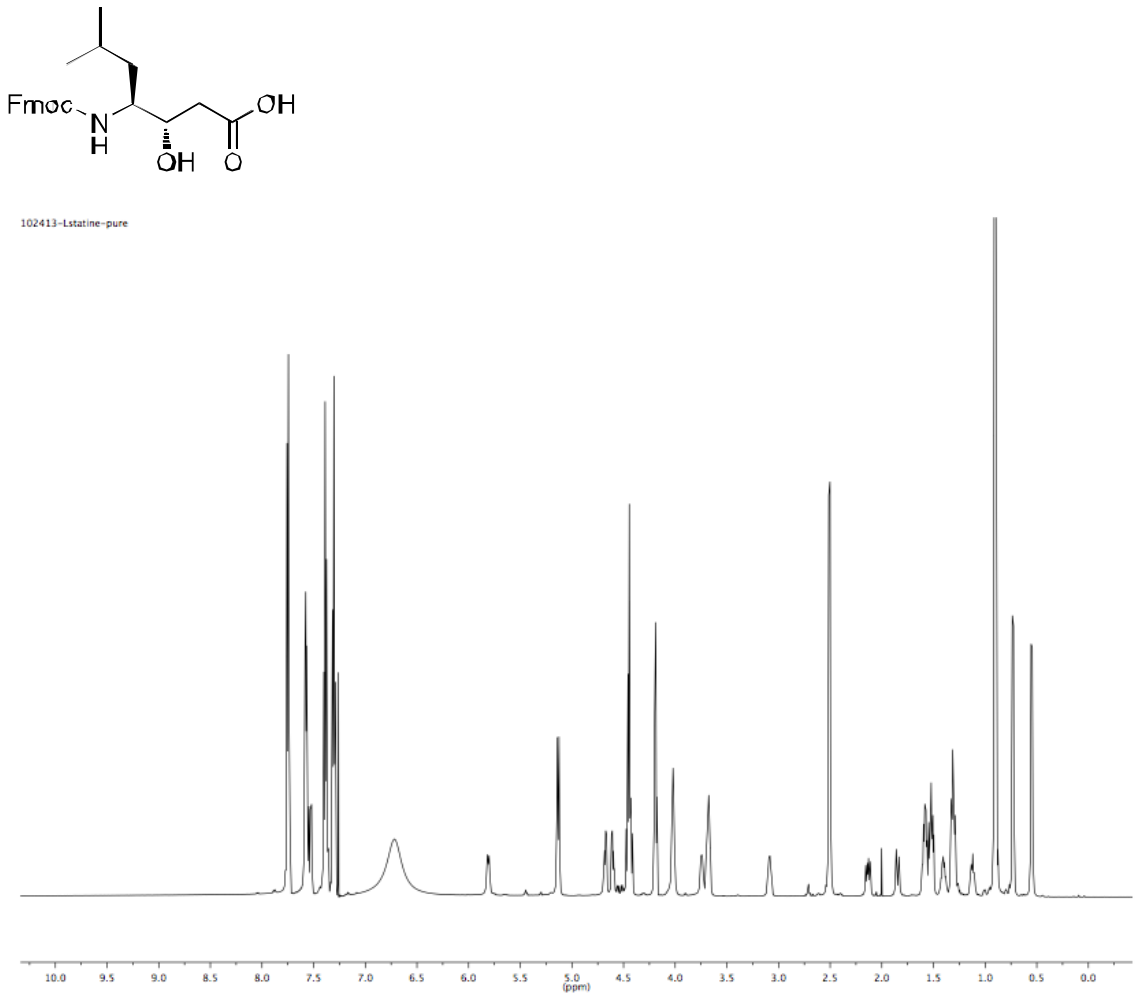

Figure S52. Fmoc-Statine Proton in $CDCl_3$

NOESY Buildup Curves

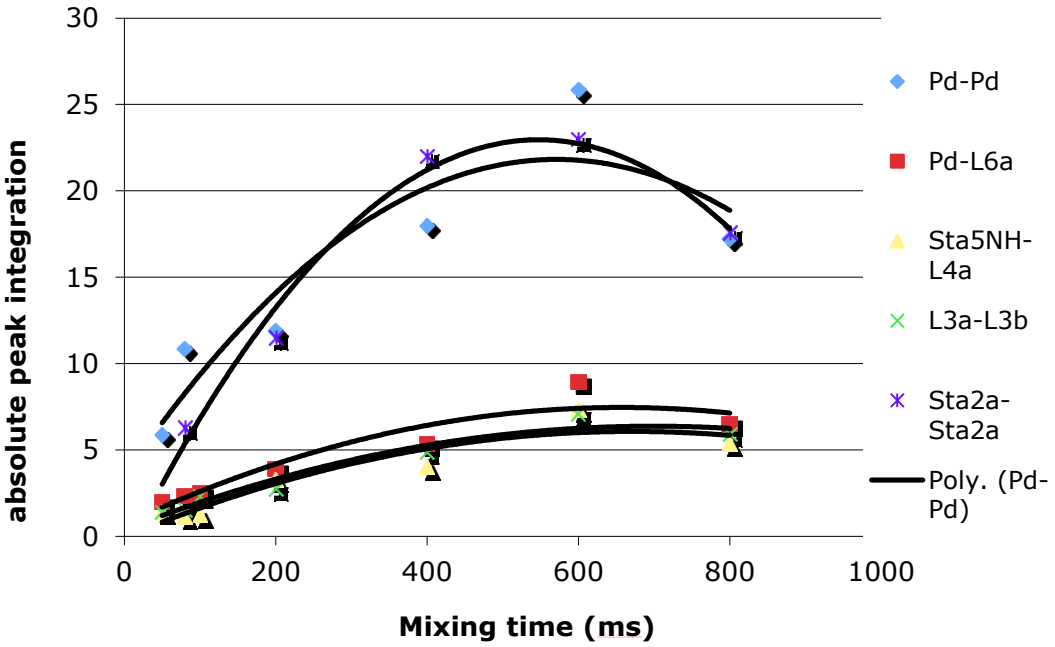

Figure S53. Macrocycle **4** NOESY Buildup Curves in $CDCl_3$ at 25 °C

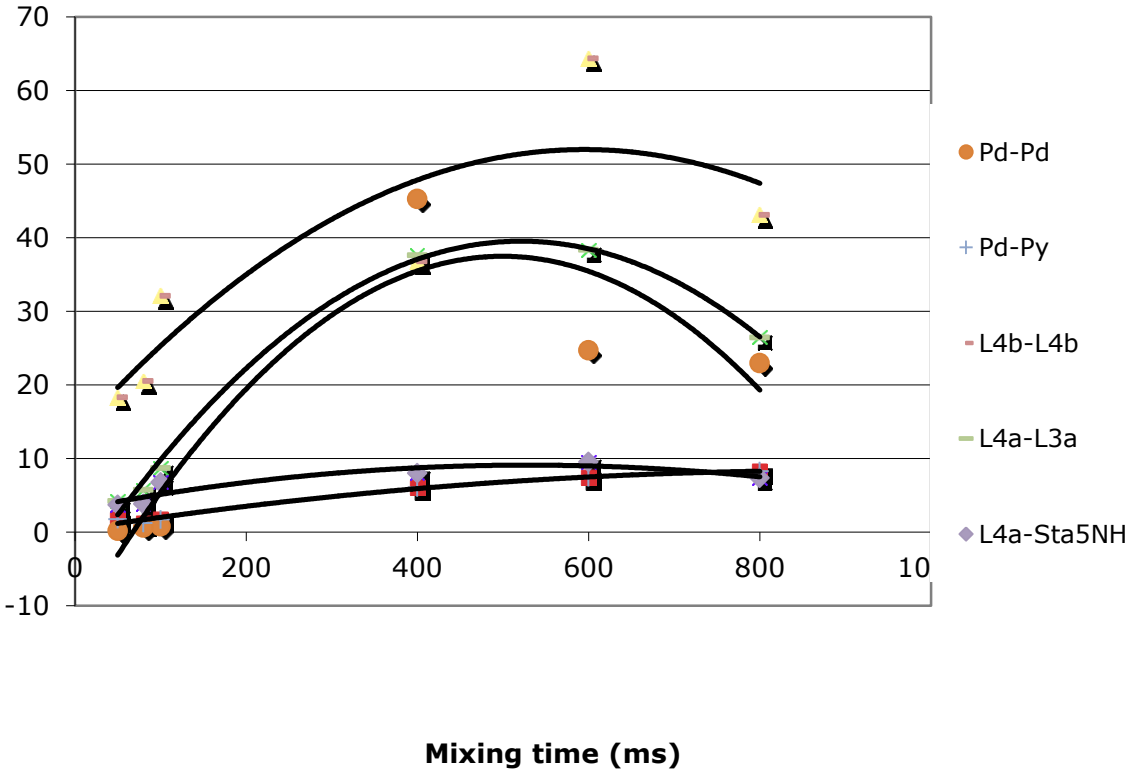

Figure S54. Macrocycle **14** NOESY Buildup Curves in $CDCl_3$ at 25 °C

VII. LC-MS SPECTRA

Monomer LC-MS

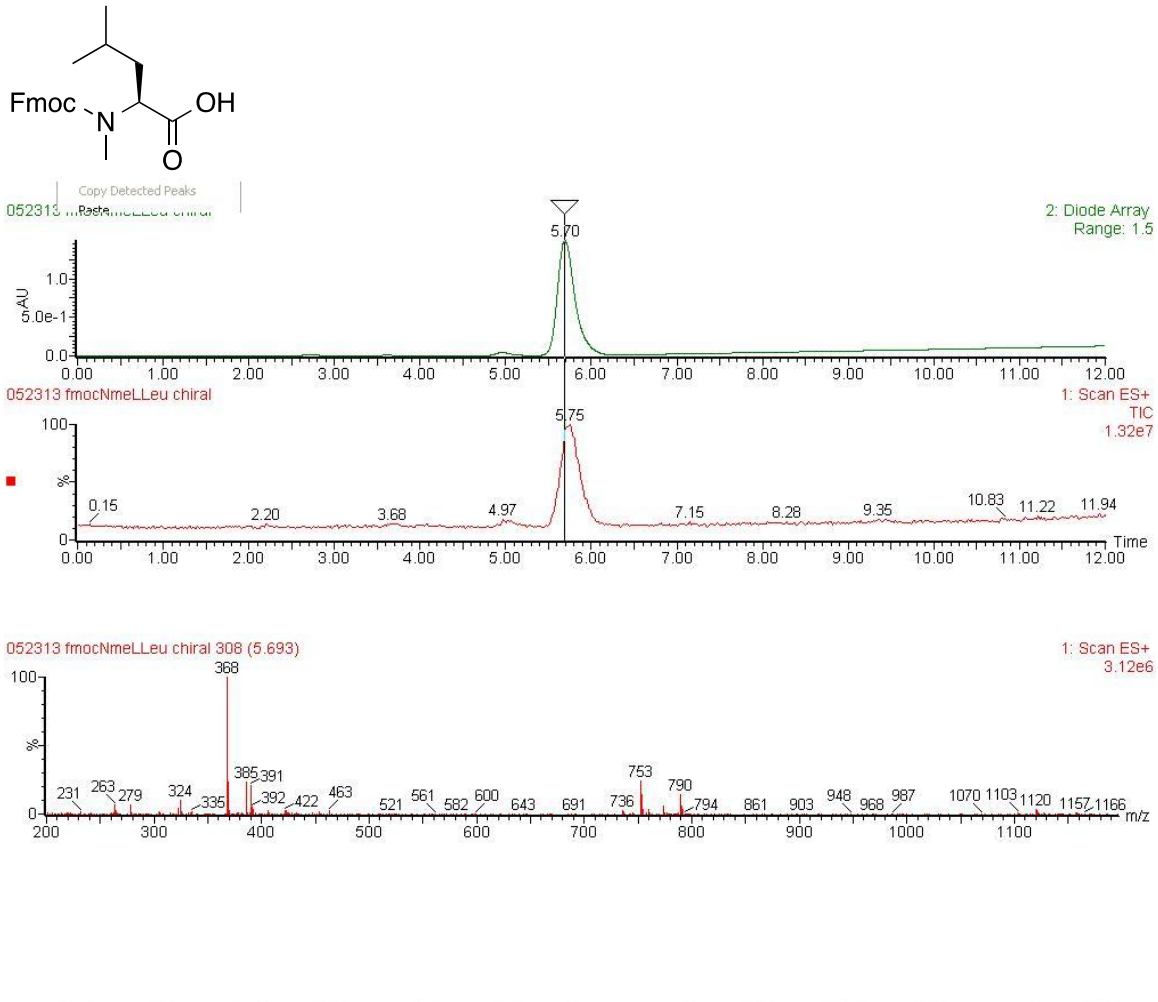

Figure S55. Fmoc-**L**-Nme-Leu Chiral LC-MS. RT = 5.75 min

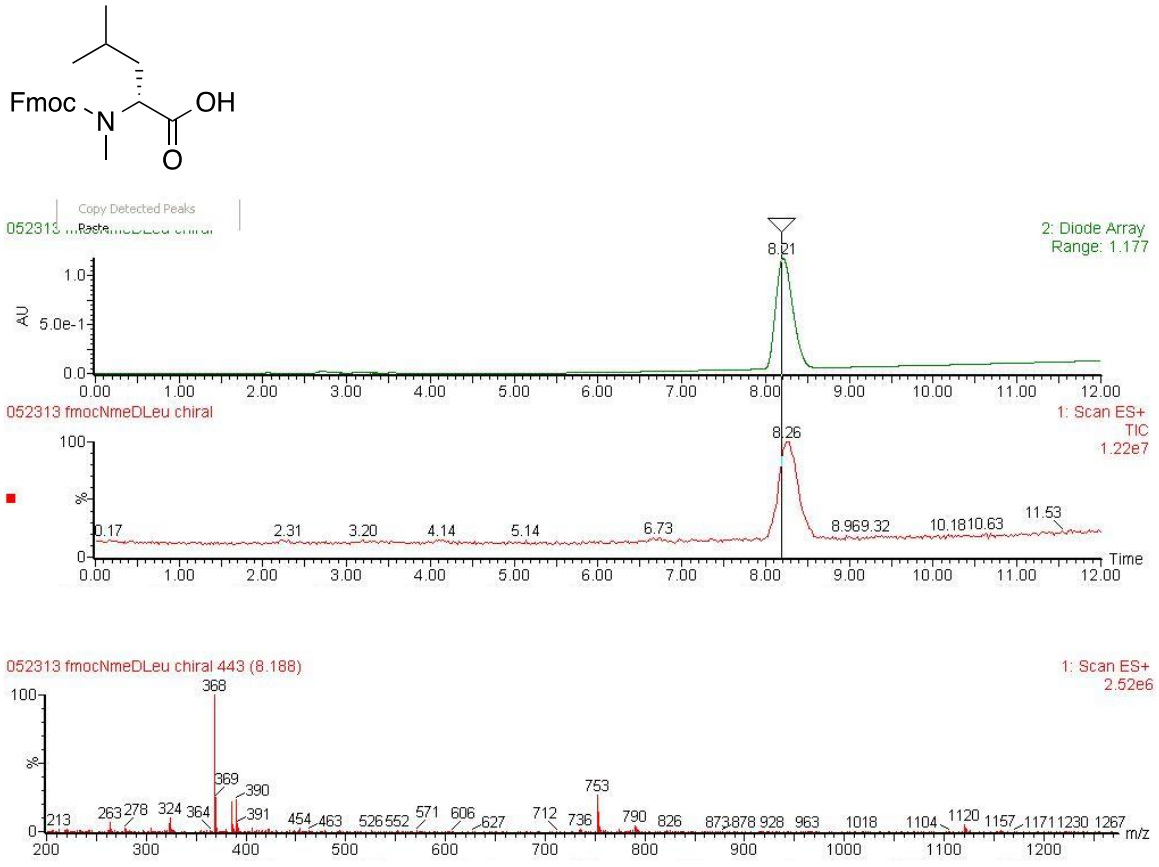

Figure S56. Fmoc-**D**-Nme-Leu Chiral LC-MS. RT = 8.26 min

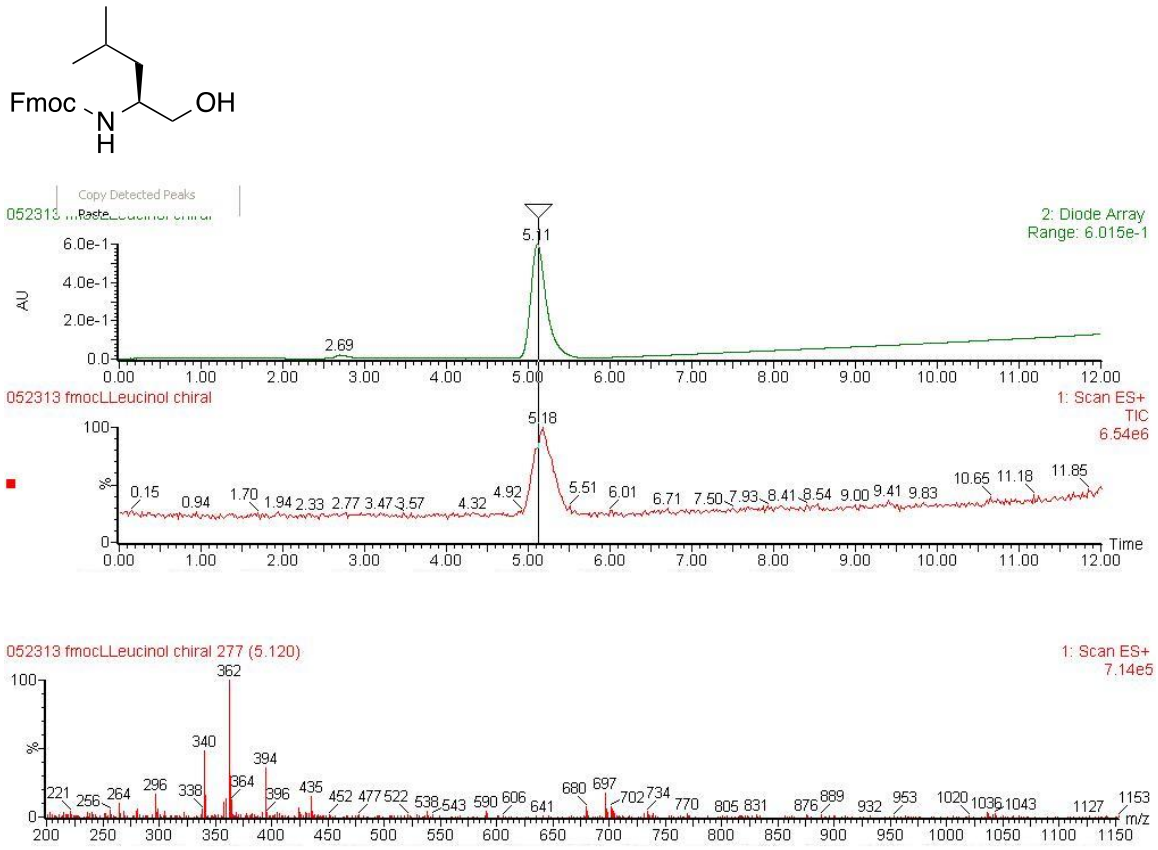

Figure S57. Fmoc-**L**-Leucinol Chiral LC-MS. RT = 5.18 min

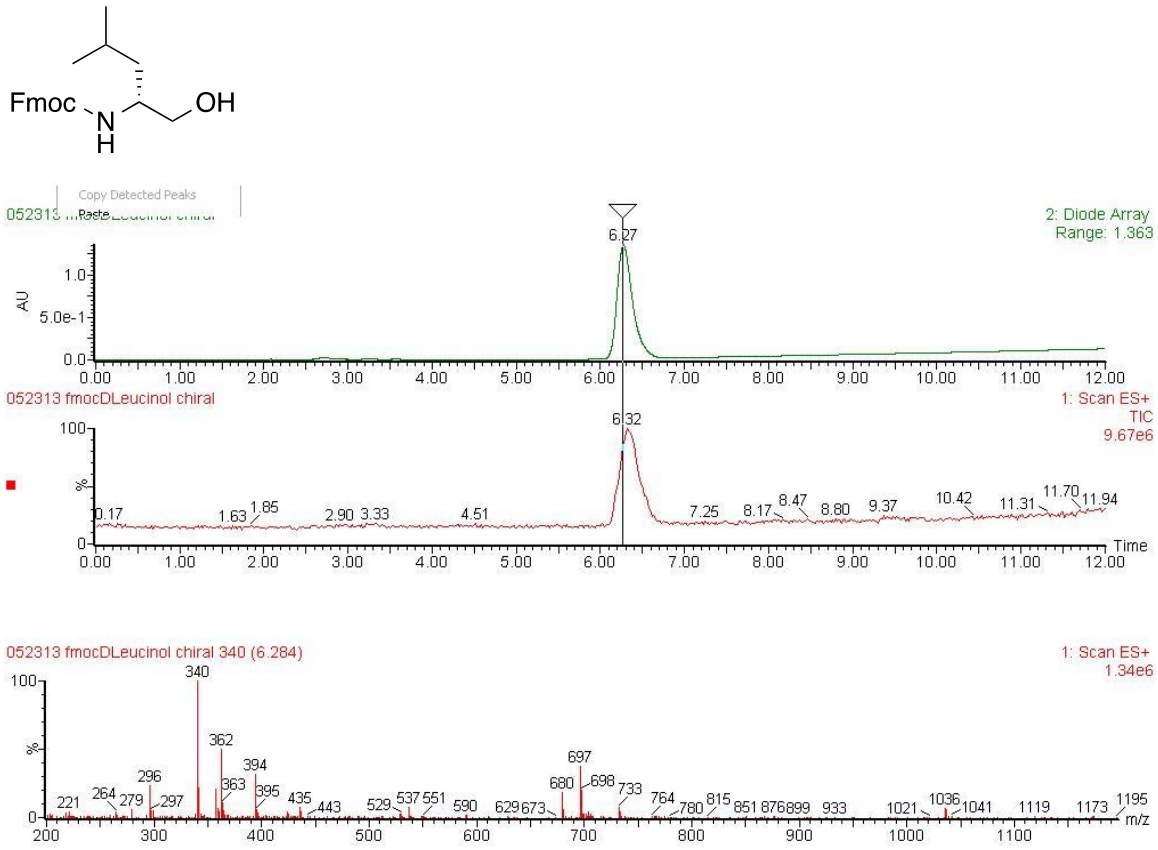

Figure S58. Fmoc-**D**-Leucinol Chiral LC-MS. RT = 6.32 min

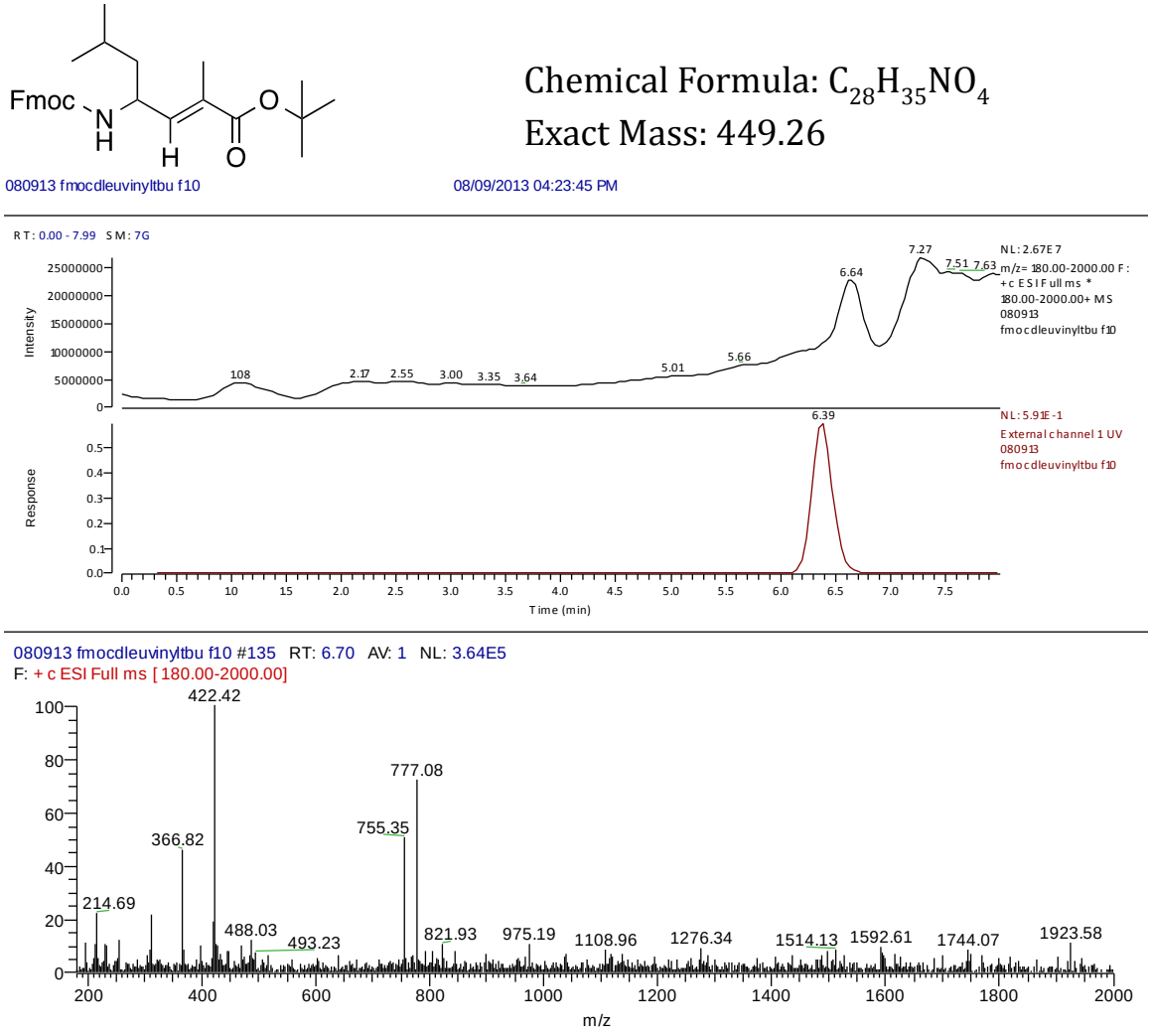

Figure S59. Fmoc-Leu-vinylogue tBu ester LC-MS

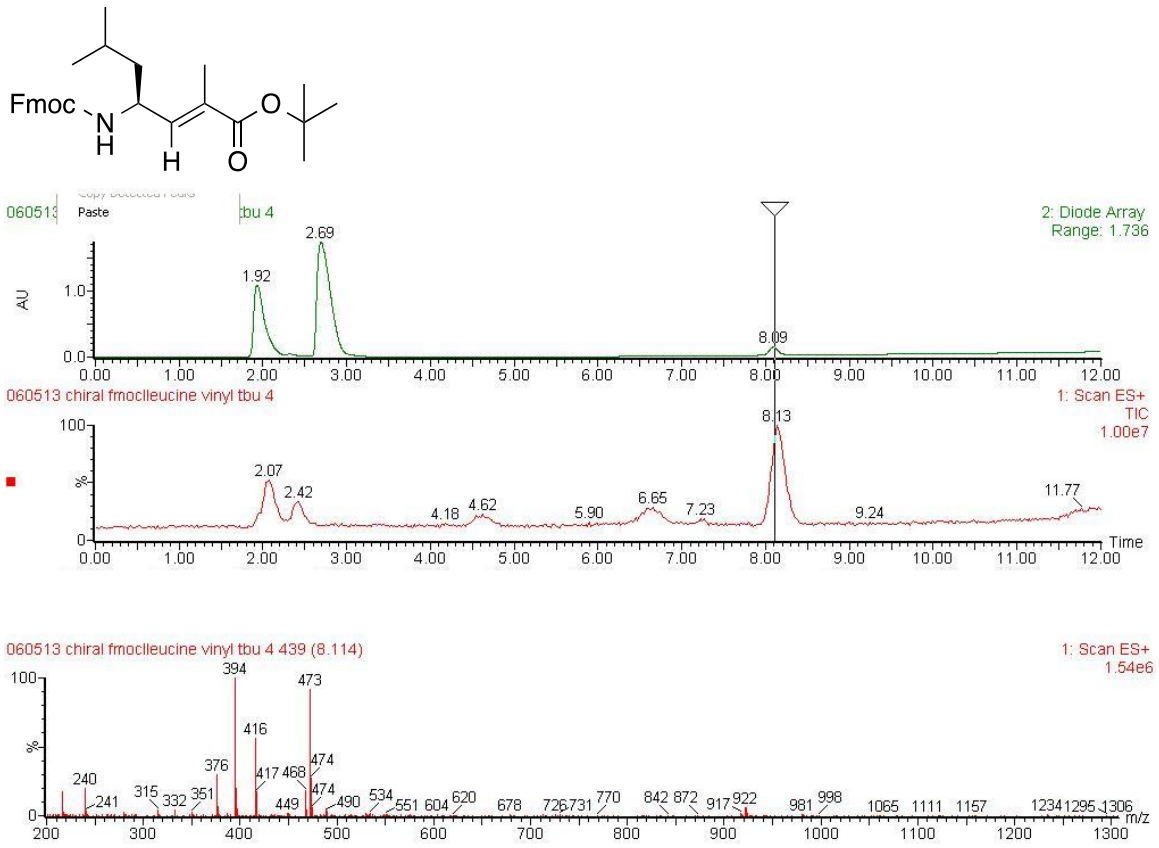

Figure S60. Fmoc-**L**-Leu-vinylogue tBu ester Chiral LC-MS. RT = 8.13 min

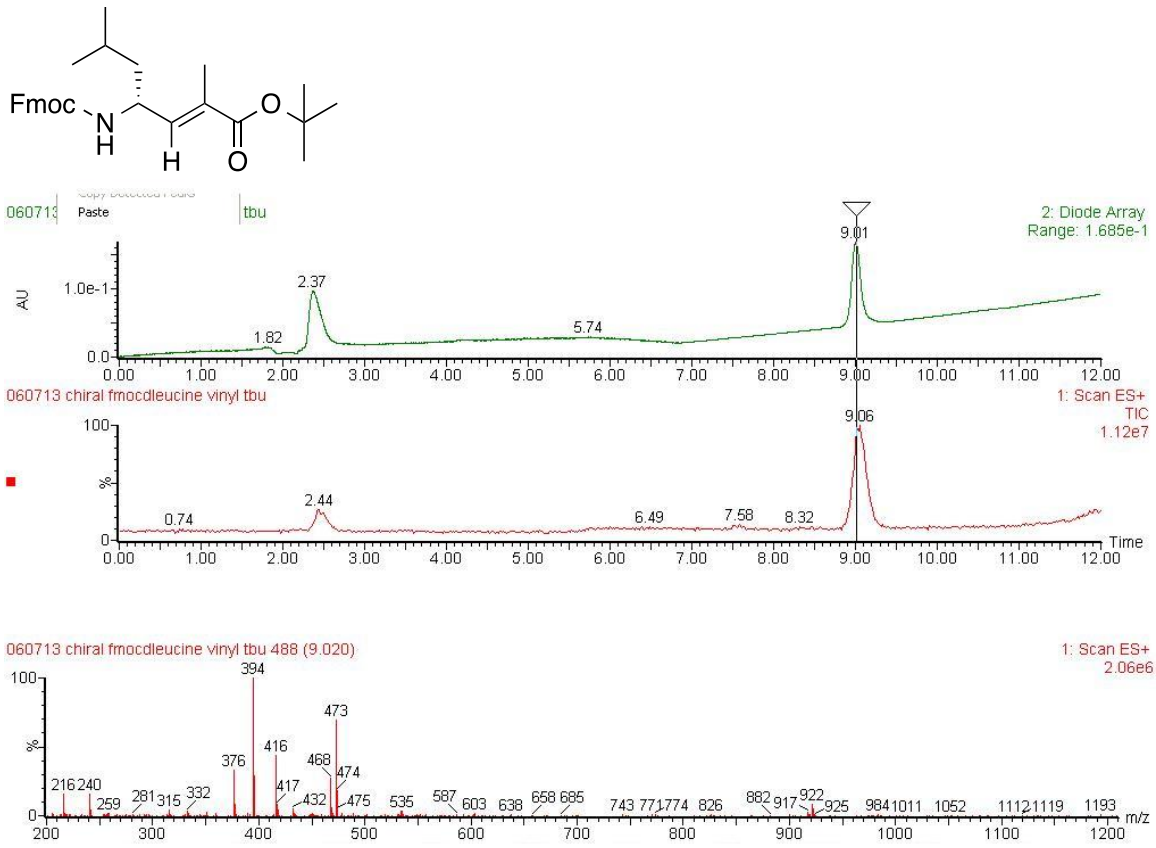

Figure S61. Fmoc-**D**-Leu-vinylogue tBu ester Chiral LC-MS. RT = 9.06 min

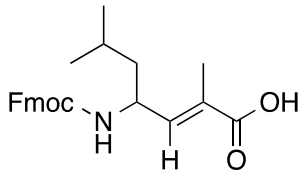

Chemical Formula: $C_{24}H_{27}NO_4$

Exact Mass: 393.19

ab 100813 dvinylogue prep

10/08/2013 05:03:04 PM

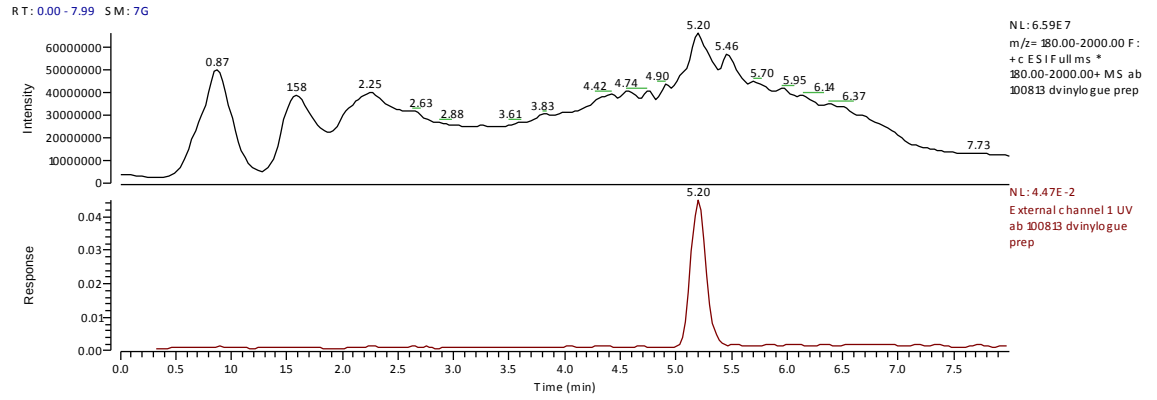

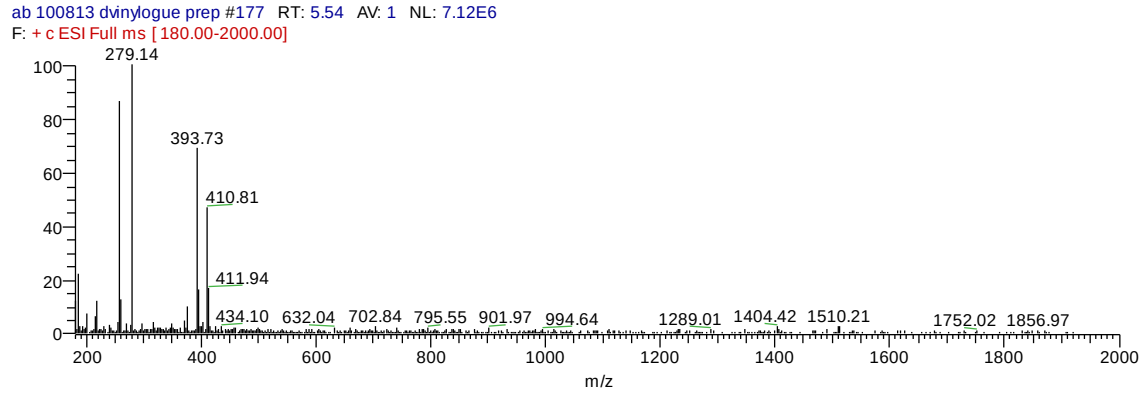

Figure S62. Fmoc-Leu-vinylogue acid LC-MS

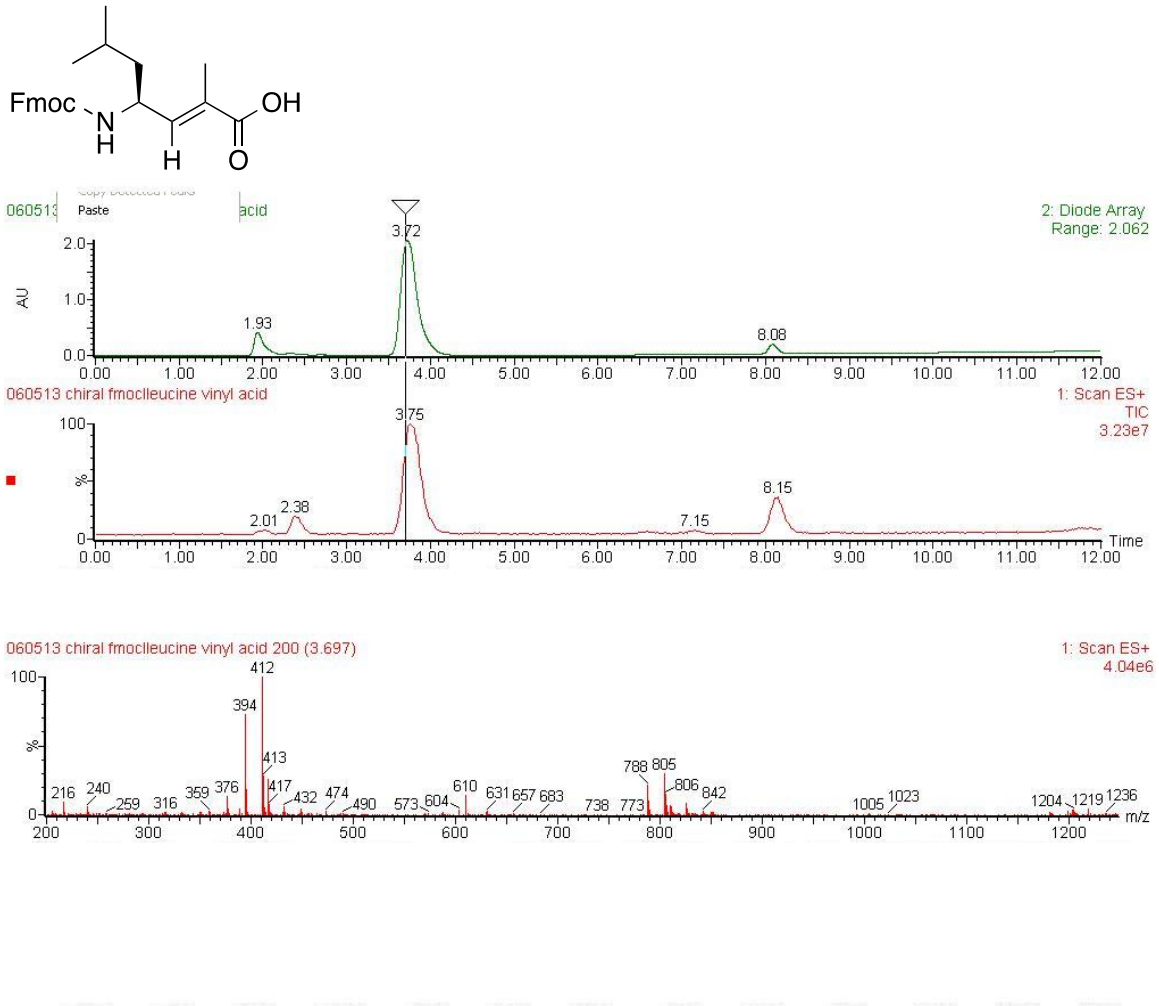

Figure S63. Fmoc-**L**-Leu-vinylogue acid Chiral LC-MS. RT = 3.75 min

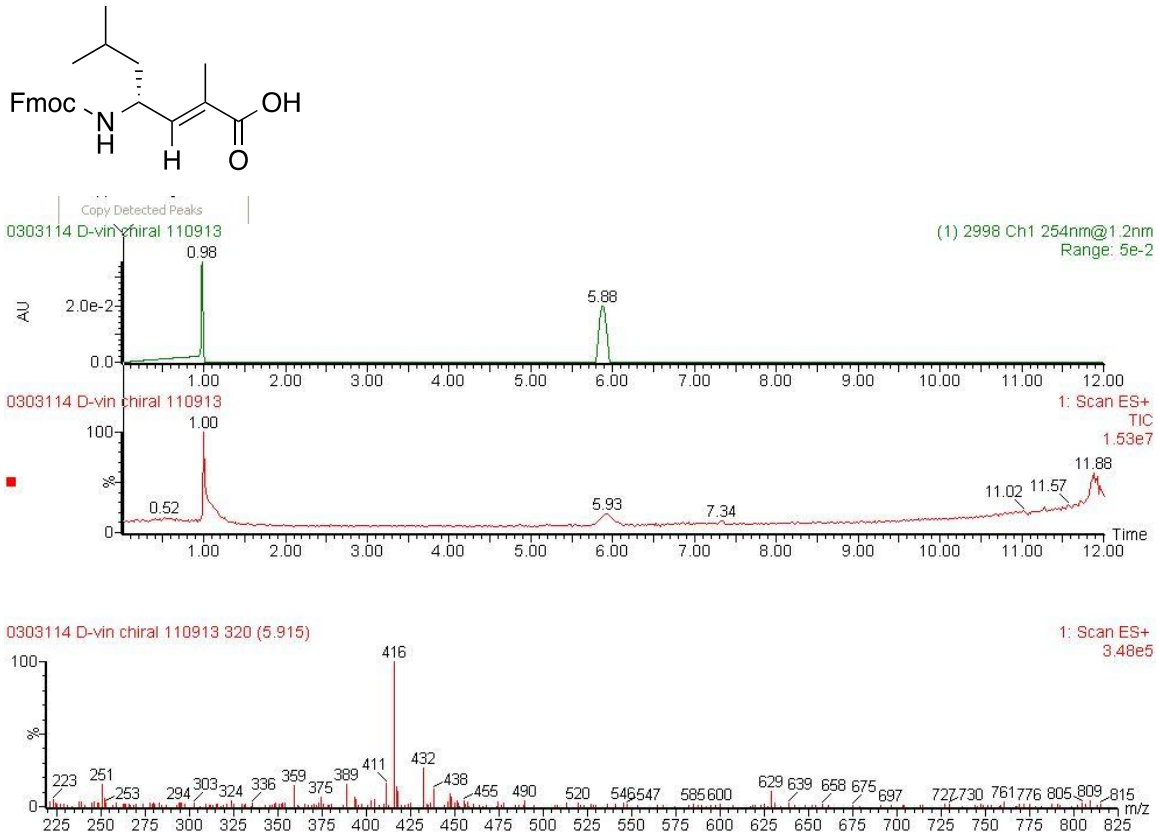

Figure S64. Fmoc-**D**-Leu-vinylogue acid Chiral LC-MS. RT = 5.93 min

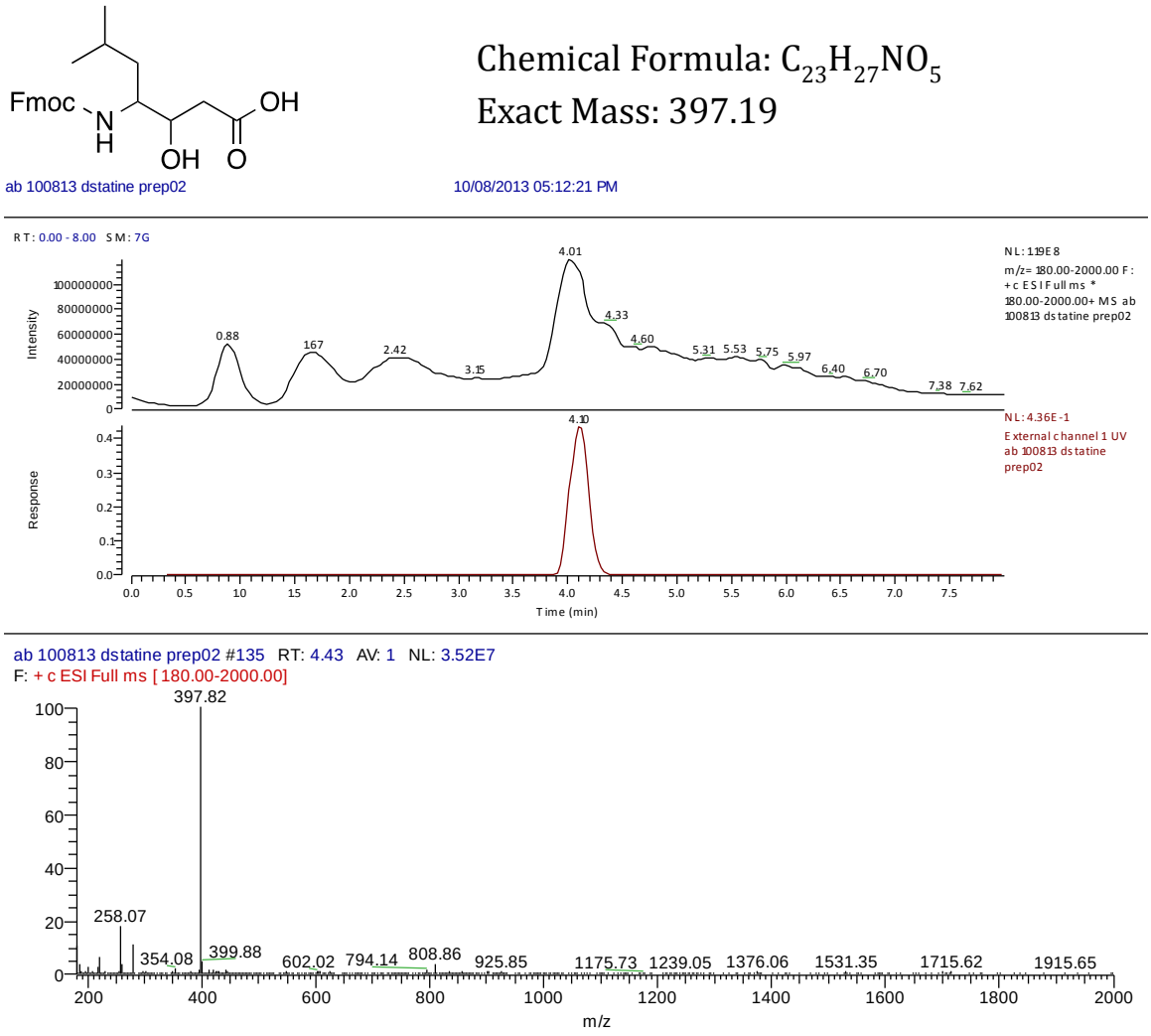

Figure S65. Fmoc-Statine LC-MS

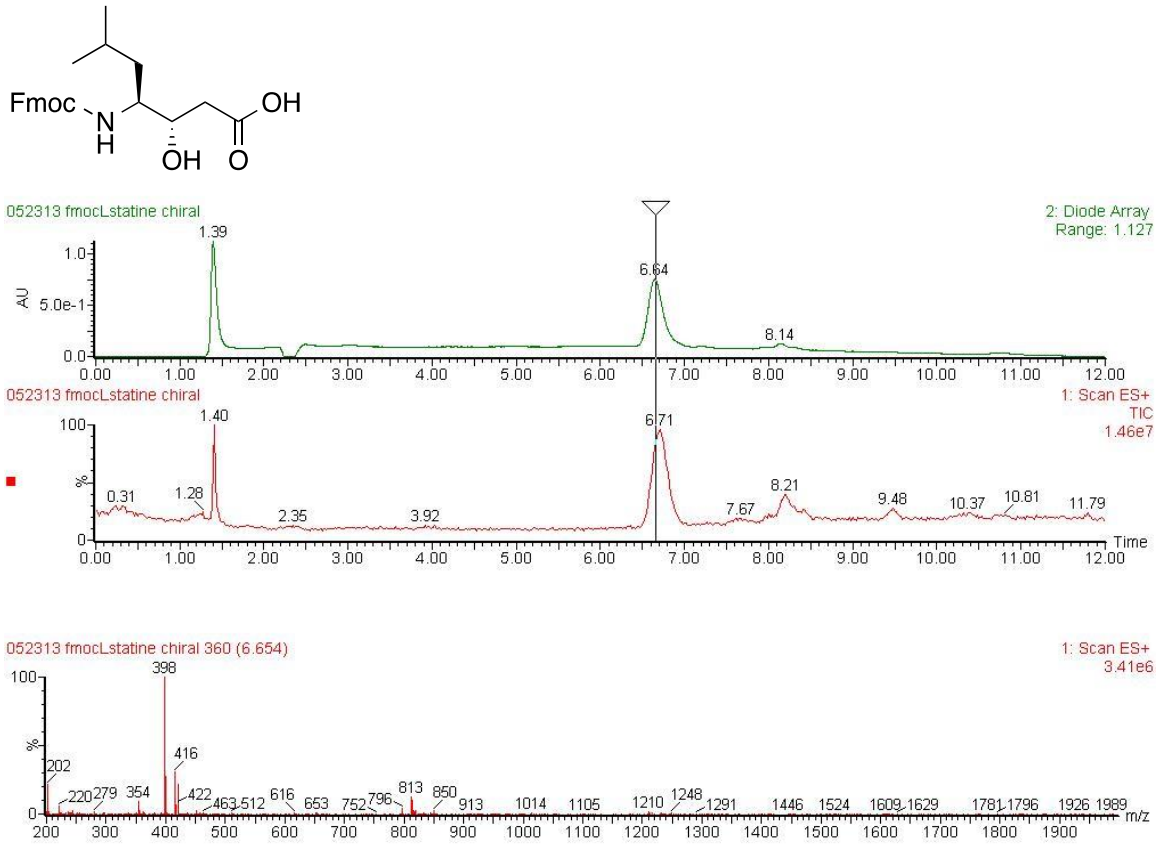

Figure S66. Fmoc-(**S,S**)-Statine Chiral LC-MS. RT = 6.71 min

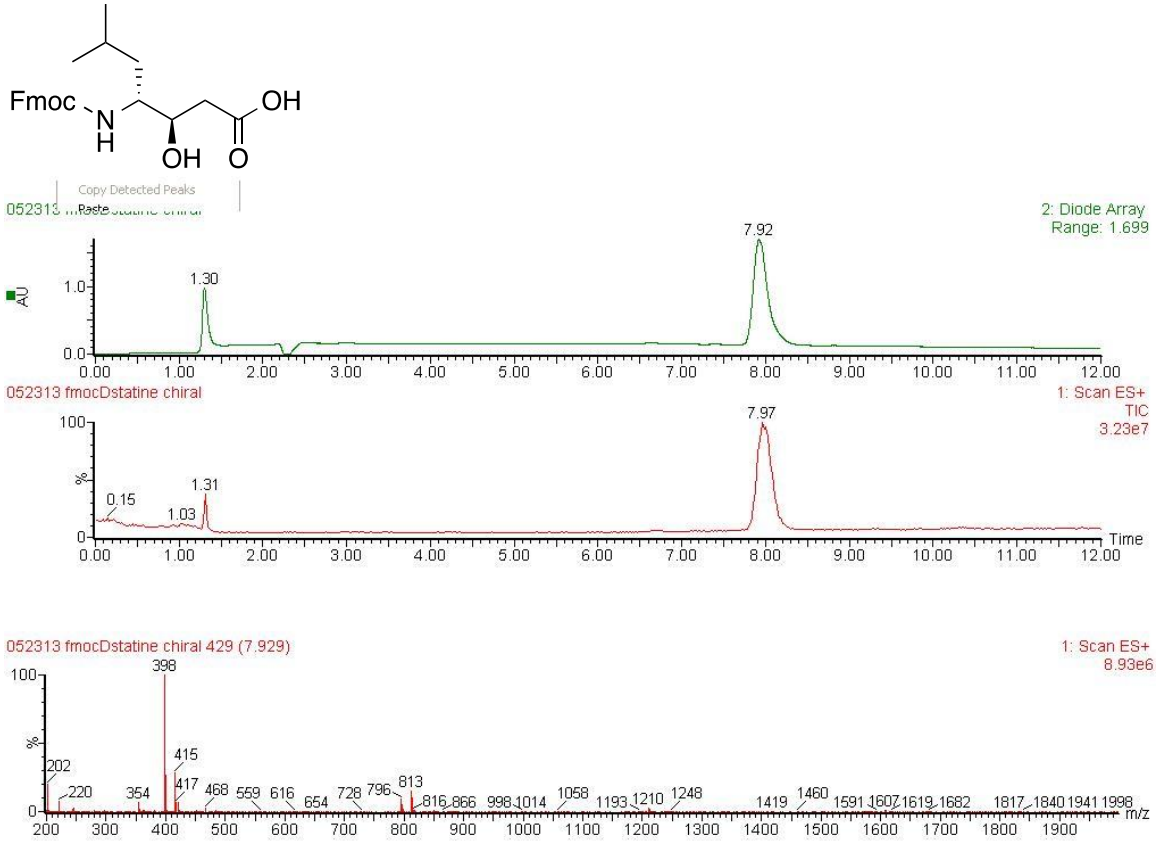

Figure S67. Fmoc-(**R,R**)-Statine Chiral LC-MS. RT = 7.97 min

Macrocycle LC-MS

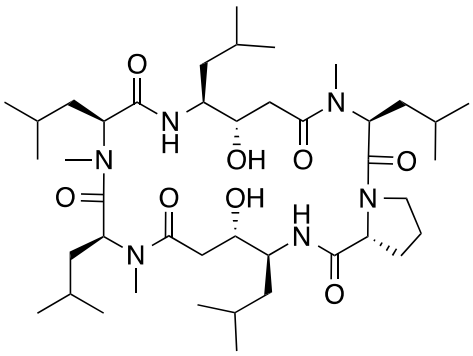

Chemical Formula: $C_{42}H_{76}N_6O_8$
Exact Mass: 792.57

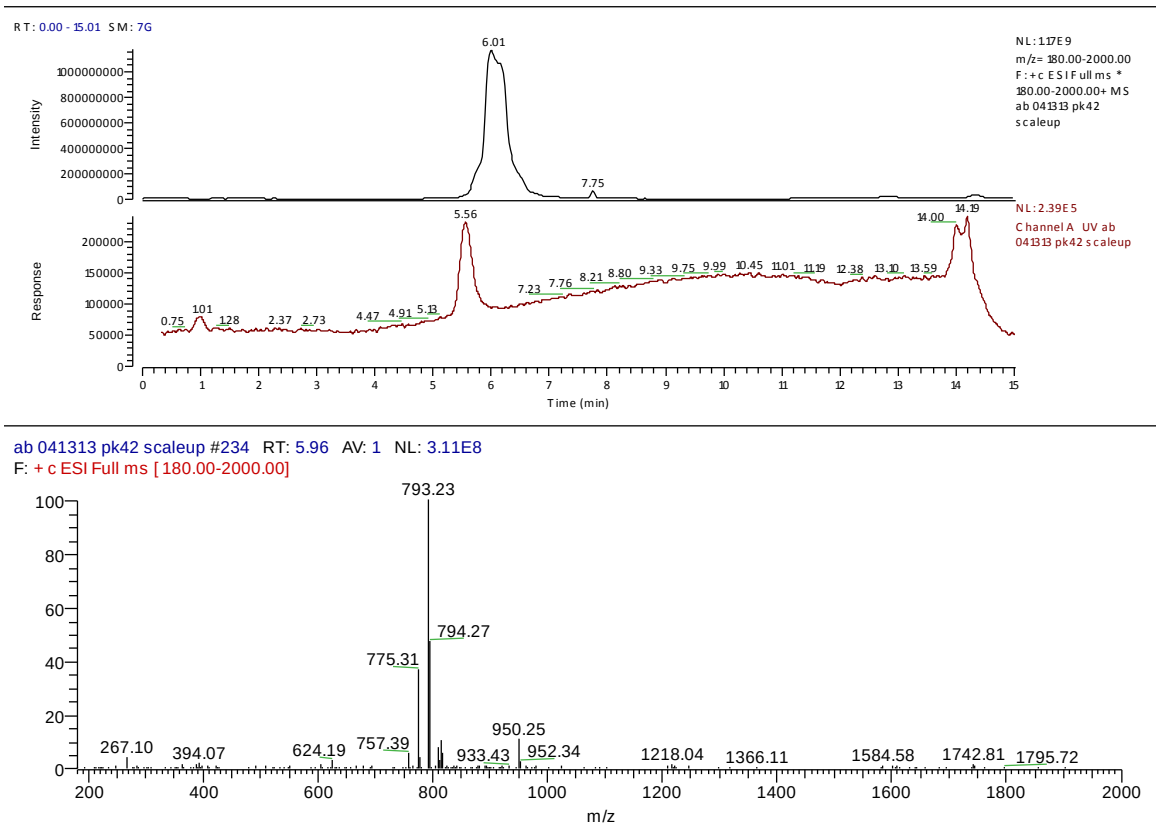

Figure S68. Cyclic **1** LC-MS

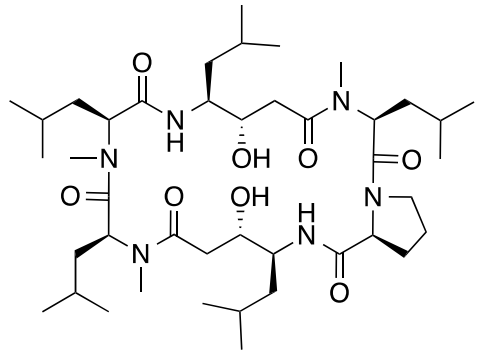

Chemical Formula: $C_{42}H_{76}N_6O_8$
Exact Mass: 792.57

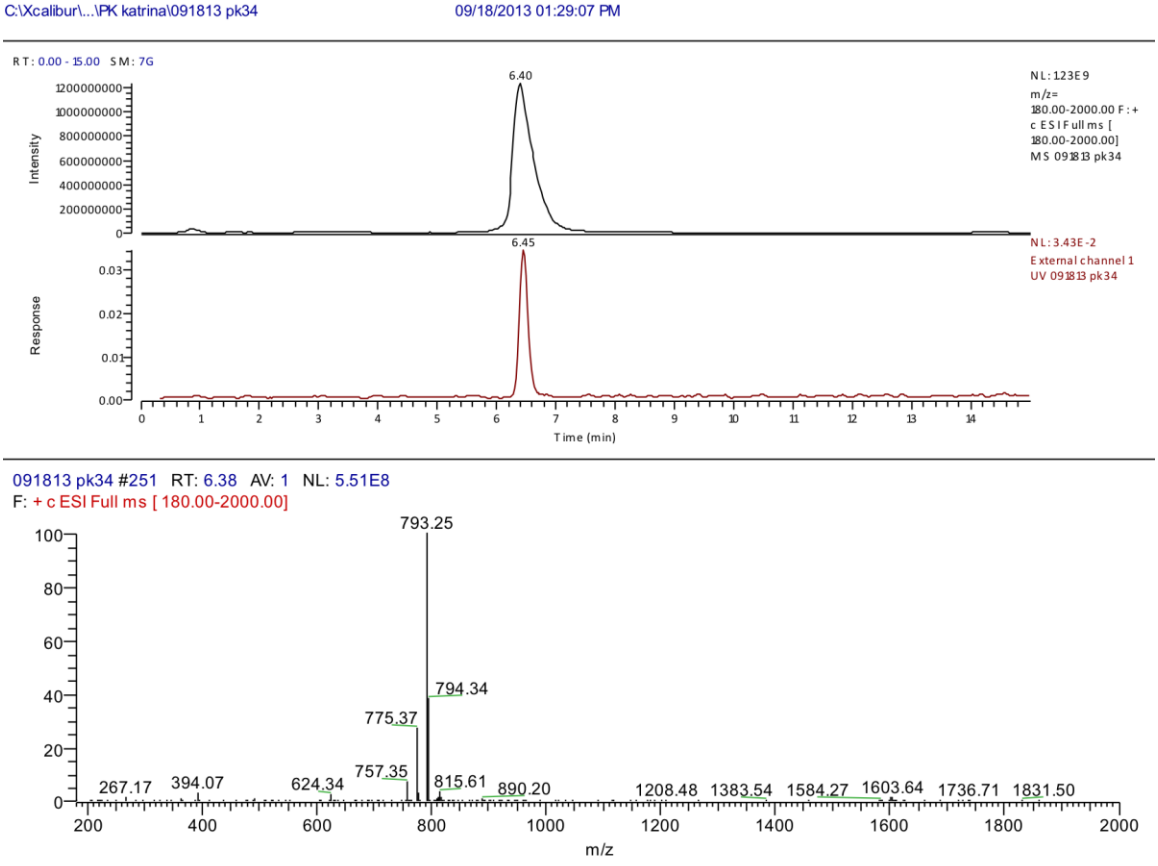

Figure S69. Cyclic **2** LC-MS

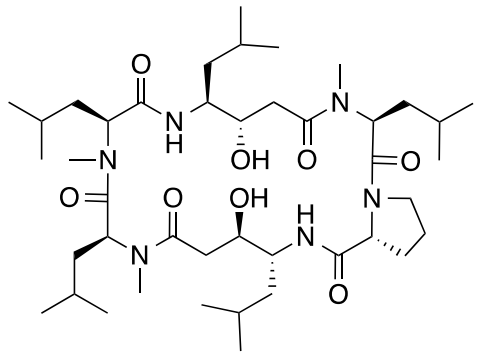

Chemical Formula: $C_{42}H_{76}N_6O_8$

Exact Mass: 792.57

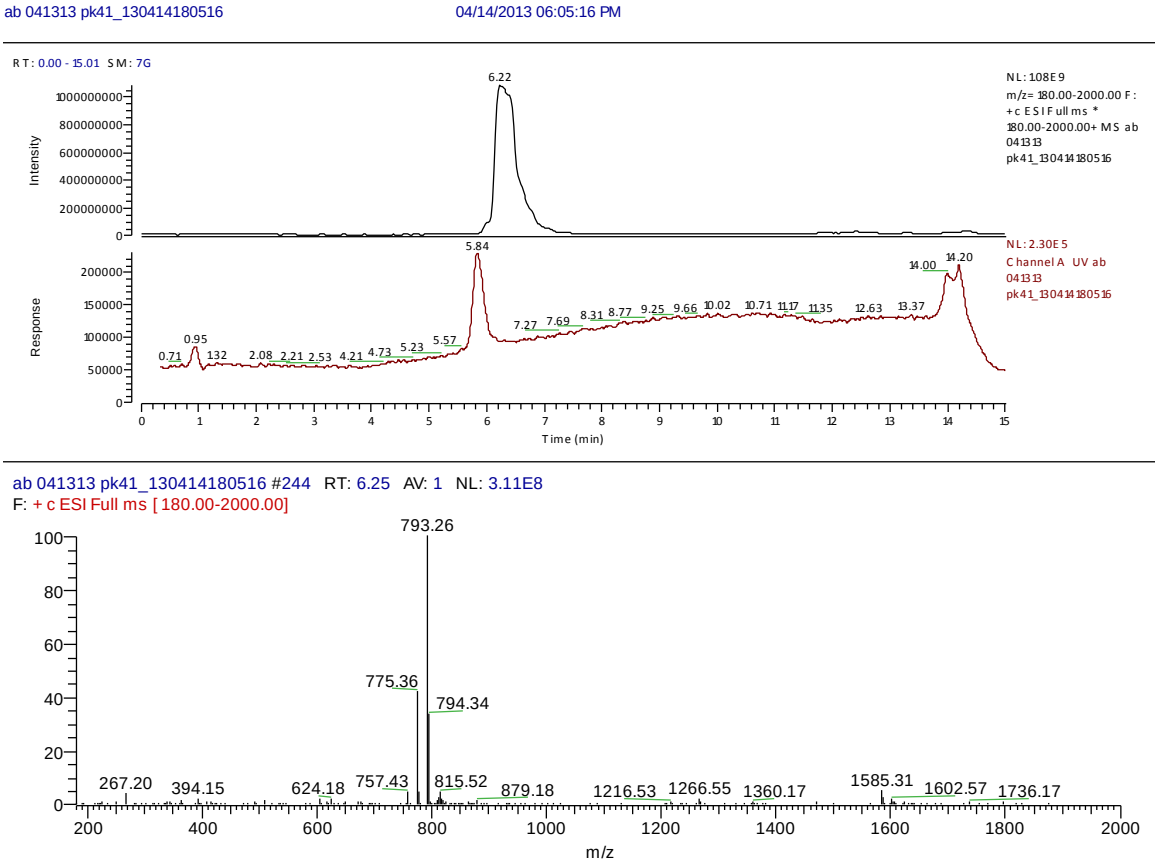

Figure S70. Cyclic **3** LC-MS

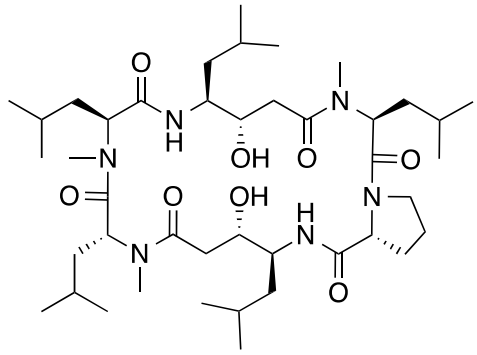

Chemical Formula: $C_{42}H_{76}N_6O_8$
Exact Mass: 792.57

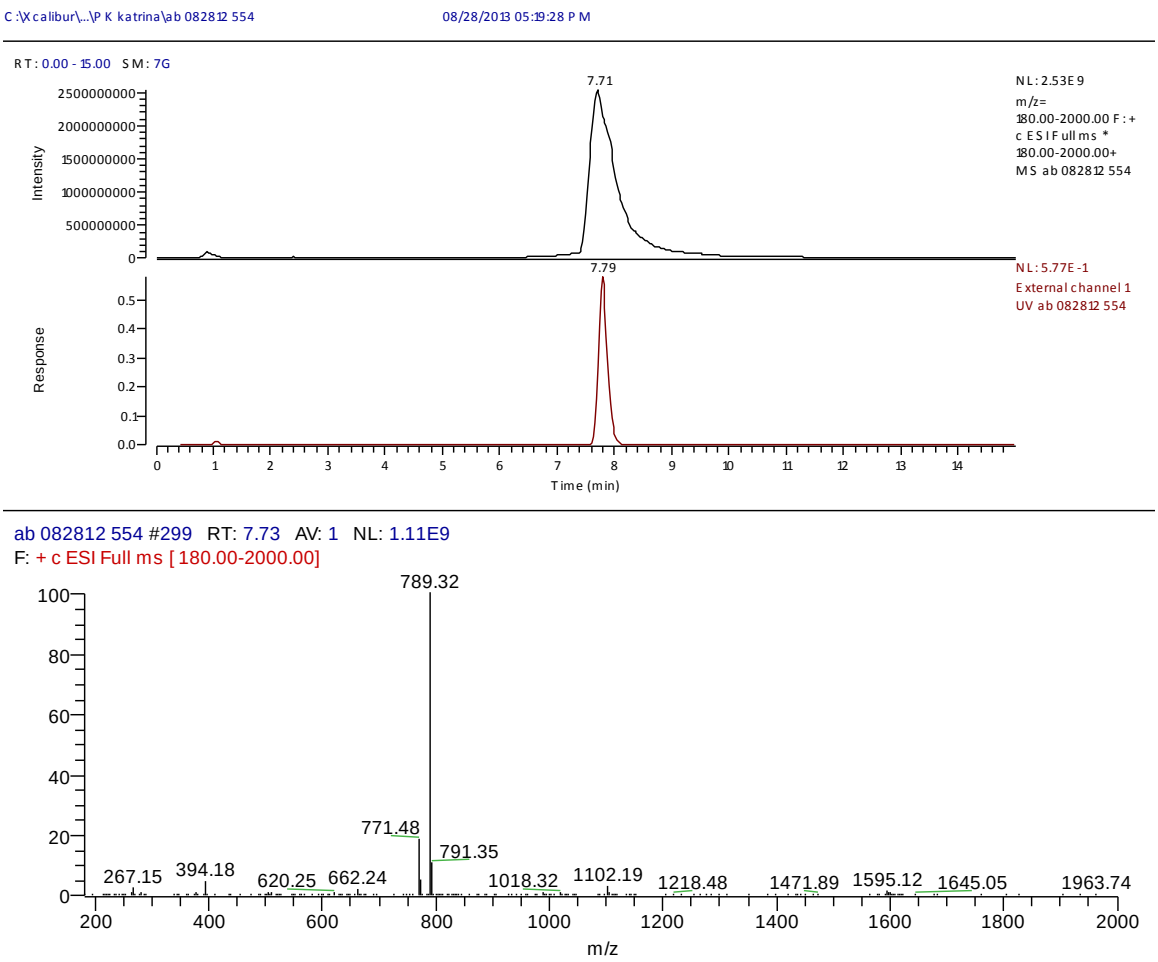

Figure S71. Cyclic **4** LC-MS

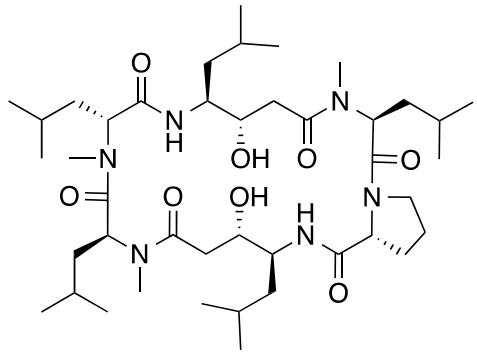

Chemical Formula: $C_{42}H_{76}N_6O_8$
Exact Mass: 792.57

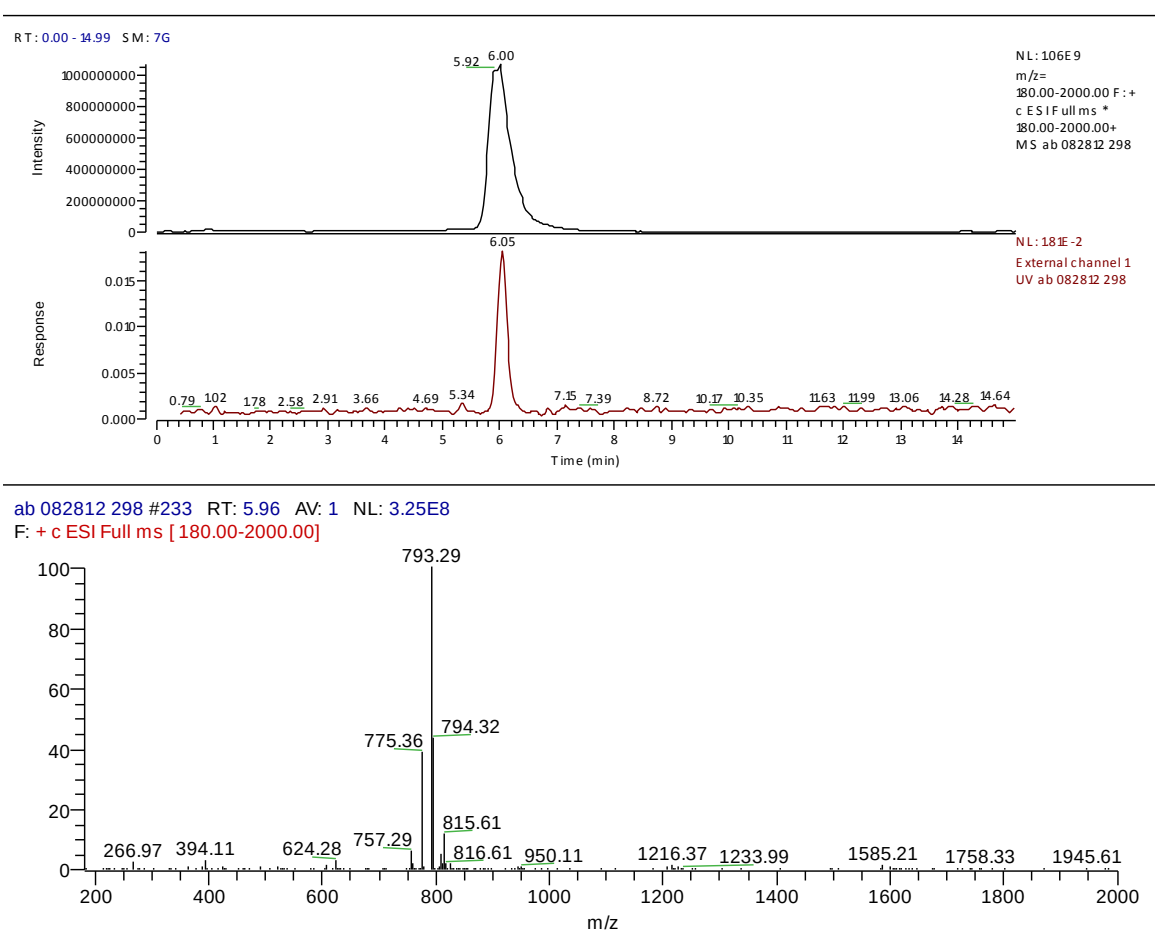

Figure S72. Cyclic **5** LC-MS

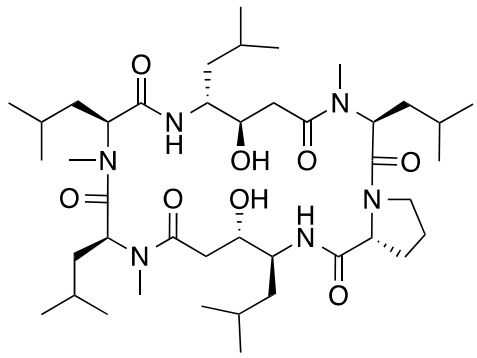

Chemical Formula: $C_{42}H_{76}N_6O_8$

Exact Mass: 792.57

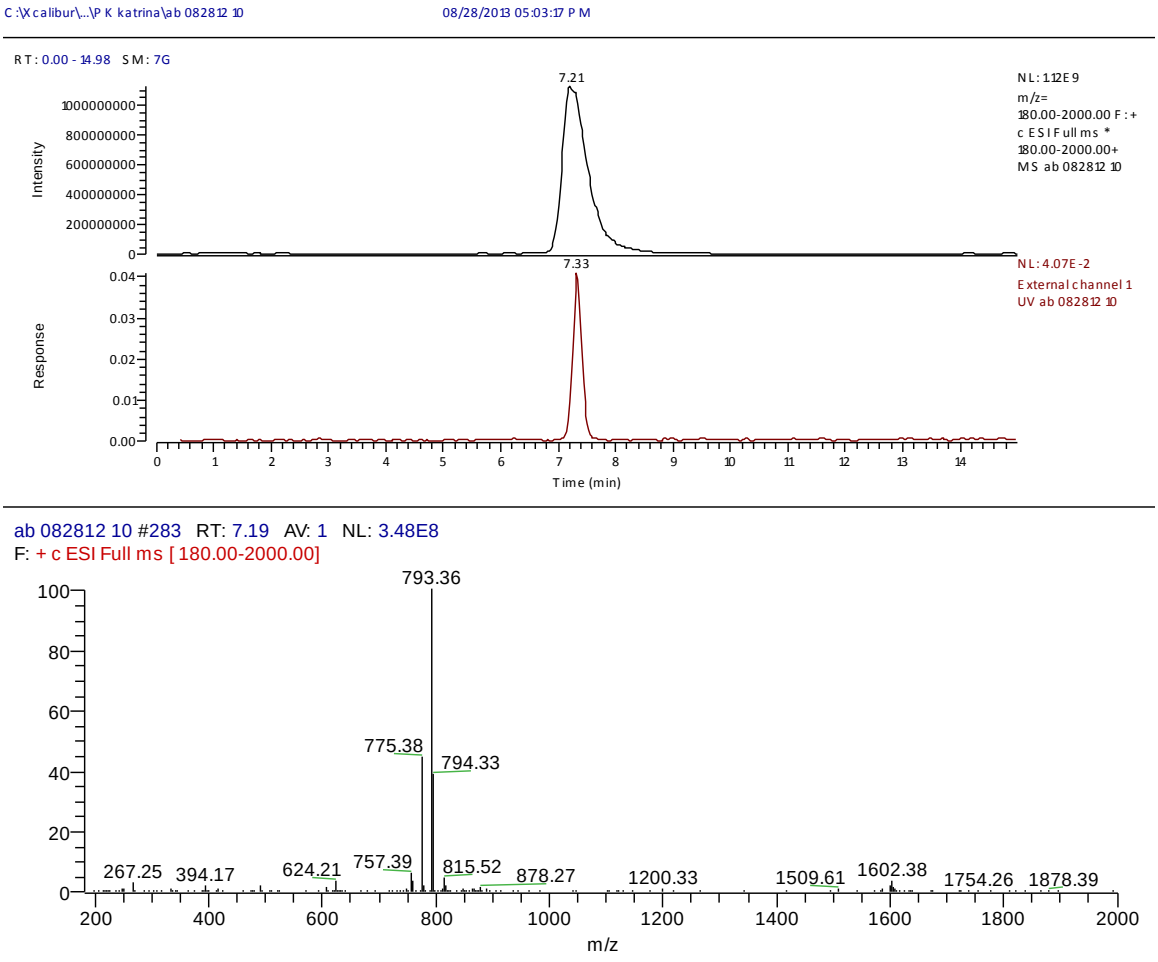

Figure S73. Cyclic **6** LC-MS

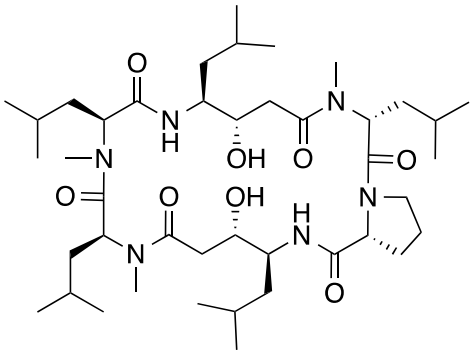

Chemical Formula: $C_{42}H_{76}N_6O_8$

Exact Mass: 792.57

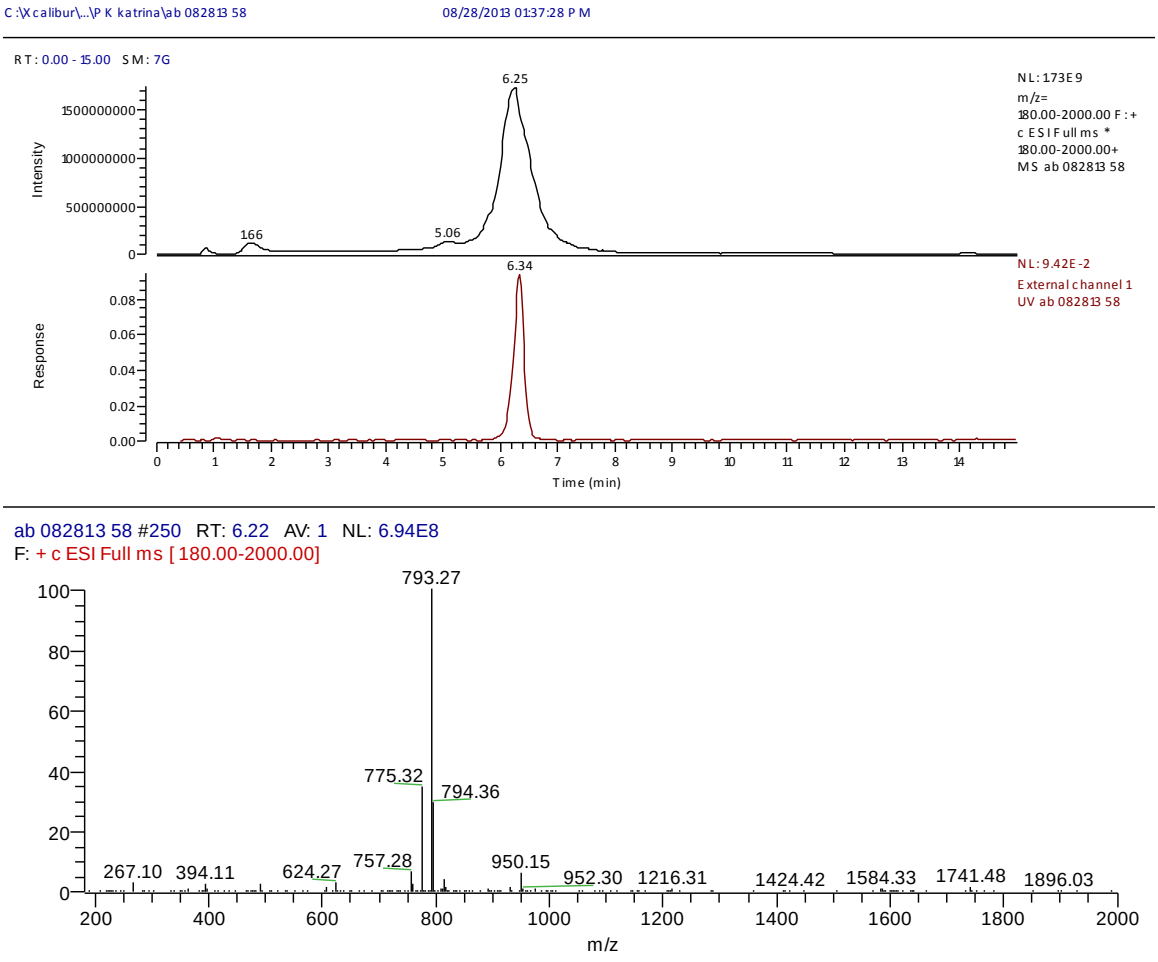

Figure S74. Cyclic **7** LC-MS

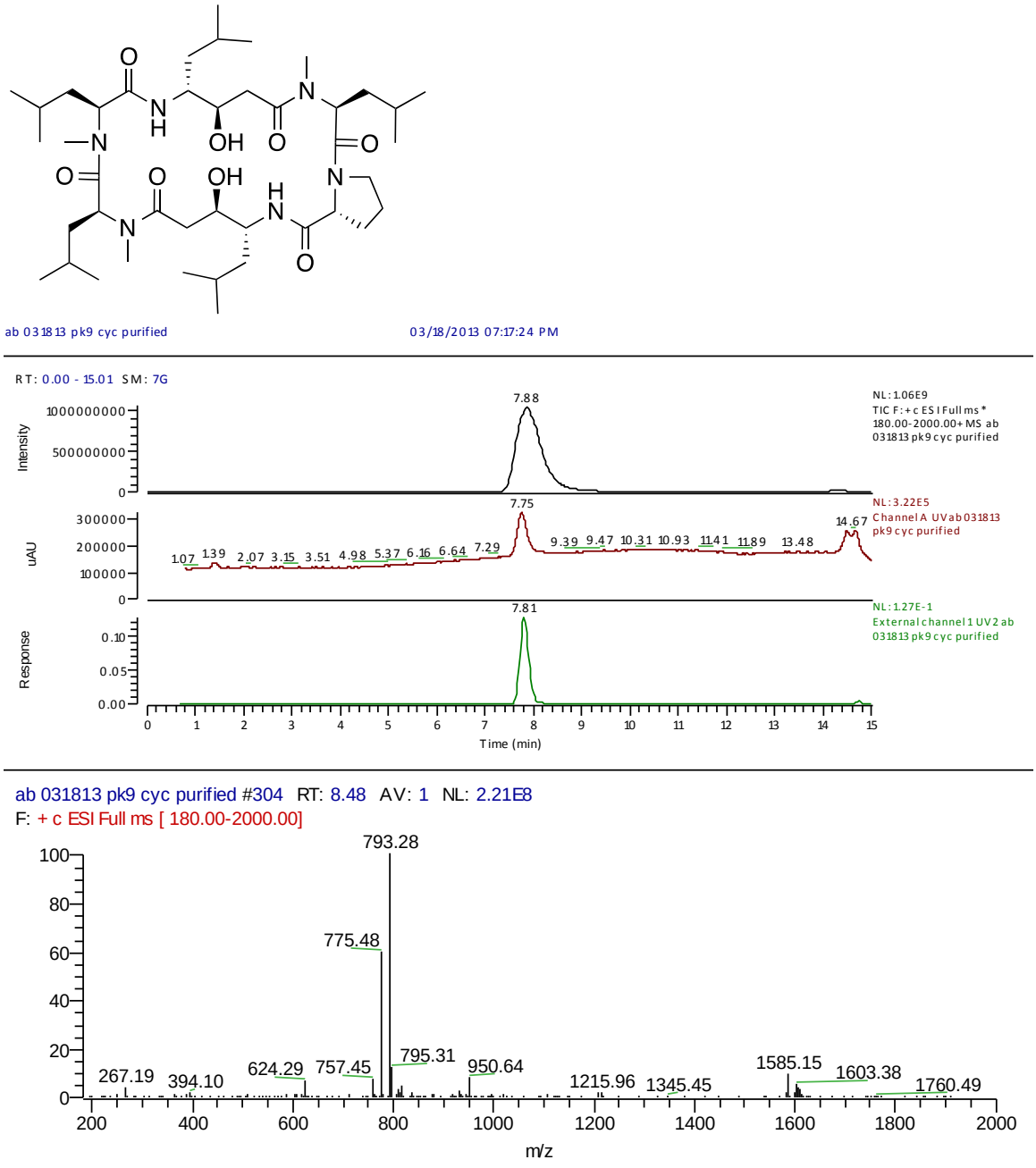

Figure S75. Cyclic **8** LC-MS

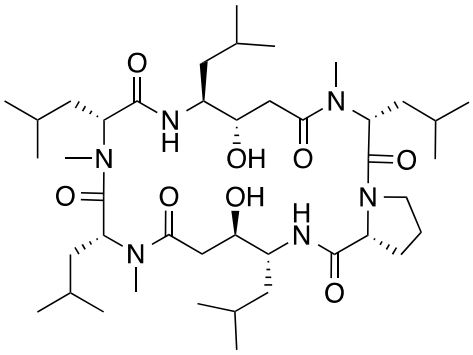

Chemical Formula: $C_{42}H_{76}N_6O_8$
Exact Mass: 792.57

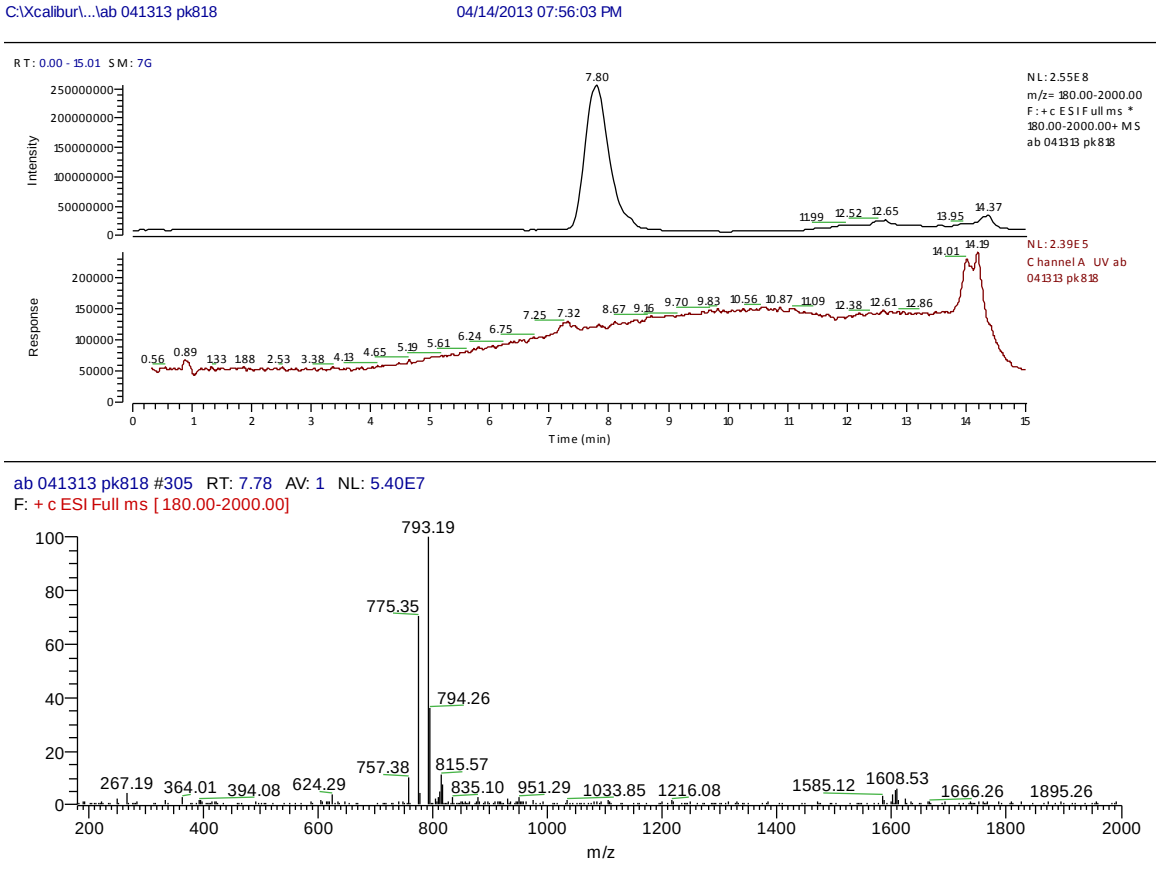

Figure S76. Cyclic **9** LC-MS

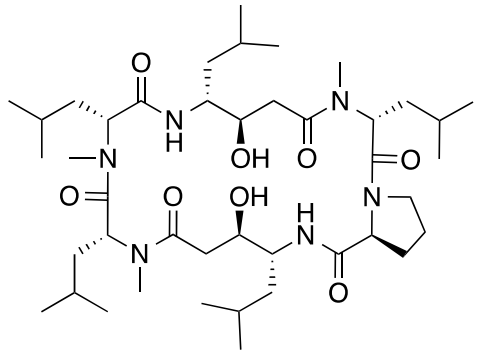

C:\Xcalibur\...\061113 pk794 f84 06/11/2013 04:48:08 AM

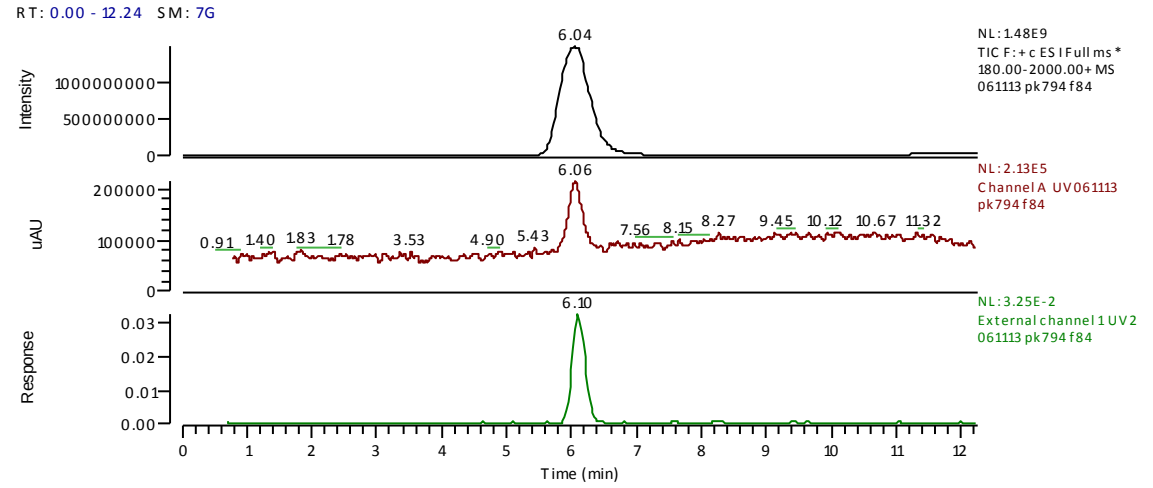

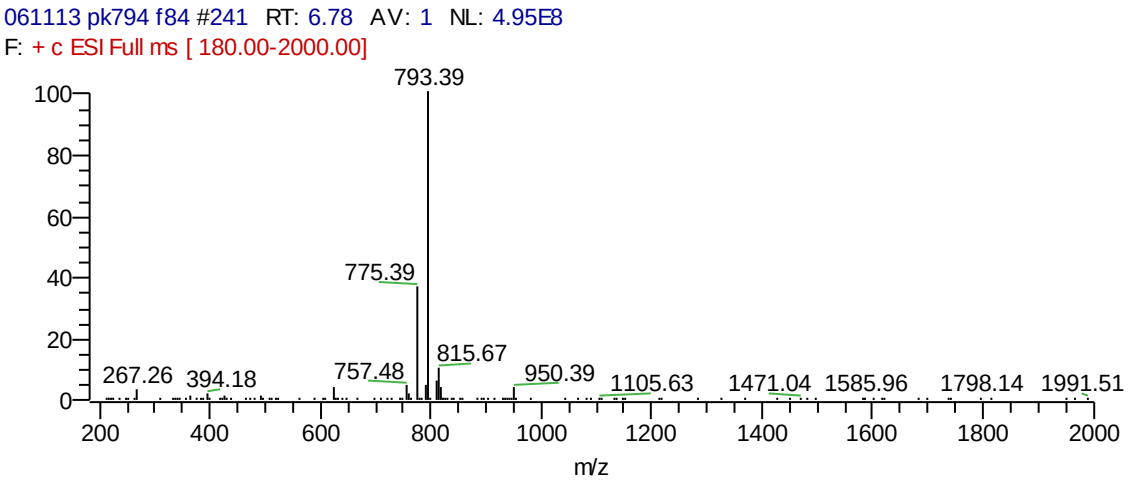

Figure S77. Cyclic **10** LC-MS

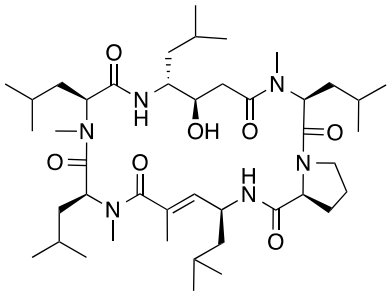

Chemical Formula: $C_{43}H_{76}N_6O_7$

Exact Mass: 788.58

ab 031713 pk6 testprep fractionwith m... 03/17/2013 02:54:13 PM

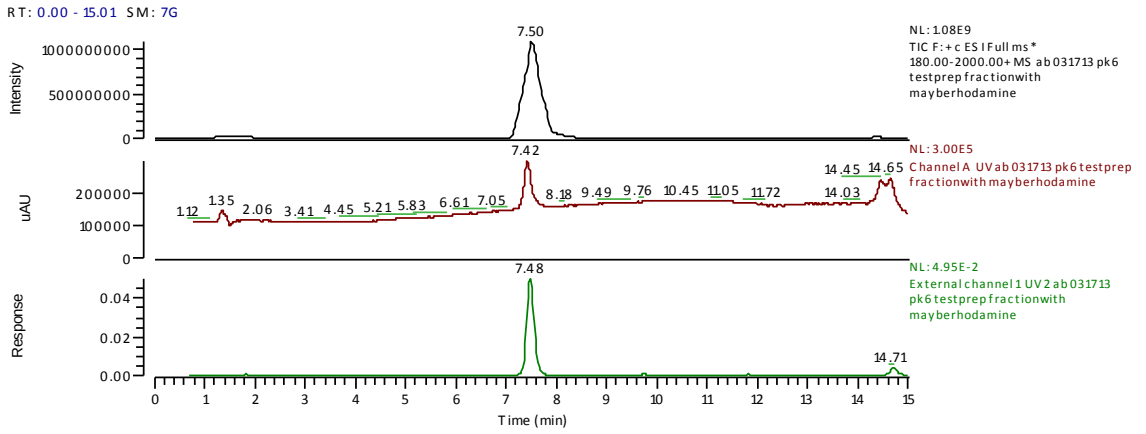

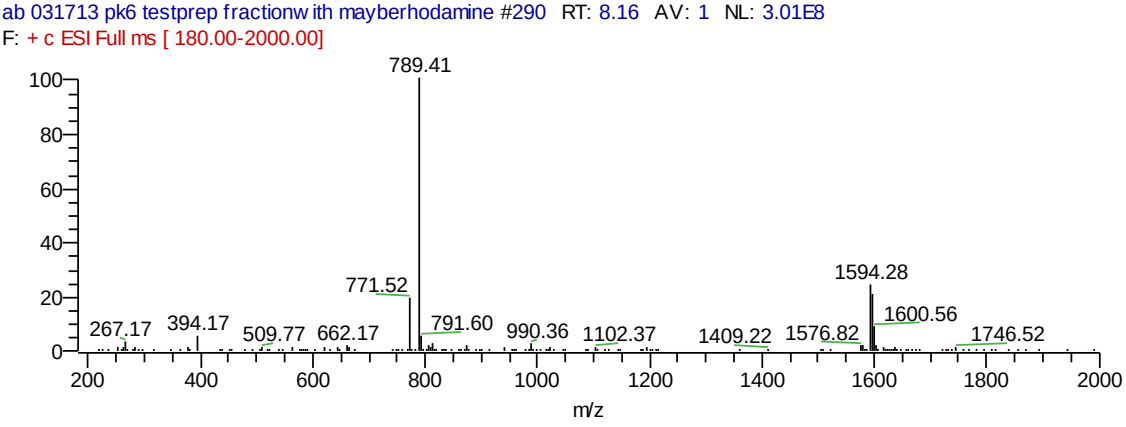

Figure S78. Macrocycle **11** LC-MS

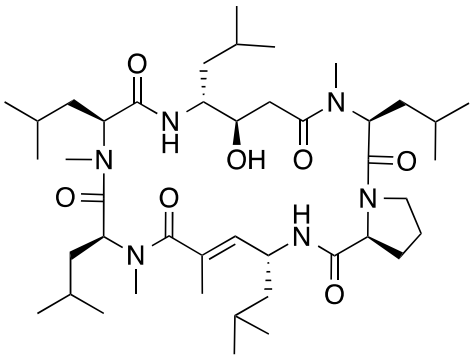

Chemical Formula: $C_{43}H_{76}N_6O_7$
Exact Mass: 788.58

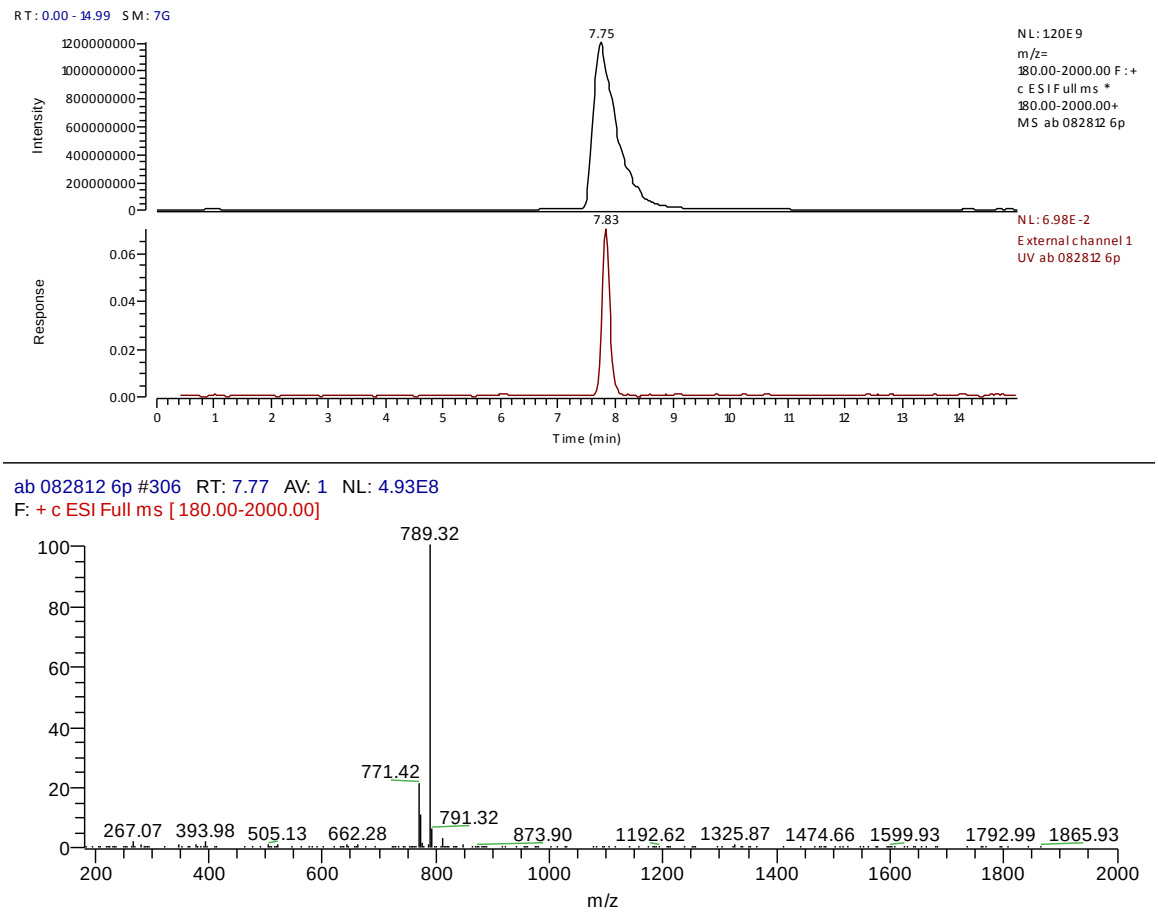

Figure S79. Macrocycle **12** LC-MS

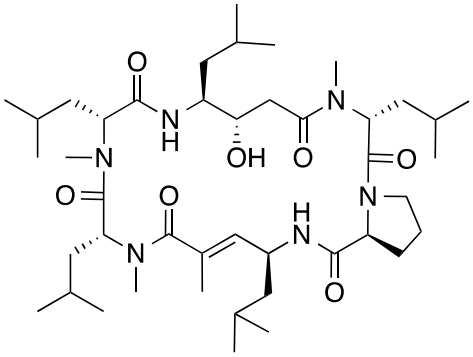

Chemical Formula: $C_{43}H_{76}N_6O_7$
Exact Mass: 788.58

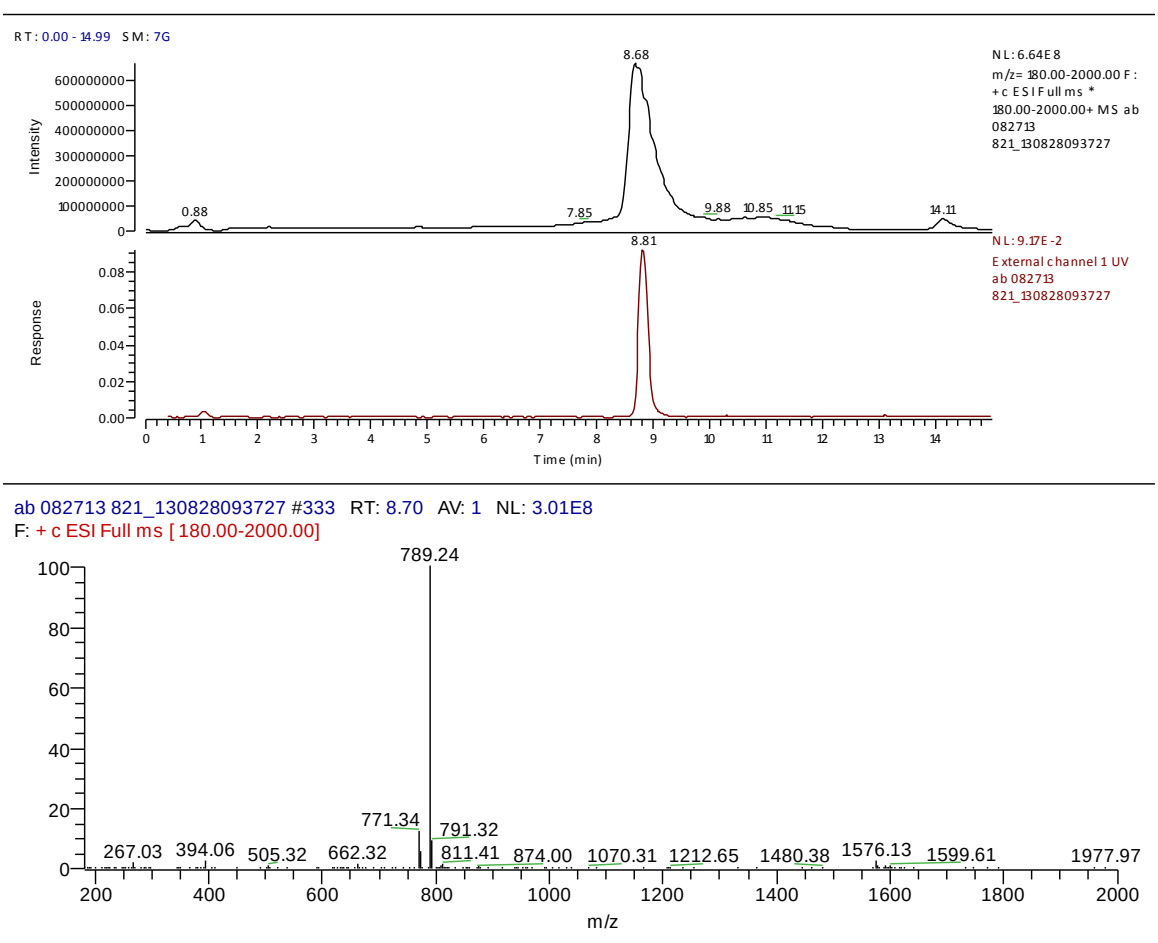

Figure S80. Cyclic **13** LC-MS

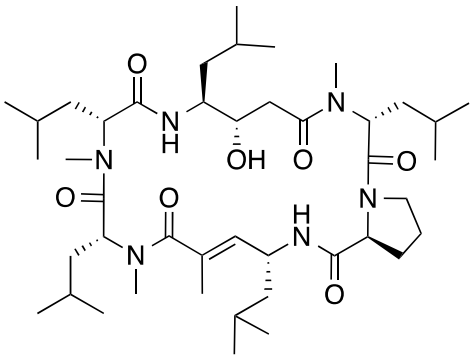

Chemical Formula: $C_{43}H_{76}N_6O_7$
Exact Mass: 788.58

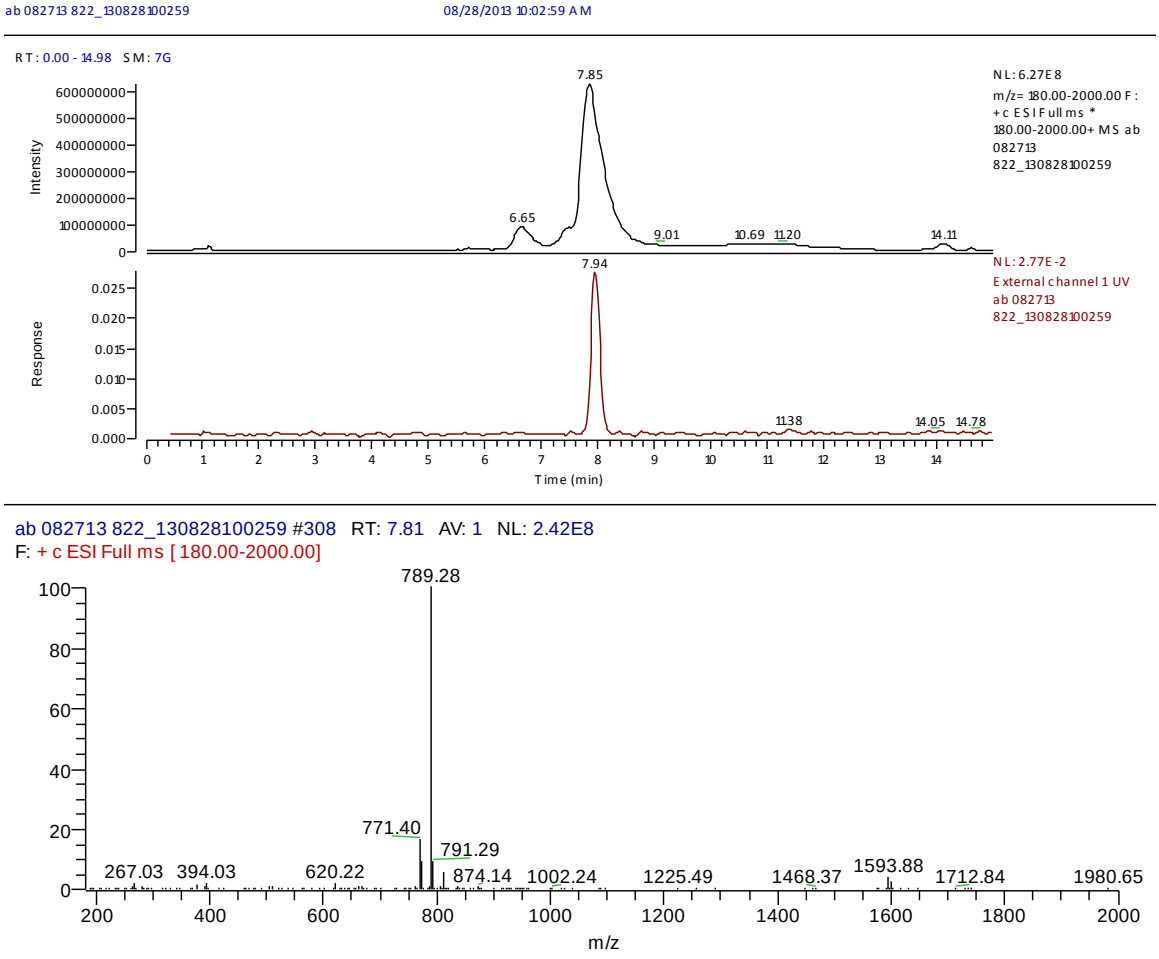

Figure S81. Cyclic **14** LC-MS

References:

(1) Freidinger, R.; Hinkle, J.; Perlow, D.; Arison, B. *Journal of Organic Chemistry* **1983**, *48*, 77.

(2) Hwang, S.-H.; Blaskovich, M. A.; Kim, H.-O. *The Open Organic Chemistry Journal* **2008**, 107.

(3) Boeckman, R. K.; Shao, P.; Mullins, J. J. **2004**, *10*, 696.

(4) Ireland, R.; Liu, L. *Journal of Organic Chemistry* **1993**, *58*, 2899.

(5) Mali, S.; Bandyopadhyay, A.; Jadhav, S.; Kumar, M.; Gopi, H. *Organic & Biomolecular Chemistry* **2011**, *9*, 6566.

(6) Gilles, A.; Martinez, J.; Cavelier, F. *Journal of Organic Chemistry* **2009**, *74*, 4298.

(7) Maryanoff, B.; Qiu, X.; Padmanabhan, K.; Tulinsky, A.; Almond, H.; Andradegordon, P.; Greco, M.; Kauffman, J.; Nicolaou, K.; Liu, A.; Brungs, P.; Fusetani, N. *Proceedings of the National Academy of Sciences of the United States of America* **1993**, *90*, 8048.

(8) Baktharaman, S.; Afagh, N.; Vandersteen, A.; Yudin, A. *Organic Letters* **2010**, *12*, 240.

(9) Cadicamo, C.; Asante, V.; Abu Ammar, M.; Borelli, C.; Korting, H.; Koksch, B. *Journal of Peptide Science* **2009**, *15*, 272.

(10) Konno, H.; Kubo, K.; Makabe, H.; Toshiro, E.; Hinoda, N.; Nosaka, K.; Akaji, K. *Tetrahedron* **2007**, *63*, 9502.

(11) El-Faham, A.; Funosas, R.; Prohens, R.; Albericio, F. *Chemistry-a European Journal* **2009**, *15*, 9404.

(12) Kansy, M.; Senner, F.; Gubernator, K. *Journal of Medicinal Chemistry* **1998**, *41*, 1007.

(13) Wohnsland, F.; Faller, B. *Journal of Medicinal Chemistry* **2001**, *44*, 923.

(14) Dorman, D. E.; Bovey, F. A. *Journal of Organic Chemistry* **1973**, *38*, 2379.

(15) Jacobson, M. P.; Pincus, D. L.; Rapp, C. S.; Day, T. J. F.; Honig, B.; Shaw, D. E.; Friesner, R. A. *Proteins-Structure Function and Bioinformatics* **2004**, *55*, 351.

(16) Atasoylu, O.; Furst, G.; Risatti, C.; Smith, A. *Organic Letters* **2010**, *12*, 1788.

(17) Cicero, D. O.; Barbato, G.; Bazzo, R. *Journal of the American Chemical Society* **1995**, *117*, 1027.

(18) Evans, D. A.; Bodkin, M. J.; Baker, S. R.; Sharman, G. J. *Magn Reson Chem* **2007**, *45*, 595.

(19) Dorman, D.; Bovey, F. *J. Org. Chem.* **1973**, *38*, 2379.